

ORNL  
MASTER COPY

JAN 12 1988

MARTIN MARIETTA

NUREG/CR-5033  
ORNL/CSD/TM-252

## Summary Description of the SCALE Modular Code System

C. V. Parks

Prepared for the  
U.S. Nuclear Regulatory Commission  
Office of Nuclear Material Safety and Safeguards  
Washington, D.C. 20555  
under Interagency Agreement DOE No. 0549-0549-A1

NRC FIN No. B-0009

OPERATED BY  
MARTIN MARIETTA ENERGY SYSTEMS, INC.  
FOR THE UNITED STATES  
DEPARTMENT OF ENERGY

### NOTICE

This report was prepared as an account of work sponsored by an agency of the United States Government. Neither the United States Government nor any agency thereof, or any of their employees, makes any warranty, expressed or implied, or assumes any legal liability or responsibility for any third party's use, or the results of such use, of any information, apparatus product or process disclosed in this report, or represents that its use by such third party would not infringe privately owned rights.

Available from

Superintendent of Documents  
U.S. Government Printing Office  
Post Office Box 37082  
Washington, D.C. 20013-7982

and

National Technical Information Service  
Springfield, VA 22161

NUREG/CR-5033  
ORNL/CSD/TM-252  
Dist. Category GM

COMPUTING AND TELECOMMUNICATIONS DIVISION  
at  
Oak Ridge National Laboratory  
Post Office Box X  
Oak Ridge, Tennessee 37831

## SUMMARY DESCRIPTION OF THE SCALE MODULAR CODE SYSTEM

C. V. Parks

Manuscript Completed: August 1987  
Date Published: December 1987

Prepared for the  
U.S. Nuclear Regulatory Commission  
Office of Nuclear Material Safety and Safeguards  
Washington, D.C. 20555  
under Interagency Agreement DOE No. 0549-0549-A1

NRC FIN No. B-0009

Prepared by the  
MARTIN MARIETTA ENERGY SYSTEMS, INC.,  
operating the  
Oak Ridge National Laboratory      Oak Ridge Y-12 Plant  
Oak Ridge Gaseous Diffusion Plant      Paducah Gaseous Diffusion Plant  
for the  
U.S. Department of Energy  
under contract DE-AC05-84OR21400



## TABLE OF CONTENTS

| SECTION   | PAGE      |
|---|-----------|
| LIST OF FIGURES .....   | v         |
| LIST OF TABLES .....  | vii       |
| PREFACE .....   | ix        |
| ABSTRACT .....  | xi        |
| <b>1. INTRODUCTION AND OVERVIEW .....</b>   | <b>1</b>  |
| 1.1 BACKGROUND .....  | 1         |
| 1.2 OVERVIEW OF SYSTEM COMPONENTS .....   | 2         |
| 1.2.1 Functional Modules .....  | 4         |
| 1.2.2 Data Base .....   | 5         |
| 1.2.3 Control Modules .....   | 6         |
| 1.2.4 Other SCALE Components .....  | 7         |
| 1.3 SUMMARY .....   | 8         |
| <b>2. CROSS-SECTION PROCESSING TECHNIQUES .....</b>   | <b>9</b>  |
| 2.1 REVIEW OF CROSS-SECTION LIBRARIES .....   | 9         |
| 2.1.1 Criticality Libraries .....   | 9         |
| 2.1.2 Shielding Libraries .....   | 10        |
| 2.2 REVIEW OF THE STANDARD COMPOSITION LIBRARY .....  | 10        |
| 2.3 REVIEW OF CROSS-SECTION PROCESSING TECHNIQUES .....                                       | 11        |
| 2.3.1 The BONAMI-S Module .....   | 12        |
| 2.3.2 The NITAWL-S Module .....   | 13        |
| 2.3.3 The XSDRNPM-S Module .....  | 14        |
| 2.3.4 The ICE-S Module .....  | 15        |
| 2.4 AUTOMATED PROCEDURE FOR CROSS-SECTION PROCESSING .....                                    | 16        |
| 2.5 SUMMARY .....   | 17        |
| <b>3. EVALUATION OF SPENT FUEL ISOTOPICS, RADIATION SPECTRA, AND<br/>    DECAY HEAT .....</b> | <b>22</b> |
| 3.1 REVIEW OF THE ORIGEN-S FUNCTIONAL MODULE .....  | 23        |
| 3.1.1 Analytic Method .....   | 23        |
| 3.1.2 ORIGEN-S Data Libraries .....   | 27        |
| 3.1.3 Calculation of Radiation Source Spectra .....   | 29        |
| 3.2 REVIEW OF THE COUPLE FUNCTIONAL MODULE .....  | 32        |
| 3.2.1 Flux Weight Factors .....   | 32        |
| 3.2.2 Cross-Section Collapse to ORIGEN-S Group Structure .....                                | 34        |
| 3.3 DEPLETION AND DECAY WITH THE SAS2 CONTROL MODULE .....                                    | 35        |
| 3.3.1 Method and Techniques .....   | 35        |
| 3.3.2 Advantages and Limitations .....  | 38        |
| 3.3.3 New Developments for SAS2 .....   | 40        |
| 3.4 GRAPHICAL DISPLAY OF ORIGEN-S RESULTS .....   | 41        |
| 3.5 SUMMARY .....   | 45        |

|  |     |
|--|-----|
| 4. COMPUTATIONAL METHODS FOR CRITICALITY SAFETY ANALYSIS .....               | 46  |
| 4.1 REVIEW OF FUNCTIONAL MODULES FOR CRITICALITY SAFETY ANALYSIS .....       | 46  |
| 4.1.1 One-Dimensional Analyses .....   | 46  |
| 4.1.2 Multidimensional Analysis .....  | 47  |
| 4.2 REVIEW OF THE CRITICALITY SAFETY ANALYSIS SEQUENCES .....                | 52  |
| 4.2.1 Description of Sequences .....   | 52  |
| 4.3 VALIDATION EXPERIENCE .....  | 56  |
| 4.4 SUMMARY .....  | 56  |
| 5. SHIELDING ANALYSIS METHODS .....  | 57  |
| 5.1 REVIEW OF THE FUNCTIONAL MODULES .....                                   | 57  |
| 5.1.1 One-Dimensional Radiation Transport and Dose Evaluation .....          | 57  |
| 5.1.2 Multidimensional Radiation Transport and Dose Evaluation .....         | 58  |
| 5.2 REVIEW OF THE SHIELDING ANALYSIS SEQUENCES .....                         | 59  |
| 5.2.1 Common Features of the Sequences .....                                 | 59  |
| 5.2.2 The SAS3 Sequence .....  | 60  |
| 5.2.3 The SAS2 Sequence .....  | 60  |
| 5.2.4 The SAS1 Sequence .....  | 62  |
| 5.2.5 The SAS4 Sequence .....  | 66  |
| 5.3 SUMMARY .....  | 71  |
| 6. HEAT TRANSFER ANALYSIS CAPABILITIES .....                                 | 75  |
| 6.1 REVIEW OF THE HEATING6 FUNCTIONAL MODULE .....                           | 75  |
| 6.1.1 Modeling Techniques .....  | 75  |
| 6.2 USER INTERFACE AND MODELING CAPABILITIES .....                           | 82  |
| 6.3 NEW FEATURES OF HEATING6.1 .....   | 93  |
| 6.4 GRAPHICAL DISPLAY CAPABILITIES .....                                     | 94  |
| 6.5 CAPABILITIES OF THE HTAS1 CONTROL MODULE .....                           | 94  |
| 6.6 VERIFICATION EFFORTS .....   | 101 |
| 6.7 SUMMARY .....  | 103 |
| 7. REFERENCES .....  | 106 |
| APPENDIX A - CHANGES AND CORRECTIONS IN THE SCALE SYSTEM:<br>1980-1986 ..... | 113 |
| APPENDIX B - FEATURES OF THE ORIGEN-S PROGRAM .....                          | 121 |

## LIST OF FIGURES

| FIGURE  | PAGE |
|---|------|
| 1.1. SCALE system components .....  | 3    |
| 2.1. Outline of Material Information Processor data .....   | 18   |
| 2.2. Material Information Processor input for CSAS2 sample problem .....  | 19   |
| 2.3. Echo of input to Material Information Processor input<br>of Fig. 2.2 .....   | 20   |
| 3.1. Computation flow path invoked by SAS2 module .....   | 36   |
| 3.2. Sample input for SAS2 sequence .....   | 39   |
| 3.3. Example of PLORIGEN plot of important nuclides .....   | 42   |
| 3.4. Example of PLORIGEN plot of gamma spectrum .....   | 43   |
| 3.5. Example of PLORIGEN plot comparing decay heat from three<br>separate burnups .....   | 44   |
| 4.1. Cross section of a typical PWR shipping cask model for KENO V.a .....  | 51   |
| 4.2. CSAS4X input for PWR assemblies in square aluminum cask .....  | 55   |
| 5.1. General SAS1 flow diagram .....  | 64   |
| 5.2. Example of SAS1 input used for ferritic steel cask analysis .....  | 65   |
| 5.3. Outline of the SAS4 analytic sequence .....  | 67   |
| 5.4. SAS4 shipping cask model for IGO=0 .....   | 68   |
| 5.5. Geometry options of source region for simplified<br>geometry input .....   | 70   |
| 5.6. Upper half of depleted uranium cask model .....  | 72   |
| 5.7. SAS4 input listing for simple cask model .....   | 73   |
| 6.1. Nodal description for three-dimensional problem .....  | 76   |
| 6.2. Surface-to-surface heat transfer .....   | 80   |
| 6.3. HEATING6 region description for two-dimensional,<br>rectangular model composed of two materials .....  | 85   |
| 6.4. HEATING6 region description for two-dimensional,<br>rectangular model with indentation .....   | 86   |
| 6.5. HEATING6 region description for two-dimensional,<br>rectangular model with various boundary conditions .....                                       | 87   |
| 6.6. Region description for two-dimensional, rectangular<br>model involving surface-to-surface boundary conditions,<br>incompatible with HEATING6 ..... | 88   |
| 6.7. HEATING6 region description for two-dimensional rectangular<br>model involving surface-to-surface boundary conditions .....                        | 89   |
| 6.8. Example of map-type temperature edit from HEATING6 .....   | 91   |
| 6.9. Zone configuration in HTAS1 general model with physical<br>dimensional labels .....  | 96   |
| 6.10. Example of REGPLOT6 output for HTAS1 sample problem 2 .....   | 99   |
| 6.11. Typical shipping cask calculational model .....   | 100  |
| 6.12. Typical shipping cask input for HTAS1 .....   | 102  |
| 6.13. Cask model problem with annular regions and radiation shield .....  | 104  |
| 6.14. HEATING6.1 and experimental results for helium-filled simulated<br>PWR assembly in an enclosure .....   | 105  |



## LIST OF TABLES

| TABLE   | PAGE |
|---|------|
| 2.1. SCALE standard response function ID numbers .....  | 11   |
| 3.1. Card-image ORIGEN-S libraries at ORNL .....  | 30   |
| 3.2. Some binary ORIGEN-S libraries at ORNL .....   | 30   |
| 3.3. Comparison of measured and computed nuclide/ <sup>238</sup> U atom<br>ratios for Turkey Point assembly ..... | 40   |
| 4.1. Functional modules executed by the Criticality Safety<br>Analysis Sequences .....                            | 52   |
| 4.2. Primary products from sequences in CSAS4 control module .....  | 53   |
| 4.3. Table of input data requirements for sequences in CSAS4<br>control module program .....                      | 54   |
| 6.1. Fin effectiveness models pictorial .....   | 83   |
| 6.2. Dependence of input parameters .....   | 92   |
| 6.3. Analysis specification keywords for HTAS1 model .....  | 95   |
| 6.4. Keywords for zones in HTAS1 model .....  | 97   |
| A.1. 16 group results for critical experiments of low-enriched,<br>slightly moderated, uranium systems .....      | 116  |



## PREFACE

This report has been compiled to provide a relatively complete description of the SCALE modular code system. The information in this report is largely condensed from the approximately 3500-page manual (NUREG/CR-0200) that documents the SCALE system and its use. Additional information based on the author's experience and discussions with the various module developers is also included. Each of the chapters represents (with slight modifications) the papers written for the proceedings of a "Workshop on the SCALE-3 Modular System," held in Saclay, France, on June 24-27, 1986. The papers were published in the October 1986 Newsletter (No. 33) of the NEA Data Bank. The workshop lectures were given by L. M. Petrie, R. M. Westfall, and the author. The workshop followed the same format as an earlier one held in April 1986 in Oak Ridge, Tennessee, under the sponsorship of the Radiation Shielding Information Center at Oak Ridge National Laboratory.

As project leader for SCALE since 1980, the author is deeply appreciative of the efforts and expertise displayed by the staff of the Computing and Telecommunications Division who developed, documented, and continue to maintain the SCALE system. The major contributors are noted below:

|                          |   |
|--------------------------|---|
| C. B. Bryan/K. W. Childs | HEATING6.1 enhancements   |
| J. A. Bucholz            | CSAS1, CSAS2, XSDOSE  |
| C. K. Cobb               | HEATPLOT-S, REGPLOT6  |
| M. B. Emmett             | JUNEBUG-II, MARS Enhancements   |
| G. E. Giles              | HEATING6  |
| N. M. Greene             | NITAWL-S, BONAMI-S, XSDRNPM-S, ICE  |
| O. W. Hermann            | ORIGEN-S, COUPLE, SAS2, PLORIGEN  |
| J. R. Knight*            | Material Information Processor, Standard<br>Composition Library, CESAR, SAS1  |
| N. F. Landers            | KENO IV, KENO V, CSAS4  |
| L. M. Petrie             | ICE-S, NITAWL-S, XSDRNPM-S, KENO V, KENO IV,<br>CSAS4, System Driver, Subroutine Library, Free-Form<br>Reading Routines, Cross-Section Libraries, Material<br>Information Processor |
| J. C. Ryman              | ORIGEN-S Data Libraries   |
| J. S. Tang               | SAS4, MORSE-SGC/S   |
| W. D. Turner             | HEATING6, HTAS1   |
| J. T. West†              | MORSE-SGC/S, JUNEBUG, MARS, SAS3  |
| R. M. Westfall           | Cross-Section Libraries, ORIGEN-S,<br>NITAWL-S, XSDRNPM-S, Project Leader 1976-1980   |

---

\*Retired.

†Presently employed at Los Alamos National Laboratory.



## ABSTRACT

SCALE — a modular code system for Standardized Computer Analyses for Licensing Evaluation — has been developed at Oak Ridge National Laboratory at the request of the U.S. Nuclear Regulatory Commission staff. The SCALE system utilizes well-established computer codes and methods within standard analytic sequences that (1) allow simplified free-form input, (2) automate the data processing and coupling between codes, and (3) provide accurate and reliable results. System development has been directed at criticality safety, shielding, and heat transfer analysis of spent fuel transport and/or storage casks. However, only a few of the sequences (and none of the individual functional modules) are restricted to cask applications. This report will provide a background on the history of the SCALE development and review the components and their function within the system. The available data libraries are also discussed, together with the automated features that standardize the data processing and systems analysis.



## 1. INTRODUCTION AND OVERVIEW

### 1.1 BACKGROUND

The Nuclear Engineering Applications Department (NEAD) of the Computing and Telecommunications Division at Oak Ridge National Laboratory (ORNL) has had a long-time relationship with the Transportation Branch of the U.S. Nuclear Regulatory Commission (USNRC). In 1969, R. H. Odegaarden approached G. E. Whitesides of NEAD concerning use of the KENO code<sup>1</sup> for criticality analysis of shipping casks. In the period 1969-1976, the USNRC (and its predecessor, the U.S. Atomic Energy Commission) funded NEAD and its sister department, Engineering Applications (responsible for thermal methods and use), to provide support in the development and use of analytical tools and cross-section libraries for the criticality, shielding, and thermal review of spent fuel packaging designs and storage pools.

As the capability and complexity of computational tools increased, use of the tools became more and more difficult for the occasional, nonexpert user. Therefore, in 1976 R. H. Odegaarden again approached NEAD with the idea of developing a computational system that would (1) use well-established computer codes and data libraries, (2) have an easy-to-use input format designed for the occasional user and/or novice, (3) combine and automate analyses requiring multiple computer codes or calculations into standard analytic sequences, and (4) be well documented and publicly available. With these general goals and a host of others that evolved over the ensuing months, R. M. Westfall and L. M. Petrie of NEAD laid out the framework for a computational system which was eventually called SCALE (Standardized Computer Analyses for Licensing Evaluation). Early papers on the development of SCALE from both a USNRC and NEAD perspective are provided in refs. 2 and 3.

From 1976-1981, funding was obtained from the USNRC Office of Nuclear Regulatory Research to develop SCALE as laid out by Westfall and Petrie. Finally, in July 1980 a limited version of SCALE was made available to the Radiation Shielding Information Center (RSIC) at ORNL. This system was packaged and released by RSIC as CCC-288/SCALE-0. Subsequent additions and modifications have resulted in the release of CCC-424/SCALE-1 in 1981, CCC-450/SCALE-2 in late 1983, and CCC-466/SCALE-3 in early 1985. With each release to RSIC, new and/or updated documentation is provided as revisions to the NRC-published SCALE Manual, NUREG/CR-0200.<sup>4</sup> A review of the major changes incorporated with each release is provided in Appendix A.

From 1982 to the present, the ongoing development and maintenance of the SCALE system has been funded primarily by the Transportation Branch within the USNRC Office of Nuclear Material Safety and Safeguards. Currently, only one major addition to the SCALE system is planned --- development of a module for predicting fuel pin temperatures in a cask. However, several new or revised modules have been completed since the 1985 release of SCALE-3. These modules, which are currently used in production work at ORNL and are scheduled for public release in SCALE-4, are discussed in this report, along with the existing modules of SCALE-3.

The SCALE-4 version of the system is planned for release in early 1988. This version will be a FORTRAN 77 version designed for enhanced portability between different computers. Both CRAY and IBM versions of SCALE-4 are planned. Outdated modules and/or those not amenable to conversion to FORTRAN 77 will not be available in SCALE-4. Several modules of SCALE-3 which are already available in FORTRAN 77 have been released through RSIC as CCC-475/SCALIAS. This package may be particularly useful to non-IBM users in the interim period prior to release of SCALE-4.

## 1.2 OVERVIEW OF SYSTEM COMPONENTS

The SCALE system draws heavily from basic neutron-transport, data-processing, and heat-transfer methods technology developed at Oak Ridge over the past two decades. The data processing is a direct outgrowth of that employed in AMPX,<sup>5</sup> a modular code system for processing coupled neutron-photon cross sections from ENDF/B. Modified versions of the AMPX problem-dependent data-processing modules NITAWL and XSDRNPM are incorporated into SCALE. However, even though some of the functions performed in AMPX and SCALE are the same, the overall purpose and organizational structure of SCALE is substantially different from that of AMPX.

The overall purpose of SCALE is systems analysis with associated data processing. For example, the objective of systems analysis may be to establish the criticality safety of the configuration under study. Then the associated data processing would involve the preparation of neutron cross sections representative of the system being analyzed. Thus, one major difference between SCALE and AMPX is that data processing in SCALE is restricted to the problem-dependent phase and, rather than being the primary objective, it is incidental to the system analysis.

The second major difference between SCALE and AMPX is the manner in which the two systems are organized. In AMPX, the user selects a sequence of modules to be executed and prepares a set of input data for each module. Back-to-back execution of individual modules is possible within SCALE, but the overall goal of the SCALE project has been to develop easy-to-use analytical sequences that are automated to perform the necessary data processing (e.g., cross-section preparation) and manipulation of well-established computer codes (functional modules) required by the sequence. Thus, the user is able to select an analytic sequence characterized by the type of analysis (criticality, shielding, or heat transfer) to be performed and the geometric complexity of the system being analyzed. The user then prepares a single set of input for the control module corresponding to this analytical sequence. The control module input is in terms of easily visualized engineering parameters specified in a simplified, free-form format. The control modules use this information to derive additional parameters and prepare the input for each of the functional modules in the analytical sequence.

The driver module resides in-core at all times and, upon various types of commands, transfers the control and functional modules to and from the central processor unit. Thus the core storage requirement for a sequence involving the execution of several modules corresponds roughly to the largest needs of any single module in the sequence. The intermediate execution paths are typically determined by the control modules. The control modules communicate with the system driver through a small common block of special parameters. Ordinarily, the user specifies the control module to be executed on a data card read by the driver. For example, to execute Criticality Safety Analysis Sequence No. 1 (CSAS1) the user submits =CSAS1 to the driver, which in turn loads CSAS1 into the central processor unit. However, provision has been made to allow the user to execute the functional modules on a stand-alone basis (e.g., =KENO5). Thus the user has the option of determining his own (or nonstandard) execution path.

The existing components of the SCALE system are shown in Fig. 1.1. The remainder of this section will provide a short description of each component. More details on the major components and their individual capabilities are provided in subsequent sections of this report.

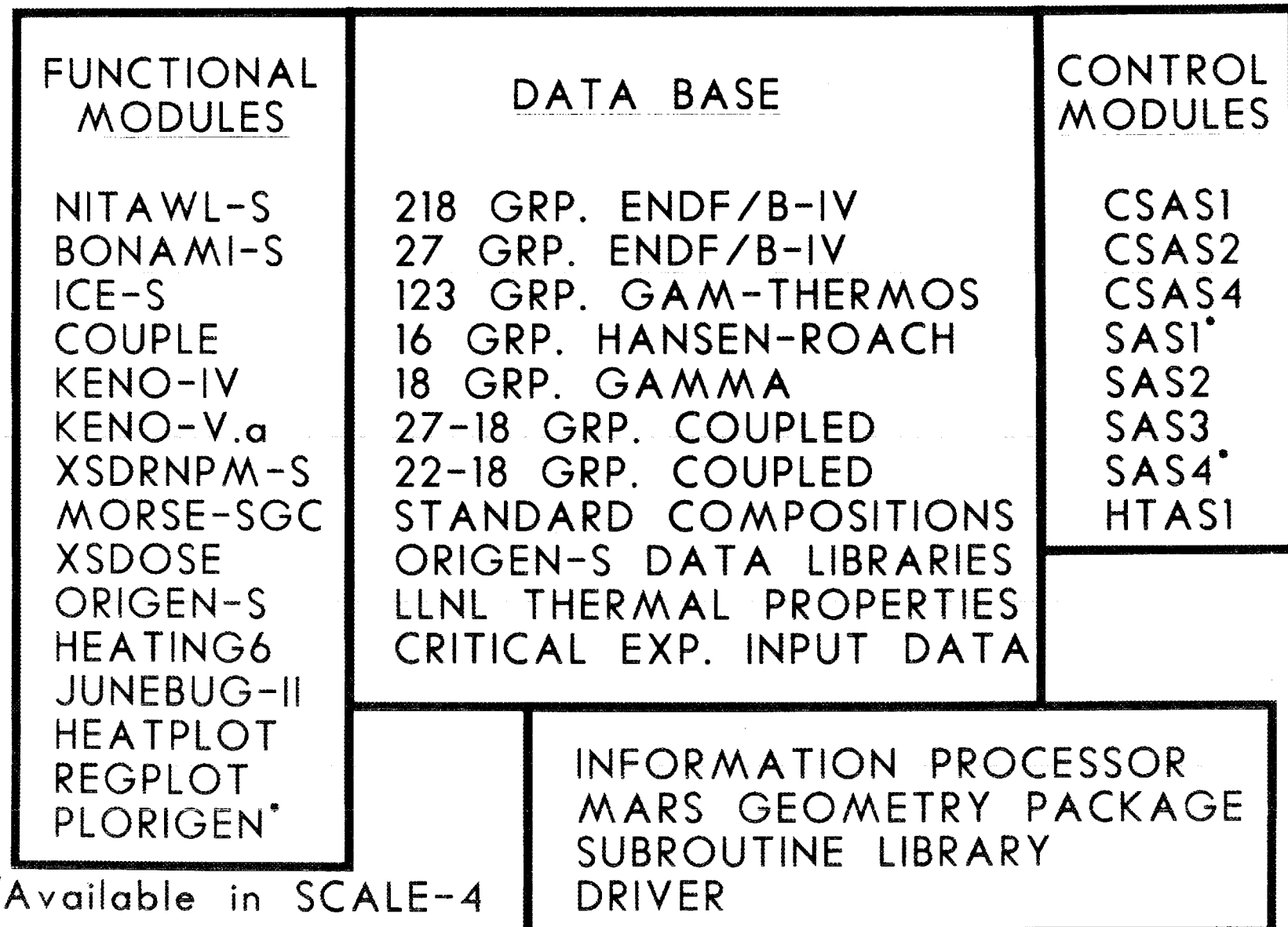


Fig. 1.1. SCALE system components.

### 1.2.1 Functional Modules

All the functional modules currently in SCALE-3 or planned for release in SCALE-4 are listed in Fig. 1.1. The SCALE functional modules were selected on a basis of both their analytic capabilities and their proven records of reliable performance. A brief summary of the capabilities of each functional module is provided below.

- **NITAWL-S** applies the Nordheim Integral Technique to perform neutron cross-section processing in the resonance energy range. This technique involves a fine energy group calculation of the slowing-down flux across each resonance with subsequent flux weighting of the resonance cross sections. The major function of NITAWL is its conversion of cross-section libraries from a problem-independent to a problem-dependent form. However, NITAWL also assembles group-to-group transfer arrays from the elastic and inelastic scattering components and performs other tasks in producing the problem-dependent working library.
- **BONAMI-S** performs resonance shielding through the application of the Bondarenko shielding factor method. As input, the program requires the presence of shielding factor data on the AMPX master library interface. As output, BONAMI-S produces a problem-dependent master library. Thus, in the SCALE sequences, it is always used in conjunction with NITAWL-S which, even if no resonance processing is done, converts the master library into an AMPX working library.
- **ICE-S** is used primarily in SCALE to mix microscopic cross-section data from an AMPX working library to produce macroscopic data in one of several available formats.
- **COUPLE** is used in the SCALE analytic sequences to update ORIGEN-S libraries with flux-weighted cross sections provided by XSDRNPM. COUPLE uses the multigroup fluxes from XSDRNPM to calculate THERM, RES, and FAST, the spectral parameters used in ORIGEN-S. This calculation is done in a manner that is consistent with the use of the data in the ORIGEN-S library for those nuclides that are not being updated with weighted cross sections from XSDRNPM. COUPLE can also be used to create and/or update binary libraries for ORIGEN-S.
- **KENO IV** and **KENO V.a** are multigroup Monte Carlo codes employed to determine effective multiplication factors ( $k$ -eff) for multidimensional systems. The basic geometrical bodies allowed for defining the model are cuboids, spheres, cylinders, hemispheres, and hemicylinders. KENO V.a differs from KENO IV in that it (1) has an enhanced geometry package that allows arrays to be defined and positioned throughout the model, (2) has a  $P_n$  scattering treatment, (3) allows extended use of differential albedo reflection, (4) can generate printer plots for checking the input model, (5) supergroups energy-dependent data, (6) has an improved restart capability, and (7) allows origin specifications to be made for spheres, cylinders, hemicylinders, and hemispheres.
- **XSDRNPM-S** is a one-dimensional discrete ordinates transport code for performing neutron or coupled neutron-gamma calculations. The code has a variety of uses within SCALE: preparation of cell-averaged cross sections for subsequent system analysis, one-dimensional criticality safety and radiation shielding analysis, and generation of a neutron spectrum used to develop spectral parameters for ORIGEN-S (via COUPLE). The latest use of XSDRNPM is to generate one-dimensional adjoint functions for use in preparing biasing parameters for MORSE-SGC.
- **MORSE-SGC/S** is the SCALE version of the MORSE family<sup>6</sup> of Monte Carlo programs for radiation shielding analysis. It utilizes the MARS geometry system with combinatorial geometry. This geometry allows ease in modeling multiple-array systems by using a repeating array feature along with an unlimited (except by computer core) array-nesting capability. MORSE-SGC/S incorporates supergroup cross-section storage and tracking.

- **XSDOSE** is a code used in conjunction with **XSDRNPM** to compute the  $n/\gamma$  flux and the resulting dose at various points outside a finite cylinder or sphere. It may also be used to compute the flux and/or dose at various points due to a finite rectangular surface source or a circular disc. The code assumes that the outgoing angular flux distribution on the rectangle, cylinder, sphere, or disc is independent of position and that the surrounding media is a void. Unlike previous codes, the numerical technique employed in **XSDOSE** is suitable for points on, close to, or far from the source.
- **ORIGEN-S** is an updated version of the **ORIGEN** code<sup>7</sup> with flexible dimensioning and free-form input processing. One of the primary objectives in developing **ORIGEN-S** was that the calculations be able to utilize multi-energy-group neutron flux and cross sections in any group structure. Utilization of the multigroup data is automated via the **COUPLE** code. **ORIGEN-S** performs point depletion and decay analyses to obtain isotopic concentrations, decay heat source terms, and radiation source spectra and strengths for use in subsequent system analyses.
- **HEATING6** is a finite-difference code for solving general multidimensional heat conduction problems. Steady-state and/or transient problems can be analyzed using a variety of boundary condition and heat generation specifications. **HEATING6.1**, which will be released as part of **SCALE-4**, provides for direct input of mode-to-mode connectors that allow multidimensional radiative heat transfer to be modeled.
- **JUNEBUG-II** is a plotting program that allows three-dimensional plotting of models for **KENO IV** and **MARS/MORSE** geometry input.
- **HEATPLOT-S** and **REGPLOT6** are graphics support programs for the **HEATING6** program. Using stored temperatures from a **HEATING6** analysis, **HEATPLOT-S** can plot a variety of temperature profiles as functions of time or space. **REGPLOT6** allows graphical verification of the **HEATING6** geometry input by plotting the region boundaries of one-, two-, or three-dimensional models.
- **PLORIGEN** is a new module of **SCALE** that allows plots of **ORIGEN-S** output. Isotopic concentrations, decay heat, and radiation source spectra can all be plotted in selected units and over selected decay time intervals. **PLORIGEN** will be available publicly as part of **SCALE-4**.

### 1.2.2 Data Base

The data base (see Fig. 1.1) available with the **SCALE** system includes the cross-section libraries, a standard composition library, data libraries required by **ORIGEN-S**, and a thermal property library. In addition, a library of **SCALE** input data required for analyzing important critical experiments is included.

Cross Sections. There are eight cross-section libraries released with the **SCALE-3** package. The user selects the desired library by specifying the appropriate alphanumeric name in the input. The libraries are all in **AMPX** master format. The **218GROUPNDF4** library is based on **ENDF/B-IV** data. It has 72 thermal groups and is suitable for criticality safety analysis of thermal systems. The group structure was chosen to fit the cross-section variation and reaction thresholds of light and intermediate nuclides, to bracket the major resonance levels of intermediate and heavy nuclides, and to "march over" the thermal resonances in fuel nuclides.<sup>8</sup> After extensive study, a 27-group format with 13 thermal groups was selected as an adequate broad group structure for collapsing the 218-group library. The resulting **27GROUPNDF4** library has been validated through the calculation of critical experiments containing the fuel, structural materials, and neutron absorbers commonly found in cask and storage pool designs.<sup>9</sup> An extension of this library (**27GROUPSHLD**) contains a large number of fission product nuclides (some with non-**ENDF/B-IV** data). This extended library is used for depletion analyses and for criticality analyses where fission products are considered. The other criticality libraries are the **HANSEN-ROACH** and **123GROUPMTH** libraries. The Hansen-Roach Bondarenko library includes

all of the original Hansen-Roach 16-group data supplemented by ENDF/B-IV data for nuclides not present in the original library. The 123-group AMPX library contains data originally compiled for the GAM-II and THERMOS programs. Although these data are old, the library is known to be quite effective in the analysis of systems containing light-water-reactor fuel. The three SCALE libraries available for shielding analyses include a 27N-18COUPLE library, a 22N-18COUPLE library, and an 18GROUPGAMMA library. The 27n-18 $\gamma$  group library uses the neutron data of 27GROUPNDF4 and gamma-ray production data of ENDF/B-IV. The 18GROUPGAMMA library uses the same gamma-ray interaction data of the 27n-18 $\gamma$  library. The 22N-18COUPLE library has been included for shielding calculations because of its fairly wide use in the past. It is derived from the data of Straker and Morrison.<sup>10</sup> This library contains no resonance data and no temperature-dependent data.

Standard Compositions. The standard composition library is used by the Material Information Processor in developing nuclide atom densities. The library contains data on each nuclide which are used in developing the input for the resonance processors and for the mesh-spacing algorithms used with the deterministic codes. The library consists of a standard composition directory, a standard composition table, an isotope distribution directory, an isotope distribution table, and a nuclide information table. The physical data contained in the library are taken from standard references. A single nuclide identification scheme is common to both the standard composition library and all of the cross-section libraries.

ORIGEN-S Libraries. The data libraries available for use by ORIGEN-S include nuclear data libraries, photon yield libraries, and a comprehensive, up-to-date photon library. All of these libraries exist in both card-image and binary form. Burnup-dependent cross-section libraries are created via standard sequences available in SCALE.

Thermal Properties. The thermal properties library included in SCALE was developed at Lawrence Livermore National Laboratory<sup>11</sup> and is made available to provide HEATING6 users with a suitable alternative to specifying their own thermal data.

CESAR. The Criticality Experiment Storage and Retrieval program assesses a data file which contains critical experiment descriptions and input for their analysis via SCALE. Nearly 450 critical experiments are currently included in the data base. The CESAR program and data are currently being updated and modified to act as an interactive information program on the Nuclear Criticality Information System (NCIS) at Lawrence Livermore National Laboratory. The updated CESAR program and data will be readily available to the criticality safety community via NCIS, thus the standard CESAR may be removed from SCALE with the SCALE-4 release.

### 1.2.3 Control Modules

As noted earlier, the modular structure of SCALE allows back-to-back execution of the functional modules to perform a system analysis. However, a variety of control modules have been developed that automate and standardize various analytic sequences. The SCALE system control module input format has been designed to minimize input errors. Upon processing the user-specified input, the SCALE system control modules immediately print an input check list in which the user (or reviewer) can easily establish that the input describes the system to be analyzed. Where appropriate, parameters are entered in an alphanumeric form. Also, associated parameters, whether alphanumeric, integer, or floating are entered in their relative logical order within a single group. For example, all the input variables required to use a standard composition are entered together.

The control modules shown in Fig. 1.1 are those developed to date. The acronyms CSAS, SAS, and HTAS stand for Criticality Safety Analysis Sequences, Shielding Analysis Sequences, and Heat Transfer Analysis Sequences, respectively. Although the control modules are typically designated by their principal analytic sequence, note that more than one sequence may exist within a control module.

- **CSAS1/CSAS2** are the analytic sequences contained in the initial SCALE control module. CSAS1 performs data processing and criticality safety analysis on systems that can be adequately modeled in one-dimensional geometries. The execution path includes the functional modules BONAMI-S, NITAWL-S, and XSDRNPM-S. CSAS2 performs data processing and criticality safety analysis on systems which must be modeled in three-dimensional geometry. The execution path includes BONAMI-S, NITAWL-S, XSDRNPM-S (if lattice cell cross-section processing is specified), and KENO IV.
- **CSAS4** is the most recent control module for criticality analysis. The analytic sequence designated by =CSAS25 follows the execution path BONAMI-S, NITAWL-S, and KENO V.a. The sequence =CSAS4 follows the same execution path but repeats the KENO V.a. analysis as part of a search for the pitch that provides the maximum or specified k-eff value. The above sequences are modified to include cell-weighting with XSDRNPM-S if =CSAS2X or =CSAS4X is designated. Some other sequences are also provided which use BONAMI-S, NITAWL-S, XSDRNPM-S, and ICE-S in various execution paths to create problem-dependent cross-section libraries for subsequent use in stand-alone functional module execution.
- **SAS1** is a new control module for performing data processing, radiation shielding analysis, and dose evaluation on systems which can be adequately modeled in one-dimensional geometries. The execution path includes BONAMI-S, NITAWL-S, XSDRNPM-S, and XSDOSE. Cell weighting is also allowed if =SAS1X is specified rather than =SAS1. This control module will be made available in SCALE-4.
- **SAS2** is a control module that processes fuel assembly cross sections, computes photon and neutron source spectra and evaluates dose rates from spent fuel casks by a one-dimensional transport shielding analysis. The execution includes: repeated passes through BONAMI-S, NITAWL-S, XSDRNPM-S, COUPLE, and ORIGEN-S for cross-section processing and fuel burnup; radiation source computations; the radial shipping cask shielding analysis applying the calculated spent-fuel composition and sources; and the final determination of dose rates by XSDOSE from the angular flux leakage.
- **SAS3** performs data processing and radiation shielding analysis on systems for which the user specifies the radiation source distribution and which must be modeled in three-dimensional geometry. The execution path includes NITAWL-S, XSDRNPM-S (if lattice cell cross-section processing is specified), ICE-S, and MORSE-SGC/S.
- **SAS4** is a new control module that allows calculation of radiation doses exterior to a transport/storage cask via a three-dimensional Monte Carlo analysis. The sequence execution path includes: BONAMI-S, NITAWL-S, and XSDRNPM-S (if lattice cell geometry is specified) for cross-section processing; XSDRNPM-S for evaluation of the adjoint flux used by the sequence for automatic generation of Monte Carlo biasing parameters; and MORSE-SGC/S for the radiation transport and dose calculation. The SAS4 module will be released publicly as part of SCALE-4.
- **HTAS1** is a control module that generates the necessary HEATING6 input and automatically manipulates the module to perform a two-dimensional (R-Z) thermal analysis for a specific class of shipping containers during the normal, fire, and post-fire conditions specified by the licensing regulations.

#### 1.2.4 Other SCALE Components

In the lower box of Fig. 1.1 are listed several of the SCALE components which cannot be readily classified as modules or data bases. The Material Information Processor is a library of subroutines assessed by all the control modules except HTAS1 (also, the CSAS1/CSAS2 control modules use an older and slightly different version). The processor reads the materials-related information, accesses the SCALE system standard compositions library, and calculates isotopic atom densities. It also prepares

the physics parameters required by the resolved resonance analysis in the NITAWL-S module. For example, the Material Information Processor includes a calculation of the Dancoff factor for problems in which a lattice cell geometry option has been specified.

The MARS geometry package is also a set of subroutines developed for use with the MORSE-SGC code system. The MARS package was developed to allow easy input specification of combinatorial geometry models containing multiple and/or nested arrays.

The Subroutine Library available in SCALE contains a number of useful subroutines that can be accessed by the functional or control modules. The SCALE free-form reading routines, a random number generator, and timing routines are examples of the routines in the library.

As noted earlier, the system driver is the foundation upon which the modular features of SCALE are based. The driver is an assembler language module developed to ensure that minimum core and running time are used in the SCALE analyses.

### 1.3 SUMMARY

As evidenced by Fig. 1.1 and the above discussion, the SCALE system is quite large and has a wide range of capabilities. The SCALE modules used for preparing problem-dependent cross-section libraries and performing criticality safety analyses are well established and in fairly routine use by much of the U.S. and foreign criticality safety communities as the primary computational tool or as a backup/review tool. Applications extend well beyond cask analysis to the areas of fuel reprocessing and handling facilities, storage facilities, and critical experiment design and analysis as well as selected reactor applications. The use of SCALE in performing shielding and heat transfer analysis is increasing. The new release of SCALE-4 with the new shielding and thermal modules will further enhance the versatility, usability, and portability of the system for these types of system analysis.

## 2. CROSS-SECTION PROCESSING TECHNIQUES

A major objective in the development of the SCALE system has been the standardization of problem-dependent cross-section data. The purpose of this section is to provide a brief summary of the SCALE features that lead to this standardization. These include standard neutron and coupled neutron-photon cross-section libraries in the AMPX master library format and a Standard Composition Library of material-dependent data. In addition to these standard data sources, other SCALE features pertinent to the standardization objective include the Material Information Processor which is applied in the analytical sequences (CSAS1, SAS1, etc.) to prepare the input specifications for those functional modules which perform the problem-dependent cross-section processing. Finally, the automated use of these functional modules (BONAMI-S, NITAWL-S, XSDRNPM-S, ICE-S) with fixed specifications of the optional input data also enhances standardization.

In summarizing these features, the scope of this section will be limited to a review of the data sources, a discussion of the analytical models applied in the functional modules, and a listing of appropriate references for more-detailed information.

### 2.1 REVIEW OF CROSS-SECTION LIBRARIES

#### 2.1.1 Criticality Libraries

Because of its performance and ease of use, the 16-group Hansen-Roach cross-section library<sup>12</sup> has been a popular favorite for criticality safety applications for many years. Its performance for low-enriched uranium systems was greatly improved by the modifications done to the <sup>238</sup>U resonance data by Knight and Whitesides at Oak Ridge. These modifications are discussed in detail in Sect. C1.C.13 of the SCALE Manual. Briefly, the <sup>238</sup>U-capture cross sections were varied in the resonance range (groups 8-12) until calculated values of the infinite medium multiplication agreed well with those derived from experiment.<sup>13,14</sup> This version became known as the Knight-Modified Hansen-Roach Library.

Several aspects of the original library should be noted. Resonance scatter, Doppler broadening, and thermal upscatter were not treated. Two data sets were provided for hydrogen, one weighted by a 1/E slowing-down spectrum, and the other weighted by a fission neutron spectrum. For light nuclides, the scattering cross sections are given in a first-order Legendre expansion with a higher-order correction to both the zero and first-order components. This correction has been observed to emphasize the forward-scattering phenomena in hydrogen.

Prior to incorporation into the SCALE system, the Knight-Modified Hansen-Roach Library was reformatted into the Bondarenko formalism of shielding factors to be applied against cross sections representing infinite dilution. This reformatting of the data provides for subsequent automated resonance self-shielding with BONAMI-S, including the determination of a heterogeneity correction to the background cross section. Also, for a number of nuclides missing in the original compilation, 16-group ENDF/B-IV data were added to the library in order to fill out the list of available materials (e.g., concrete).

The 218-group Criticality Safety Reference Library<sup>15</sup> was developed for the Nuclear Regulatory Commission utilizing all of the general-purpose files in the ENDF/B-IV compilation. It served as the reference source for an extensive series of tests<sup>16</sup> through which the 27-energy group structure was identified. Both the 218- and 27-group versions of this data were designed to utilize the Nordheim resonance shielding treatment of NITAWL-S. Each of the libraries has a P<sub>3</sub>-scattering expansion order and treats thermal upscatter to 3 eV. A special version of the 27-group library (27GROUPSHLD), which includes additional data for fission products, is available for application in burnup studies.

The 123-group GAM-THERMOS library was named after the popular early codes<sup>17,18</sup> from which the 90 epithermal and 33 thermal group structures were adapted. It was originally developed at Oak Ridge as part of the Molten Salt Reactor Program. Generally, the data came from mixed sources: some GAM-II data, some FLANGE thermal data, and some early compilations of ENDF/B. This library also utilizes the Nordheim treatment, has a  $P_3$ -scattering expansion order, and treats thermal upscatter. It contains many of the fission products required for analysis of reactor control.

Various levels of effort have been taken in the validation of the Knight-Modified Hansen-Roach, the 123-group GAM-THERMOS, and the 27-group ENDF/B-IV libraries. Westfall and Knight<sup>9</sup> applied all three libraries in the analysis of some 70 experiments performed to simulate various aspects of nuclear fuel shipping casks. More recently, extensive validation studies for low-enriched<sup>19</sup> and high-enriched<sup>20</sup> systems have been performed. Generally, the libraries perform acceptably well, the ENDF/B-IV data perform worst for low-enriched and best for high-enriched systems.

### 2.1.2 Shielding Libraries

Presently, there are two standard cross-section libraries available within the SCALE system for performing radiation shielding analyses. The 22 neutron-18 gamma group library<sup>10,21</sup> was developed for the Atomic Energy Commission with ENDF/B-II data. The neutron data were originally generated with SUPERTOG in a 104-group structure. Then, the 22-group data were obtained by averaging over a 104-group spectrum calculated with ANISN for a uranium-water mixture. The library has a  $P_3$ -scattering expansion order. It does not have provision for problem-dependent resonance shielding or thermal upscatter. The original library was supplemented with ENDF/B-III and -IV data and released by the Radiation Shielding Information Center as DLC-23/CASK in March 1975. The library has been used in a wide variety of applications since that time.

The other standard shielding library in SCALE is the coupled 27 neutron-18 gamma group library developed from the 218-group ENDF/B-IV criticality library described above. This is an unusual shielding library in that it does treat resonance shielding and thermal upscatter on a problem-dependent basis. Generally, these processes are not considered to be important for shielding applications. However, for certain situations, such as neutron multiplication in water-flooded casks or secondary gamma generation due to thermal neutron capture, the additional capability can be significant. A recent study also indicates that adequate resonance self-shielding is very important for iron-shielded spent fuel sources.<sup>22</sup> The neutron group structure is sparse in the high MeV range. Thus, the library should not be applied in the analysis of accelerator or fusion-energy devices. The 18-group gamma-ray cross sections were generated from the ENDF/B-IV data compilation through the application of the AMPX modules LAPHNGAS and SMUG. The gamma cross sections include a  $P_3$ -scattering expansion order. Uncoupled neutron and gamma-ray versions of this library also exist.

Many of the standard SCALE libraries include a variety of dose factor data. Table 2.1 shows the response functions available for the various libraries. The SCALE shielding analytical sequences automatically select the ANSI Standard Dose Factors<sup>23</sup> for dose quotations.

## 2.2 REVIEW OF THE STANDARD COMPOSITION LIBRARY

The Standard Composition Library is a compilation of physical properties data for the elements, their isotopes, various chemical compounds, metallic alloys along with information that summarizes available cross-section data (resonance, thermal-scattering kernels, etc.) by isotope and cross-section library. The physical properties data are taken from standard reference sources such as the "Handbook of Chemistry and Physics"<sup>24</sup> and the "Chart of the Nuclides."<sup>25</sup>

Table 2.1. SCALE standard response function ID numbers

| ID no. | Response Function  | Availability <sup>a</sup> |
|--------|--|---------------------------|
| 9001   | Hurst dose factors (mrad/h)/(neutrons/cm <sup>2</sup> /s)  | 1,5                       |
| 9002   | Snyder-Neufeld dose factors (mrad/h)/(neutrons/cm <sup>2</sup> /s)   | 1,5                       |
| 9026   | Snyder-Neufeld conversion from flux to biological dose (mrem/h)/(neutrons/cm <sup>2</sup> /s)                | 1,5                       |
| 9027   | Henderson conversion from neutron flux to absorbed dose rate in tissue (rad/h)/(neutrons/cm <sup>2</sup> /s) | 1,5                       |
| 9028   | Straker-Morrison conversion factors (mrem/h)/(neutrons/cm <sup>2</sup> /s)                                   | 1                         |
| 9029   | ANSI standard neutron flux-to-dose-rate factors (rem/h)/(neutrons/cm <sup>2</sup> /s)                        | 1,2,3,5                   |
| 9501   | Straker-Morrison conversion factors (mR/h)/(photons/cm <sup>2</sup> /s)                                      | 1,4                       |
| 9502   | Henderson conversion factors (rad/hr)/(photons/cm <sup>2</sup> /s)   | 1,4                       |
| 9503   | Claiborne-Trubey conversion factors (rad/h)/(photons/cm <sup>2</sup> /s)                                     | 1,4                       |
| 9504   | ANSI standard gamma-ray flux-to-dose-rate factors (rem/h)/(photons/cm <sup>2</sup> /s)                       | 1,2,3,4                   |

<sup>a</sup>Reference numbers of cross-section libraries : 1 - 22N-18COUPLE; 2 - 27N-18COUPLE; 3 - 27GROUPEHLD; 4 - 18GROUPEGAMMA; and 5 - 123GROUPEMTH.

Section M8.2 of the SCALE manual provides a useful summary of the Standard Composition Library. This section includes four tabulations. The first table gives a brief description of each of the approximately 300 standard compositions, including the constituents of compounds by chemical formula, and of alloys by weight percent. The second table lists the theoretical densities of the standard compositions, their constituent nuclides, and their availability in the various cross-section libraries. The third table lists the available fissile solutions that the user can specify by heavy metal density and acid molarity. The fourth table summarizes information on which elements may have their isotopic compositions specified by the user.

The Standard Composition Library is generated and updated by a computer program called COM-POZ. Since it is structured as a directly addressable data set, its implementation on non-IBM equipment may pose special problems for new SCALE users. However, the FORTRAN 77 version available in CCC-475/SCALIAS or with SCALE-4 should not present a problem to users. The Standard Composition Library and the user-specified input information constitute the principal sources of data used by the Material Information Processor in preparing standardized input for the SCALE analytical sequences.

### 2.3 REVIEW OF CROSS-SECTION PROCESSING TECHNIQUES

Within the SCALE system analytical sequences, cross-section processing always begins with an AMPX master library and always ends with an AMPX working library. The objective is to treat those aspects of the problem where space-energy coupling produces significant variations in the neutron spectrum such that broad-group, spatially averaged constants can be obtained for calculating reactions rates on a macroscopic basis. To this end, various solutions are developed for the time-independent form of the neutron transport equation.

In performing resonance shielding analyses (BONAMI-S, NITAWL-S), an approximate spatial treatment is applied in performing a detailed energy slowing-down calculation. In performing a subsequent spatial weighting analysis (XSDRNPM-S), broad energy group constants are applied in performing a detailed space-angle calculation of the neutron spectrum over the entire energy range. Then, spatial weighting can be performed over fuel pins, lattice cells, or even larger regions.

The analytical models and capabilities of each of these functional modules is briefly described.

### 2.3.1 The BONAMI-S Module

BONAMI-S performs resonance shielding through the application of the Bondarenko shielding factor method. As input, the program requires the presence of shielding factor data on the AMPX master library interface. As output, BONAMI-S produces a problem-dependent master data set. Thus, in the SCALE sequences, it is always used in conjunction with NITAWL-S, which converts the problem-dependent data set into an AMPX working library.

Presently, the only standard SCALE system cross-section library containing shielding factors is the Knight-Modified Hansen-Roach 16-group set. However, new cross-section libraries generated from recent versions of ENDF/B include shielding factors for the unresolved resonance energy range and for those resolved resonances whose parameters are not specified in the single-level Breit-Wigner formulation contained in NITAWL-S. After sufficient validation, these libraries will probably become available in SCALE.

For each energy group, the shielding factors are tabulated as functions of two parameters: background cross section and nuclide temperature. The essential tasks performed by BONAMI-S are the determination of the appropriate background cross section, interpolation in the shielding factor tables, and application of the shielding factors against reference unshielded values of the groupwise cross sections to produce the problem-dependent data.

The fundamental theory applied in the shielding-factor method rests upon simplified slowing-down approximations for the absorber material and the treatment of external sources through elementary integral transport approximations. In both the Bondarenko and Hansen-Roach derivations of the methodology, the dependence of the shielding factors on the background cross sections is initially developed for an infinite medium. The original derivations included the narrow resonance approximation for the calculation of slowing-down sources. However, more recent methodology includes slowing-down calculations. The kinematics of neutron scattering with the resonance nuclide are explicitly treated. Under this approach, the shielding factor methodology becomes closely related to the Nordheim Integral Treatment.

For multizone systems, the equivalence theorem relating homogeneous and heterogeneous systems is invoked to modify the background cross section to include the effect of external sources. This modification is called the escape cross section which, for convex bodies, is obtained from the Wigner rational approximation,  $\sigma_e = 1/(\bar{\ell}N)$ , where  $\bar{\ell}$  is the mean chord length and  $N$  is the nuclide's number density. In lattice cell geometries, the escape cross section is reduced by a Dancoff factor to account for absorption in neighboring cells. Escape cross sections for moderator regions are obtained through two-region reciprocity relations.

In addition to the homogeneous option, BONAMI-S, through various Dancoff factor formulations, will treat symmetric and asymmetric slab cells and cylindrical cells in either hexagonal or square lattices. Also, for cylindrical cells, the effects of cladding around the absorber can be treated. Since the escape cross sections depend on the total cross sections for each zone, which themselves are subject to

shielding, an iterative solution is required to converge the determination of the background cross sections. For interpolating the shielding factor data, a novel interpolation scheme is used in BONAMI-S. This scheme avoids many of the problems of the Lagrangian schemes widely employed in other programs.

Assuming an adequate treatment of the slowing-down phenomena in the generation of the shielding factors, BONAMI-S can accurately produce cross sections suitably shielded for a wide variety of applications.

### 2.3.2 The NITAWL-S Module

The NITAWL program was originally developed as part of the AMPX cross-section processing system to perform resonance shielding and cross-section format conversion. Resonance shielding can be done with several analytical models, the most rigorous of which is the Nordheim Integral Technique. Nordheim's methods, as programmed in NITAWL-S, have been extensively enhanced. NITAWL-S is applied in all SCALE system analytical sequences which include problem-dependent cross-section processing.

Nordheim's method involves a solution of the integral form of the transport equation for the detailed spectral variation of the neutron flux across the energy range of each resonance. The slowing-down source, due to neutron scatter with the resonance nuclide as well as with two admixed moderator nuclides (non-absorbing), is calculated explicitly over a fine mesh in the lethargy variable. At each point in this mesh, a neutron balance is performed to determine the neutron flux for subsequent use in spectral weighting and for the calculation of down-scattered sources to successive points.

Spatial transport in Nordheim's method is treated with first-flight escape and transmission probabilities for a two-region model in cylindrical, spherical, or slab geometry. The inner region contains the absorber nuclide and the admixed moderators. The outer region, if present, is assumed to contain a non-absorbing moderator with an associated  $1/E$  variation of the slowing-down flux and a Maxwellian thermal neutron distribution. Escape probabilities for the inner region are determined under the assumption of uniform, isotropic sources. Escape probabilities for the outer region are obtained with two-region reciprocity relationships. These probabilities are modified for lattice-cell geometry by a Dancoff factor which accounts for transmission from the inner region through the moderator to neighboring absorbers. Transmission through the absorber region is treated with a "grayness" factor.

Instead of performing an explicit calculation of the slowing down sources, the user has the option of specifying the narrow resonance and infinite mass approximations for the absorber nuclide and the asymptotic flux approximation for the admixed moderators. The narrow resonance and asymptotic flux approximations essentially state that the flux in the slowing-down range is unperturbed by the resonance nuclide and therefore has an asymptotic form, either  $1/E$  or Maxwellian. These forms allow analytic evaluations of the slowing-down source integrals. The infinite mass approximation states that there is no neutron energy loss due to scattering with the resonance nuclide. For typical cases involving uranium-238, the narrow resonance approximation seriously overestimates the absorption cross section due to the broad, predominantly absorbing levels and it seriously underestimates the absorption cross sections due to the broad, predominantly scattering levels. The infinite mass approximation does somewhat better. In the SCALE system analytical sequences, the Nordheim Integral Technique is generally applied.

In addition to down-scattered sources and escape probabilities, point values of the Doppler broadened resonance cross sections must be determined prior to each neutron balance calculation. The cross sections are reconstructed from the resonance parameters with the single-level Breit-Wigner formulation as specified in the ENDF/B documentation.

Given the basic strategy in Nordheim's method of treating one resonance at a time, there is no opportunity to treat resonance interference and overlap effects. Also, it is necessary to make certain "wing corrections" in the process of producing group-averaged values. These corrections are done with analytic flux assumptions such as the narrow resonance and infinite mass approximations.

In the unresolved resonance range, the NITAWL-S algorithm is essentially the same as that developed for the original GAM program. It involves the narrow resonance approximation, averaging over the Porter-Thomas distribution of reduced neutron widths and treating spatial dependence with Wigner's rational approximation. The 123-group GAM-THERMOS library is the only SCALE system library which applies this treatment.

The version of NITAWL-S to be released with SCALE-4 contains new procedures for incorporating the wing corrections into the group-dependent background data. Also, the unresolved resonance treatment for the 123-group GAM-THERMOS library is done with the Bondarenko method. Thus, the latest version of NITAWL prepared for SCALE-4 no longer performs wing corrections or unresolved resonance processing.

Several extensions to Nordheim's method have been implemented into the algorithm contained in NITAWL-S.

1. Elements containing more than one isotope can be treated.
2. Self-shielding is applied to resonance scattering. Transfer matrices are adjusted.
3. P-wave as well as S-wave levels can be treated.
4. The asymptotic flux approximation in the thermal energy range is assumed to have a Maxwellian distribution in energy.
5. A refined procedure for generating the energy mesh over which reaction rates are integrated has been developed.
6. The user has the option of averaging the multigroup constants over the absorber region or with a cell-averaging formulation.

Given the constraints of the geometric model and the applicability of the isolated resonance treatment, the Nordheim method as programmed in NITAWL-S has proven to be a very efficient and effective procedure for performing resonance shielding.

### 2.3.3 The XSDRNPM-S Module

The XSDRNPM-S module is a highly evolved one-dimensional discrete-ordinates transport program that has a wide variety of features. Its origins trace back to the popular ANISN program which pioneered the treatment of anisotropic scattering in discrete-ordinates calculations. XSDRNPM-S is capable of performing neutron or coupled neutron-gamma calculations with the scattering anisotropy represented to any arbitrary order. The primary emphasis in the solution algorithm is on the accurate calculation of detailed spectral variations. However, with sufficient angular quadrature and spatial mesh specifications, highly precise solutions to one-dimensional transport problems are obtained. For simpler systems, alternative solutions with diffusion, infinite medium and  $B_n$  (buckling loss) theories can be specified.

XSDRNPM-S is applied in a number of SCALE analytical sequences. It is used to cell-weight cross sections in both criticality and shielding analytical sequences. In CSAS1, XSDRNPM-S is also used to determine the system multiplication factor. In SAS1, it provides the angular fluxes for a subsequent

dose determination with XSDOSE. In SAS4, XSDRNPM-S is used in the adjoint mode to produce biasing parameters for a subsequent MORSE Monte Carlo analysis.

The finite-differencing in XSDRNPM-S is done with the weighted diamond-difference model with weighting parameters chosen on the basis of experience with the DOT IV code.<sup>26</sup> By default, angular quadrature sets are calculated in an automatic fashion for the appropriate one-dimensional geometry. Scattering expansion can be treated to whatever order is provided in the cross-section sets.

Boundary conditions on the angular fluxes can be specified as vacuum, reflected, periodic, white or user-supplied albedos. Also, transport in the transverse direction can be approximated with geometric buckling losses or with void streaming corrections.

Two types of fixed sources can be specified. Boundary sources are angle- and group-dependent. Volumetric sources specified by spatial interval are group-dependent and isotropic in angular variation.

Convergence in XSDRNPM-S is determined by tests on several quantities. The point values of the scalar fluxes must vary by less than a prescribed amount between outer iterations. Also, the ratio of source terms and scattering rates (up and down in energy) between outer iterations must converge. Provision is made for banding thermal groups and thereby accelerating upscatter convergence.

Cross-section output options are extensive. In addition to group collapsing, spatial weighting can be performed by cell, zone, region, or "inner cell" prescriptions. Either inscatter or outscatter formulations with an option of five current specifications may be used to obtain transport cross sections. Cross-section libraries can be output in ANISN (BCD or Binary), CCCC ISOTXS, or AMPX working formats.

In addition to the parameters and data described above, XSDRNPM-S produces extensive balance tables, and it may be used to produce reaction rates by nuclide with a variety of spatial and energy group options. It is an efficient and highly evolved program which performs several important functions in SCALE.

#### 2.3.4 The ICE-S Module

The purpose of the ICE-S module is to read problem-dependent microscopic data from an AMPX Working Library, mix macroscopic constants on the basis of the nuclide number densities specified for the various problem material zones, and produce macroscopic libraries in one of several formats for subsequent use in systems analysis. In addition, ICE-S provides five options for producing material-dependent fission neutron spectra, and it can interpret the data in scattering transfer arrays to produce the group-to-group scattering probabilities required in Monte Carlo analyses.

The simplest option for picking the fission spectrum involves summing the values of  $\nu\Sigma_f$  for each fissionable nuclide and selecting the spectrum for that nuclide with the highest sum. The second option allows the user to input a groupwise flux spectrum to be folded into this procedure. The third option allows the user to specify a fission-1/E-Maxwellian spectrum with arbitrary coefficients and energy ranges. The fourth option allows the selection of a typical fast breeder reactor flux spectrum. The final option triggers the use of the weighting functions (MT = 1099) originally used to generate the multi-group values from ENDF/B data.

The output library options for the macroscopic data include the AMPX Working Library, the standard and group-independent ANISN, and the Monte Carlo processed library formats. Advantages of applying ICE-S in the SCALE analytical sequences include reducing computer storage requirements for the systems analysis programs and providing additional flexibility in preparing data for a number of material mixtures.

## 2.4 AUTOMATED PROCEDURE FOR CROSS-SECTION PROCESSING

The first step activated by the criticality and shielding analysis sequences is to access the Data Preprocessor and Material Information Library which were developed to centralize the procedure for automated cross-section processing. The Data Preprocessor and Material Information Library make up a subroutine library referred to in the SCALE package as MIPLIB. This subroutine library is used by all the sequences of the CSAS4 control module and all the shielding analysis sequences. However, the first SCALE control module --- the CSAS1/CSAS2 control module --- has built-in routines that perform the basic functions of MIPLIB, but does not use MIPLIB directly. In fact, many of the MIPLIB routines were lifted from the CSAS1/CSAS2 program and subsequently altered or updated to add additional features. The input data for both processors are very similar. Their functions are the following:

1. read the user-specified input on material compositions and geometry pertinent to cross-section processing;
2. access information from the Standard Composition Library to determine nuclide atom densities and resonance data; and
3. establish the input data and execution sequence for those functional modules involved in cross-section processing.

The Data Preprocessor carries out operations to prepare and check data that will be used by the functional modules which are activated for the cross-section portion of the sequence. The Material Information Processor reads and processes the composition and geometric information used for calculating material number densities and the parameters required for the cross-section resonance treatment. The composition and geometric information is input in engineering terms, with only the detail necessary to properly define the problem. Keywords describing the system, as well as associated numerical data, are used when they are appropriate. Commonly used values of some of the parameters may be obtained by default, or may be easily changed to the quantities needed. After all of the description has been entered, the data arrays necessary to run BONAMI-S, NITAWL-S and XSDRNPM-S are prepared. A flexibly dimensioned array is used to store all of the information.

All materials used in the composition description must be included in the Standard Composition Library available with SCALE. The library gives full information about each composition, such as the amount of each element in the material, the density, the element's cross-section library identification number, etc. This information is used to calculate number densities for each isotope and to prepare some of the resonance data. Resonance data (e.g., Dancoff factors) are calculated for use by NITAWL-S using the material and geometric descriptions.

All the sequences use either NITAWL-S to do resonance self-shielding of cross-sections using the Nordheim treatment or BONAMI-S to process cross sections using Bondarenko self-shielding factors. Input data for XSDRNPM-S is prepared by the Material Information Processor whenever cell-weighted cross sections are required for the subsequent systems analysis. The cross sections obtained via this pass through XSDRNPM-S allow a homogeneous representation of the geometric cell specified in the processor input.

Three types of basic geometry descriptions can be specified by alphanumeric keyword:

- **INFHOMMEDIUM** is used for an infinite homogeneous medium. The cross sections are treated as if each mixture is infinite. Thus, the self-shielding calculations will not account for any geometrical effects.
- **LATTICECELL** is used when the geometry can be described as a lattice. It is especially suited for arrays of cylindrical rods or spherical pellets. The use of **LATTICECELL** requires the entry of

additional geometry information which describes the unit cell. When the problem consists of an array of fuel bundles or similar geometry, the cross sections are corrected for both geometric and resonance self-shielding. The Material Information Processor utilizes information on the lattice type, the lattice pitch, and the moderator total cross section to obtain the Dancoff factor by numerical integration with a program called SUPERDAN.<sup>27</sup> This determination of the Dancoff factor and its utilization in input specifications is an example of the automated procedure for cross-section processing in SCALE.

- **MULTIREGION** may be used to define a geometric configuration that is more complicated than that allowed by **LATTICECELL**. It can also be used for a system involving large geometric regions where geometry effects may be minimal. The cross sections utilized in the unit cell are corrected for resonance self-shielding, but the geometric correction uses a Dancoff factor of 0, thus ignoring the effects due to a lattice geometry.

The geometry input to the Material Information Processor is used to prepare appropriate resonance data for the designated materials. Mixtures not included in the simple geometric description have resonance processing performed with infinite homogeneous data. The new MIPLIB package released with SCALE-3 optionally allows the user to override the default resonance data for any mixture and input a simple geometry description by utilizing the **MORE DATA** option. Note, however, that when this option is used, the Dancoff factor for the mixture is not automatically produced, but must be input by the user. An outline of the Material Information Processor data and an example of its specification in a sample problem are given in Figs. 2.1-2.3.

## 2.5 SUMMARY

This section has reviewed the current cross-section libraries and data processing techniques employed within the SCALE system. The libraries and procedures used are common to all of the neutronic analysis modules found in SCALE and provide a sound basis for automation and standardization within the sequences.

| Data position | Type of data                             | Data entry  | Comments   |
|---------------|--|---|--|
| 1             | TITLE                                    | Enter a title.  | 80 characters.   |
| 2             | Cross-section library name               | HANSEN-ROACH,<br>27GROUPNDF4,<br>123GROUPGMTH,<br>218GROUPNDF4,<br>etc. | Alphanumeric name for available libraries.   |
| 3             | Type of calculation                      | INFHOMMEDIUM<br>LATTICECELL<br>MULTIREGION                              | These are the available options. See the explanation in Sect. C4.4.3 of ref. 4.  |
| 4             | Standard compositions specification data | Enter the appropriate data.   | Terminate this data block with END COMP.<br>See Table C4.4.4 of ref 4.   |
| 5             | Cell geometry specification              | Enter the appropriate data.<br>(Omit for INFHOMMEDIUM.)                 | Omit for INFHOMMEDIUM. See Table C4.4.5 of ref. 4 for LATTICECELL and MULTIREGION.   |
| 6             | Optional parameter data                  | Enter the desired data.   | Precede this data block by MORE DATA, if more parameter data is to be entered. Otherwise, omit this data entirely. See Sect. C4.4.7 of ref. 4. |

Fig. 2.1. Outline of Material Information Processor data.

ORNL DWG. 87-13384

```

=CSAS2X
7 PWR FUEL ASSM IN A SHIPPING CASK(HOMOGENIZED) AT ROOM TEMP
27GROUPNDF4 LATTICECELL
UO2 1 0.95 293.0 92235 3.2 92238 96.8 END
ZIRCALLOY 2 1.0 END
H2O 3 1.0 END
ARBMTL-B4C 2.64 2 1 1 0 5000 4 6012 1 4 0.015 END
ARBMTL-AL 2.64 1 0 0 0 13027 100.0 4 0.985 END
H2O 5 1.0 END
SS304 6 1.0 END
UO2 7 .90 293.0 92235 0.2 92238 99.8 END
END COMP
SQUAREPITCH 1.26 0.819 1 3 0.95 2 0.836 0 END

```

Fig. 2.2. Material Information Processor input for CSAS2 sample problem.

7 PWR FUEL ASSM IN A SHIPPING CASK(HOMOGENIZED) AT ROOM TEMP

\*\*\*\* PROBLEM PARAMETERS \*\*\*\*

LIB 27GROUPNDF4 LIBRARY  
 MXX 7 MIXTURES  
 MSC 8 COMPOSITION SPECIFICATIONS  
 IZM 4 MATERIAL ZONES  
 GE LATTICECELL GEOMETRY  
 MORE 0 0/1 DO NOT READ/READ OPTIONAL PARAMETER DATA  
 MSLM 0 FUEL SOLUTIONS

\*\*\*\* PROBLEM COMPOSITION DESCRIPTION \*\*\*\*

SC UO2 STANDARD COMPOSITION  
 MX 1 MIXTURE NO.  
 VF 0.9500 VOLUME FRACTION  
 TEMP 293.0 DEG KELVIN  
 92235 3.20%  
 92238 96.80%  
 END

SC ZIRCALLOY STANDARD COMPOSITION  
 MX 2 MIXTURE NO.  
 VF 1.0000 VOLUME FRACTION  
 END

SC H2O STANDARD COMPOSITION  
 MX 3 MIXTURE NO.  
 VF 1.0000 VOLUME FRACTION  
 END

SC ARBMTL-B4C STANDARD COMPOSITION  
 MX 4 MIXTURE NO.  
 VF 0.0150 VOLUME FRACTION  
 ROTH 2.6400 DENSITY  
 NEL 2 NO. ELEMENTS  
 IVIS 1 0/1 NO VARIABLE ISOTOPE/VARIABLE ISOTOPE  
 ICP 1 0/1 MIXTURE/COMPOUND  
 IRS 0 0/1 NO RESONANCE MTL./RESONANCE MTL.  
 5000 4.00  
 6012 1.00  
 END

Note that mixture No. 4 has a density of 1.64 g/cc and is 1.5 wt % B<sub>4</sub>C and 98.5 wt % Al. This particular boral mixture was conveniently described using the Standard Composition Specification Cards.

SC ARBMTL-AL STANDARD COMPOSITION  
 MX 4 MIXTURE NO.  
 VF 0.9850 VOLUME FRACTION  
 ROTH 2.6400 DENSITY  
 NEL 1 NO. ELEMENTS  
 IVIS 0 0/1 NO VARIABLE ISOTOPE/VARIABLE ISOTOPE.  
 ICP 0 0/1 MIXTURE/COMPOUND  
 IRS 0 0/1 NO RESONANCE MTL./RESONANCE MTL.  
 13027 100.00  
 END

Fig. 2.3. Echo of input to Material Information Processor input of Fig. 2.2.

SC H2O            STANDARD COMPOSITION  
 MX                5 MIXTURE NO.  
 VF                1.0000 VOLUME FRACTION  
 END

SC SS304         STANDARD COMPOSITION  
 MX                6 MIXTURE NO.  
 VF                1.0000 VOLUME FRACTION  
 END

SC UO2            STANDARD COMPOSITION  
 MX                7 MIXTURE NO.  
 VF                0.9000 VOLUME FRACTION  
 TEMP             293.0 DEG KELVIN  
                   92235 0.20%  
                   92238 99.80%  
 END

\*\*\*\* PROBLEM GEOMETRY \*\*\*\*

CTP SQUAREPITCH CELL TYPE  
 PITCH            1.2600 CM CENTER TO CENTER SPACING  
 FUELOD          0.8190 CM FUEL ROD DIAMETER OR SLAB THICKNESS  
 MFUEL            1 MIXTURE NO. OF FUEL  
 MMOD             3 MIXTURE NO. OF MODERATOR  
 CLADOD          0.9500 CM CLAD OUTER DIAMETER  
 MCLAD            2 MIXTURE NO. OF CLAD  
 GAPOD            0.8360 CM GAP OUTER DIAMETER  
 MGAP             0 MIXTURE NO. OF GAP

ZONE SPECIFICATIONS FOR LATTICECELL GEOMETRY

ZONE 1 IS FUEL  
 ZONE 2 IS GAP  
 ZONE 3 IS CLAD  
 ZONE 4 IS MOD

\*\*\*\* XSDRN MESH INTERVALS \*\*\*\*

6 MESH INTERVALS IN ZONE 1  
 4 MESH INTERVALS IN ZONE 2  
 4 MESH INTERVALS IN ZONE 3  
 14 MESH INTERVALS IN ZONE 4

Note that mixture No. 5 is the same as mixture No. 3. Two or more mixtures having identical specifications should be defined whenever one is inside the lattice cell and the others are not.

These data will be used for the resonance self-shielding calculation in NITAWL and for the spatial self-shielding (i.e., the cell-averaging) calculation in XSDRNPM.

These mesh intervals are automatically determined by the control module and printed here for your inspection and approval. The size of the spatial mesh intervals may be increased or decreased using the SZF parameter (i.e., one of the optional control parameters).

Fig. 2.3 (continued)

### 3. EVALUATION OF SPENT FUEL ISOTOPICS, RADIATION SPECTRA, AND DECAY HEAT

The primary reason for including an isotopic generation, depletion, and decay scheme in the SCALE computational system is to provide a means for calculating the radiation and heat generation source terms for use by the shielding and heat transfer analysis modules. It was determined that the ORIGEN code<sup>7</sup> and its data libraries should be updated and/or modified to provide a point depletion and decay capability within the SCALE system. The funding sponsor (the U.S. Nuclear Regulatory Commission) wanted the entire SCALE system to utilize and interface with multi-energy-group nuclear libraries processed from evaluated data files (e.g., ENDF/B). Also, envisioning the transport and storage of different fuel assembly types and irradiation histories, the sponsor wanted ORIGEN-S to be able to execute using neutronic data prepared for any user-specified assembly and irradiation history. Unfortunately, neither the original ORIGEN code nor the planned update, ORIGEN2,<sup>28</sup> provided this desired flexibility.

The original ORIGEN code had four libraries designed for the analysis of fuel irradiated in each of four reactor types — light water reactors (LWR), liquid metal fast breeder reactors (LMFBR), high-temperature gas-cooled reactors (HTGR), and molten salt breeder reactors (MSBR). In several instances, the cross sections and resonance integrals in these libraries were adjusted<sup>7</sup> to obtain agreement between calculated and measured fuel mass balances. Likewise, the ORIGEN2 code uses neutron cross-section and fission product yield libraries which have been developed for a number of specific reactor models. Here, a reactor model means a combination of a particular kind of reactor and a specified fuel cycle — for example, a uranium-fueled PWR using a once-through fuel cycle. Several cross-section libraries are available for different reactor models,<sup>29</sup> and work is currently being done at ORNL to update the libraries for the latest LWR designs. The cross-section libraries for ORIGEN2 were developed by performing detailed multigroup reactor physics and depletion calculations for each of the reactor models, and collapsing the multigroup libraries to one group for use by ORIGEN2. Burnup-dependent cross sections for the important actinide nuclides are built into ORIGEN2 for each reactor model.

The SCALE developers produced the ORIGEN-SCALE (ORIGEN-S for short) code<sup>30</sup> to provide the specific features desired by the NRC and required for use within SCALE. Utilization of the multigroup data is automated via the COUPLE code which was developed in conjunction with ORIGEN-S. COUPLE uses the multigroup data to update nuclide cross sections and calculate appropriate ORIGEN-S special parameters (THERM, RES, FAST) to be used for nuclides where multigroup cross sections are not provided.

Within SCALE, multigroup fluxes and cross sections are provided to COUPLE via the XSDRNPM module — a 1-D discrete ordinates transport code (see Sect. 2.3.3). Resonance processing of cross sections is performed via BONAMI-S or NITAWL-S. Burnup-dependent libraries are created for ORIGEN-S by employing successive passes through XSDRNPM-S and COUPLE using the desired multigroup cross-section library. Each successive XSDRNPM-S calculation uses irradiation time-dependent compositions evaluated by ORIGEN-S and pertinent information on the reactor history which affects the lattice cell flux calculation. This procedure is automated in SCALE with the SAS2 (Shielding Analysis Sequence No. 2) control module.

The purpose of this section is to review the ORIGEN-S data libraries and the SCALE system modules utilized for evaluation of nuclide isotopics, radiation spectra, and decay heat of spent fuel assemblies. In addition, this section will discuss the features of the new PLORIGEN module which provides a graphical display of the ORIGEN-S output variables. Development work aimed at improving the SAS2 module is also briefly discussed. Much of the material presented here is condensed from Sects. S2, F6, F7, F15, and M6 of the SCALE manual.<sup>4</sup>

### 3.1 REVIEW OF THE ORIGEN-S FUNCTIONAL MODULE

ORIGEN-S computes time-dependent concentrations and source terms of a large number of isotopes, which are simultaneously generated or depleted through neutronic transmutation, fission, radioactive decay, input feed rates, and physical or chemical removal rates. The calculations may pertain to fuel irradiation within nuclear reactors, or the storage, management, transportation, or subsequent chemical processing of removed fuel elements. The matrix exponential expansion model of the ORIGEN code is unaltered in ORIGEN-S. Essentially all features of ORIGEN were retained, expanded, or supplemented within new computations.

The primary objective of ORIGEN-S, as requested by the Nuclear Regulatory Commission, is that the calculations may utilize the multi-energy-group cross sections from any currently processed standardized ENDF/B data base. Complementary codes within SCALE compute flux-weighted cross sections, simulating conditions within any given reactor fuel assembly, and convert the data into a library that can be input to ORIGEN-S. Time-dependent libraries may be produced, reflecting fuel composition variations during irradiation. Some of the other objectives included in ORIGEN-S are: the convenience of free-form input, flexible dimensioning of storage to avoid size restrictions on libraries or problems; the computation of gamma and neutron source spectra in any requested energy group structure, applying a more complete standardized data base; the determination of neutron absorption rates for all nuclides; and the integration of fission product energies and sources over any decay interval, by applying the Volterra multiplicative integral method. ORIGEN-S can also produce an output file containing the information required to provide graphical display of the results using the PLORIGEN code. A complete list of the ORIGEN-S features is provided as Appendix B. This appendix lists the output units and quantities available from ORIGEN-S and gives an overall review of the large amount of flexibility and versatility provided with the code.

#### 3.1.1 Analytic Method

In determining the time dependence of nuclide concentrations, ORIGEN-S is primarily concerned with developing solutions for the following equation:

$$\frac{dN_i}{dt} = \text{Formation Rate} - \text{Destruction Rate} - \text{Decay Rate.} \quad (3.1)$$

ORIGEN-S considers radioactive disintegration and neutron absorption (capture and fission) as the processes appearing on the right-hand side of Eq. (3.1). The time rate of change of the concentration for a particular nuclide,  $N_i$ , in terms of these phenomena can be written as

$$\begin{aligned} \frac{dN_i}{dt} = & \sum_j \gamma_{ji} \sigma_{f,j} N_j \phi + \sigma_{c,i-1} N_{i-1} \phi + \lambda_i' N_i' \\ & - \sigma_{f,i} N_i \phi - \sigma_{c,i} N_i \phi - \lambda_i N_i, \end{aligned} \quad (3.2)$$

where ( $i = 1, \dots, I$ ), and

$$\sum_j \gamma_{ji} \sigma_{f,j} N_j \phi \text{ is the yield rate of } N_i \text{ due to the fission of all nuclides } N_j,$$

|                               |   |
|-------------------------------|---|
| $\sigma_{c,i-1} N_{i-1} \phi$ | is the rate of transmutation into $N_i$ due to radiative neutron capture by nuclide $N_{i-1}$ ,                                 |
| $\lambda_i' N_i'$             | is the rate of formation of $N_i$ due to the radioactive decay of nuclides $N_i'$ ,   |
| $\sigma_{f,i} N_i \phi$       | is the destruction rate of $N_i$ due to fission,  |
| $\sigma_{c,i} N_i \phi$       | is the destruction rate of $N_i$ due to all forms of neutron capture ( $n,\gamma$ ; $n,\alpha$ ; $n,p$ ; $n,2n$ ; $n,3n$ ), and |
| $\lambda_i N_i$               | is the radioactive decay rate of $N_i$ .  |

Equation (3.2) is written for a homogeneous medium containing a space-energy averaged neutron flux,  $\phi$ , with flux-weighted average cross sections,  $\sigma_f$  and  $\sigma_c$ , representing the reaction probabilities. In reality, the flux as a function of space, energy, and time is dependent upon the nuclide concentrations. ORIGEN-S assumes that the space-energy averaged flux can be considered constant over time steps  $\Delta t$ . For a given time step, these assumptions are necessary if Eq. (3.2) is to be treated as a first-order, linear, differential equation. However, for successive time steps,  $\Delta t_k$ ,  $\Delta t_{k+1}$ , ...  $\Delta t_n$ , ORIGEN-S provides the capability of using updated values for the space-energy averaged flux and, therefore, for the flux-weighted cross sections.

Proceeding with the description of the ORIGEN-S analytical model, for all nuclides  $N_i$ , Eq. (3.2) represents a coupled set of linear, homogeneous, first-order differential equations with constant coefficients. As such, Eq. (3.2) can be written in matrix notation as

$$\dot{\tilde{N}} = \tilde{A} \tilde{N} , \quad (3.3)$$

where  $\tilde{N}$  is a vector of nuclide concentrations and  $\tilde{A}$  is the transition matrix containing the rate coefficients for radioactive decay and neutron absorption. Equation (3.3) has the known solution

$$\tilde{N}(t) = \tilde{N}(0) e^{\tilde{A}t} , \quad (3.4)$$

where  $\tilde{N}(0)$  is a vector of initial nuclide concentrations. Analogous to a series expansion for the exponential function, the matrix exponential function,  $\exp(\tilde{A}t)$ , appearing in Eq. (3.4) can be expanded such that Eq. (3.4) is written as

$$\tilde{N}(t) = \tilde{N}(0) \sum_{m=0}^{\infty} \frac{(\tilde{A}t)^m}{m!} . \quad (3.5)$$

Equation (3.5) constitutes the matrix exponential method, which yields a complete solution to the problem.

A straightforward solution of Eq. (3.5) would require the in-core storage of the complete transition matrix. To avoid this storage requirement, a recursion relation has been developed by defining

$$\tilde{C}_0 = \tilde{N}(0)I = \tilde{N}(0) \quad (3.6)$$

and

$$\tilde{C}_{m+1} = \frac{\tilde{C}_m \tilde{A} t}{m+1}, \quad (3.6b)$$

where I is the identity matrix. Use of Eq. (3.6) into Eq. (3.5) yields

$$\tilde{N}(t) = \sum_{m=0}^{\infty} \tilde{C}_m. \quad (3.7)$$

A solution for the system of nuclides as given in Eq. (3.7) requires the storage of only two vectors,  $\tilde{C}_m$  and  $\tilde{C}_{m+1}$ , in addition to the current value of the solution.

Various tests are conducted in ORIGEN-S to assure that the summations indicated in Eq. (3.7) do not lose accuracy due to relative magnitudes or small differences between positive and negative rate constants. Nuclides with large rate constants are removed from the transition matrix and treated separately. For example, in the decay chain  $A \rightarrow B \rightarrow C$ , if the rate constant for B is large, a new rate constant is inserted in the matrix for  $A \rightarrow C$ . Tests for removal depend on the value of the diagonal element, d, for each nuclide. In the current version of ORIGEN-S, all nuclides for which  $\exp(-dt) < 0.001$  are removed from  $\tilde{A}$  and must be handled by alternative procedures. Increasing this restriction value would result in more computer time and possibly other numerical problems.

The short-lived nuclides removed from the transition matrix are solved using the nuclide chain equations. In testing for possible removal, a queue is formed of the short-lived precursors of each long-lived isotope. These queues extend back up the several chains to the last preceding long-lived precursor. The queues include all nuclides whose half-lives (loss due to decay and neutron absorption) are less than 10% of the time interval. A generalized form of the Bateman equations<sup>31</sup> is used to solve for the concentrations of the short-lived nuclides at the end of the time step. The applied equation for  $N_i$  is

$$N_i = N_i(0)e^{-a_{ii}t} + \sum_{k=1}^{i-1} N_k(0) \prod_{n=k}^{i-1} \frac{a_{n+1,n}}{a_{nn}} \left[ \sum_{j=k}^{i-1} \frac{e^{-a_{jj}t} - e^{-a_{ii}t}}{a_{ii} - a_{jj}} \prod_{\substack{n=k \\ n \neq j}}^{i-1} \frac{a_{nn}}{a_{nn} - a_{jj}} \right]. \quad (3.8)$$

The solution given by Eq. (3.8) is applied to calculate all contributions to the "queue end-of-interval concentrations" of each short-lived nuclide from initial concentrations of all others in the queue described above. The beginning-of-interval concentrations of long-lived or stable daughter products are augmented by the appropriate contribution from all nuclides of the queue divided by  $e^{-dt}$ , where d is the diagonal element. While dividing  $e^{-dt}$  produces a more correct concentration of the long-lived nuclide, it overpredicts its daughter concentrations. This adjustment is normally a small fraction of these concentrations in the usual reactor applications intended for the code (i.e., the ratio of the concentrations of long-lived daughters to that of their short-lived precursors is large).

Equation (3.8) is applied in making adjustments to certain elements of the final transition matrix, which now excludes the short-lived nuclides. The value of the element must be determined for the new transition between the long-lived precursor and the long-lived daughter of a short-lived queue. The element is adjusted such that the end-of-interval concentration of the long-lived daughter calculated from

the single link between the two long-lived nuclides (using the new element) is the same as what would be determined from the chain including all short-lived nuclides. The method assumes zero concentrations for precursors to the long-lived precursor. The computed values asymptotically approach the correct value with time as successive time intervals are executed. (For this reason, at least five to ten time intervals are recommended in place of one or two during a typical reactor exposure period. Larger intervals during the decay of discharged fuel are reasonable because long-lived nuclides have built up by that time.)

In the instance that a short-lived nuclide has a long-lived precursor, an additional solution is required. First, the amount of short-lived nuclide  $i$  due to the decay of the initial concentration of long-lived precursor  $j$  is calculated as

$$N(t)_{j \rightarrow i} = N_j(0)a_{ij} \frac{e^{-a_{ij}t}}{a_{ii} - a_{ij}} \quad (3.9)$$

from Eq. (3.8) with  $a_{kk} = d_k$  and assuming  $\exp(-d_i t) \ll \exp(-d_j t)$ . However, the total amount of nuclide  $i$  produced depends upon the contribution from the precursors of precursor  $j$ , in addition to that given by Eq. (3.9). The quantity of nuclide  $j$  not accounted for in Eq. (3.9) is denoted by  $N'_j(t)$ , the end-of-interval concentration minus the amount which would have remained had there been no precursors to nuclide  $j$ ,

$$N'_j(t) = N_j(t) - N_j(0)e^{-a_{jj}t} . \quad (3.10)$$

Then the short-lived daughter and subsequent short-lived progeny are assumed to be in secular equilibrium with their parents, which implies that the time derivative in Eq. (3.2) is zero.

$$N_i = 0 = \sum_j a_{ij} N_j . \quad (3.11)$$

The "queue end-of-interval concentrations" of all the short-lived nuclides following the long-lived precursor are augmented by amounts calculated with Eq. (3.8). The concentration of the long-lived precursor used in Eq. (3.10) is that given by Eq. (3.9). The set of linear algebraic equations given by Eq. (3.11) is solved by the Gauss-Seidel iterative technique. This algorithm involves an inversion of the diagonal terms and an iterated improvement of an estimate for  $N_i$  through the expression

$$N_i^{k+1} = - \frac{1}{a_{ii}} \sum_{j \neq i} a_{ij} N_j^k . \quad (3.12)$$

Since short-lived isotopes are usually not their own precursors, this iteration often reduces to a direct solution.

So far, in the discussion of the analytical model applied in ORIGEN-S, we have considered the solution of the homogeneous equation, Eq. (3.3). This equation is applicable to reactor fuel burnup calculations and therefore its solution is of primary interest for incorporation into the SCALE system analytical sequences. However, an additional capability resides in the ORIGEN-S program to consider an externally imposed time rate-of-change for the nuclide concentrations. This capability would be

applicable to various phases of fuel reprocessing. Mathematically, the consideration of such rate changes results in a nonhomogeneous form of Eq. (3.3).

$$\tilde{\dot{N}} = \tilde{A} \tilde{N} + \tilde{B} . \quad (3.13)$$

For a user-specified set of rate changes,  $\tilde{B}$ , the particular solution of Eq. (3.13) is sought to be added to the solution of the homogeneous equation, Eq. (3.3). As before, the matrix exponential method is used for the long-lived nuclides, and secular equilibrium is assumed for the short-lived nuclides. Details of the solution procedure can be found in ref. 30.

The ORIGEN-S user has the option of inputting a fixed value for the neutron flux or the specific power. The SCALE analytical sequences call for the power per fuel assembly history and fuel volume data from which the specific power is determined. The average neutron flux over the time interval is obtained from the specific power, microscopic fission cross sections, and an approximate expression for the fissioning nuclide concentrations as a function of time. Likewise, if a fixed value of the neutron flux is specified, the average power over the time interval is obtained. A Taylor series expansion of the macroscopic cross sections about the interval initial time and a time integration over the interval are employed to obtain the average value. Since only a few terms are retained in the expansions, they are accurate only for slowly varying functions of time. Therefore, the user may have to reduce the specified time step to ensure an accurate calculation of the average flux or the average power. If either of these quantities differs from the value at the beginning of the time step by more than 20%, a warning is printed to use smaller time steps.

Although a constant energy/fission value can be input to ORIGEN-S, the default option is to determine the average energy per fission (constant for each time step) on the basis of the neutron absorptions occurring during each time step. The total thermal energy from neutron absorption is the sum of the yields,  $Q_{ij}$ , for nuclides  $i$  and reaction types  $j$  (fission, radiative capture, etc.) weighted by their probability of occurrence. The energy carried off by neutrinos is not included. Values for the thermal yields for twenty-four fissile isotopes and other important nuclides have been taken from ENDF/B files. A thermal yield of 5 MeV is used for radiative capture of nuclides that are not important or for which ENDF/B data are not available. This value is typical of known thermal yields, and the total contribution from these nuclides is usually less than 0.3% of the average energy per fission.

As implied above, the primary problem typically solved by ORIGEN-S is the determination of time-dependent nuclide concentrations. While the matrix exponential solution has been described in this section, an alternative matrix operator method for calculating radioactive decay is available in ORIGEN-S. This model produces: (1) the "instantaneous-concentrations" of nuclides similar to that determined by Eq. (3.4); and (2) the "time-integrated-concentrations" from the integration of Eq. (3.4) over any specified time interval. The second model is called the Volterra multiplicative integral method and is useful in computing either the total disintegrations or the total energy released from fission products during various cooling intervals. These integrals more correctly simulate counting measurements, total heat, or radiation exposure than those derived from directly "averaging" the instantaneous values from the matrix exponential method. The theory and method of solutions applicable to the integral solution option will not be presented here but are discussed in detail in ref. 30.

### 3.1.2 ORIGEN-S Data Libraries<sup>32</sup>

The original version of the ORIGEN code<sup>7</sup> used two kinds of data libraries in card-image format. The nuclear data libraries contained decay data, natural abundances of nuclides, radioactivity concentration guides, cross sections, and fission yields. The photon yield libraries contained multigroup photon yields (photons per disintegration) for decay gamma- and X-rays, for bremsstrahlung from beta particles

slowing down in a  $\text{UO}_2$  fuel matrix, and for some gammas accompanying spontaneous fission and  $(\alpha, n)$  reactions in oxide fuels. There were three libraries of each kind, one for 253 light element nuclides (structural materials and activation products), one for 101 actinide nuclides (fuel materials, transplutonium nuclides, and decay daughters), and one for 461 fission product nuclides. The nuclear data libraries included cross sections and fission yields for four reactor types: the high-temperature gas-cooled reactor (HTGR), the light-water reactor (LWR), the liquid metal fast breeder reactor (LMFBR), and the molten salt breeder reactor (MSBR). Since the original ORIGEN code and its libraries were primarily intended for use in generic studies of spent fuel and waste characteristics, cross sections for a number of nuclides were adjusted to give agreement between calculated and measured fuel mass balances.<sup>7</sup>

As the ORIGEN code became more widely used for more complex applications, more nuclear data libraries were added. A large light element library<sup>33,34</sup> for 674 nuclides, with cross sections for HTGRs and LWRs, was created. About the same time a large fission product library<sup>34</sup> for 821 nuclides, with cross sections and fission yields for LWRs and LMFBRs, was generated from ENDF/B-IV data.<sup>35</sup>

In addition to the data libraries, a certain amount of nuclear data for ORIGEN was programmed into the code itself. Photon yields for prompt and equilibrium fission product gamma rays were stored in an 18-energy-group structure for estimating gamma-ray sources from spontaneous fission. The average number of neutrons released by spontaneous fissions,  $\nu$ , and the number of neutrons produced per alpha disintegration in  $\text{UO}_2$  fuel were calculated from empirical functions. These data were used to estimate spontaneous fission and  $(\alpha, n)$  reaction neutron sources from actinides in spent fuel.

Thus, at the time that the development of ORIGEN-S began, the data necessary to run ORIGEN were contained in five card-image nuclear data libraries, three card-image photon yield libraries, and in the code itself. The customary manner of running ORIGEN was to use three nuclear data libraries and the three photon yield libraries, although provisions existed to skip the use of certain of these libraries.

The ORIGEN-S code can still be run in this manner and, in fact, can be run with the original ORIGEN libraries if the user desires. Henceforth, the term "original ORIGEN libraries" is defined as the five nuclear data libraries and three photon yield libraries still being distributed with the 1979 edition of the ORIGEN code.<sup>36</sup> These libraries are not distributed with ORIGEN-S, but revised libraries, described in the remainder of this section, are distributed with the SCALE code package.

The major revision to the card-image nuclear data libraries has been the inclusion of new decay data. Nearly all the cross-section data have been left the same as in the original ORIGEN libraries. The updating of cross-section data is now performed (for the binary data libraries discussed later) with the COUPLE code, using problem-dependent multigroup cross sections from a detailed neutronics calculation. The photon yield libraries have completely new data taken from the ORNL Master Photon Data Base<sup>37</sup> discussed below. In addition to using the photon yield libraries described in this report, the user of ORIGEN-S can generate photon yield libraries in an energy-group structure of his choice.<sup>30</sup>

In addition to the card-image nuclear data and photon yield libraries, the ORIGEN-S code can read data from three other kinds of libraries: a binary (unformatted) data library, an ENDF/B-IV fission product data base, and the ORNL Master Photon Data Base.

The use of a binary ORIGEN-S data library is one of the most significant features of ORIGEN-S. A binary data library is generated with the COUPLE code. It contains, in a single library, the same kinds of data as the card-image nuclear data and photon yield libraries, but for only one reactor type. The ORIGEN-S code is normally run with one or more (time-dependent) binary data libraries for the reactor type of interest. The binary data library has many advantages over the card-image data libraries. Its principal advantage is that the cross sections within the library can be replaced with cross

sections derived from a detailed multigroup neutronics (e.g., unit cell) calculation. Cross-section updating is performed with the COUPLE code that reads the multigroup cross sections from an AMPX weighted (working) cross-section library. Within SCALE, automated generation of time-dependent (i.e., burnup-dependent) binary data libraries can be performed with the SAS2 control module. Another advantage is that any portion of the photon yield data from the ORNL Master Photon Data Base can be placed in the binary library with any desired energy group structure. Furthermore, any item of data in a binary library can be replaced (using COUPLE) by a user-specified value. Finally, execution of ORIGEN-S is slightly faster when a binary library is used.

The ENDF/B-IV fission product data base used by ORIGEN-S contains fission product decay data in ENDF/B-IV card-image (BCD) format. These data were compiled from file (MF) 1, reaction-type (MT) 457 data of the ENDF/B-IV fission product tapes.<sup>35</sup> They can be used by ORIGEN-S to generate multigroup fission product photon source spectra or to make a card-image photon yield library for fission products.<sup>30</sup> For either use, the photon energy group structure can be specified by the user.

The ORNL Master Photon Data Base was originally developed for the ORIGEN2 code.<sup>28</sup> In its card-image form, it consists of six data sets for six kinds of photon sources. One data set contains decay gamma- and X-ray line data from the Evaluated Nuclear Structure Data File (ENSDF).<sup>38,39</sup> Another data set contains spectra for gamma rays accompanying spontaneous fission and ( $\alpha$ ,n) reactions. Two data sets contain bremsstrahlung spectra from decay beta (negatron and positron) particles slowing down in a UO<sub>2</sub> fuel matrix. The last two data sets contain bremsstrahlung spectra from decay betas slowing down in water. These data sets can be concatenated in any user-chosen combination to form a card-image master photon data base for use with ORIGEN-S. In addition, ORIGEN-S can be used to create a binary (unformatted) master photon data base, containing data from any combination of the card-image data sets, for use in subsequent ORIGEN-S runs. It has been customary at ORNL to run ORIGEN-S with a binary master photon data base, since execution is somewhat more efficient for that mode of operation. The ORNL Master Photon Data Base is the most comprehensive and up-to-date photon library available to ORIGEN-S. It can be used to generate multigroup photon source spectra, to make card-image photon yield libraries, or to update photon yield data in a binary data library. The spectra and photon yield data can be generated in any energy group structure for all light-element, actinide, and fission product nuclides having photon data.

Table 3.1 provides a summary of the card-image libraries distributed with ORIGEN-S. Examples of various binary libraries that can be created by the user are shown in Table 3.2. Instructions and, in many cases, the actual input for creating the binary libraries are provided with the SCALE package.

### 3.1.3 Calculation of Radiation Source Spectra

One of the major features of the ORIGEN-S code is the capability to produce radiation source strengths and spectra in any desired multigroup format. This feature is tremendously useful for the shielding analyst who requires sources in a multigroup format corresponding to available cross-section sets.

There are four types of photon source spectra that can be computed by ORIGEN-S. There are photon spectra for the three libraries (light element, fission product, actinide), computed in the energy group structures of the input photon libraries (commonly called the "photon tables"). Also, there may be "special gamma source spectra" computed for the total spectrum from all three libraries as well as that for individual libraries, using an input energy group structure. For gamma sources, the code first converts inventories of all nuclides of the cooled fuel assembly to disintegrations per second. Then, applying the ORNL Master Photon Data Base it sums individual nuclide photon spectra to determine the total gamma source spectrum. The intensity of a line at energy E, from the data base, is normalized to E, the

Table 3.1. Card-image ORIGEN-S libraries at ORNL

| Member name | Description   |
|-------------|---|
| ACTINIDE    | Actinide nuclear data library (101 nuclides)  |
| BIGFISP     | Big fission product nuclear data library (821 nuclides)                               |
| BIGLITE     | Big light element nuclear data library (687 nuclides)                                 |
| ENDFB4FP    | ENDF/B-IV fission product decay library   |
| MPBRH2OM    | Master photon data for bremsstrahlung from negatrons slowing down in water            |
| MPBRH2OP    | Master photon data for bremsstrahlung from positrons slowing down in water            |
| MPBRUO2M    | Master photon data for bremsstrahlung from negatrons slowing down in UO <sub>2</sub>  |
| MPBRUO2P    | Master photon data for bremsstrahlung from positrons slowing down in UO <sub>2</sub>  |
| MPDKXGAM    | Master photon decay x- and gamma-ray line data  |
| MPSFANGM    | Master photon gamma-ray spectra from spontaneous fission and ( $\alpha$ ,n) reactions |
| PHOACT      | Actinide photon yield library (18 groups)   |
| PHOFISP     | Fission product photon yield library (12 groups)                                      |
| PHOLITE     | Light element photon yield library (12 groups)  |
| SMALFISP    | Small fission product nuclear data library (461 nuclides)                             |
| SMALLITE    | Small light element nuclear data library (253 nuclides)                               |

Table 3.2. Some binary ORIGEN-S libraries at ORNL

| Member name | Description  |
|-------------|--|
| BASICLWR    | Basic LWR ORIGEN-S Binary Working Library described in ref. 32. It has ( $\beta$ ,n) decay data for fission products, so it cannot be used with the integral option.   |
| BASLMFBR    | Basic LMFBR ORIGEN-S Binary Working Library. This library was converted from the large light-element, actinide, and large fission product card-image nuclear data libraries. It has the same ( $\beta$ ,n) decay data and photon yield data as the Basic LWR Binary Working Library. It cannot be used with the integral option. |
| MAPHH2OB    | Binary master photon library with the photon data from members MPDKXGAM, MPSFANGM, MPBRH2OM, and MPBRH2OP of the card-image library.   |
| MAPHNOBR    | Binary master photon library with the photon data from members MPDKXGAM and MPSFANGM of the card-image library.  |
| MAPHUO2B    | Binary master photon library with the photon data from members MPDKXGAM, MPSFANGM, MPBRUO2M, and MPBRUO2P of the card-image library.   |
| PWR33CY1    | Binary working library for cycle 1 of a "typical" PWR, as described in ref. 32. It cannot be used with the integral option.  |
| PWR33CY2    | Binary working library for cycle 2 of a typical PWR. It cannot be used with the integral option.   |
| PWR33CY3    | Binary working library for cycle 3 of a typical PWR. It cannot be used with the integral option.   |

average energy of the group, using direct multiplication by the factor  $E/\bar{E}$ , with one exception. In cases where  $E-E_1$  or  $E_2-E$  is less than  $0.03(E_2-E_1)$ , where  $E_1$  and  $E_2$  are the boundaries of a group, one-half the initial intensity is applied to each of the two groups having the boundary near the line. These procedures maintain the conservation of energy rather than photon intensity, which should give a more correct computation of dose rates in the shielding analysis. As a final correction, the ratio of total nuclide gamma energy, from data in the ORIGEN-S working library, to the gamma energy of only those nuclides having line data, is multiplied times the spectrum computed from the data base to account for nuclides that do not have line data (typically a small fraction). The gamma spectrum is supplied in the energy group structure specified by the user.

The major part of the neutron source is produced from spontaneous fission of the heavy nuclides. Data required to compute the neutron production rate from this process include the spontaneous fission half-life, the average neutron yield per spontaneous fission,  $\nu_{sf}$ , and the concentration for each contributing nuclide. Spontaneous fission half-lives for the more significant nuclides are those from the ORIGEN-S card-image actinide nuclear data library. These half-lives are taken from ENSDF<sup>38,39</sup> and from Kocher's compilation of decay data,<sup>40</sup> both of which contain evaluated measured data. For several less important nuclides, unmeasured half-lives are taken from ref. 41. These data were estimated with a correlation between measured data and so-called fissility parameters.<sup>42</sup> The  $\nu_{sf}$  data are taken from ref. 41. Measured values are available for 21 nuclides, including the most significant. An equation, derived<sup>41</sup> to compute  $\nu_{sf}$ , produces values which are within two experimental standard deviations for all except three nuclides. This equation is applied for nuclides that do not have measured data.

A significant neutron source is also often produced by  $^{17}\text{O}(\alpha,n)$  reactions in the  $\text{UO}_2$  and other oxygen compounds of the spent fuel. Thin target cross sections for these reactions and alpha stopping power data may be applied to compute neutron yields of the fuel material. Measurements<sup>43</sup> of thin target cross sections for the  $^{17}\text{O}(\alpha,n)$  and  $^{18}\text{O}(\alpha,n)$  reactions produced improvement over earlier data.<sup>44,45</sup> Additionally, thick target energy-dependent  $(\alpha,n)$  yields for  $^{238}\text{U}^{\text{NAT}}\text{O}_2$  were computed,<sup>43</sup> having estimated accuracies within 10%. ORIGEN-S applies yield data from ref. 43 to weighted energy averages of alpha energy-intensity data<sup>40</sup> of all nuclides except for those reported<sup>46</sup> for  $^{214}\text{Bi}$ ,  $^{241}\text{Pu}$ , and  $^{249}\text{Bk}$ , which have very small alpha branching fractions. Decay constants and alpha decay branching fractions are required to compute the  $(\alpha,n)$  source. The decay constants are provided directly from the ORIGEN-S data libraries. However, since alpha decay branching fractions are not supplied directly from an ORIGEN-S data library, the data are provided in the Block Data COMMON /SPECDDT/. The data were copied from the current version (updated in 1981-1982) of the ORIGEN-S card image nuclear data library. Also, since alpha energies are not explicitly included in ORIGEN-S libraries, the weighted averages of the most current (1981) evaluation<sup>40</sup> are also supplied in COMMON /SPECDDT/. All of the nuclide yields and associated data can be edited during the execution.

The isotopes  $^{242}\text{Cm}$  and  $^{244}\text{Cm}$  characteristically produce all except a small percentage of the spontaneous fission and  $(\alpha,n)$  neutron source in spent PWR fuel over a 10-year decay time. The next largest contribution is usually from the  $(\alpha,n)$  reaction of alphas from  $^{238}\text{Pu}$ , which is approximately 1 to 2% of the source. Neutron energy spectra of both the spontaneous fission and  $(\alpha,n)$  reactions have been determined for the curium isotopes<sup>47,48</sup> and  $^{238}\text{Pu}$ .<sup>49</sup> The measured spontaneous fission neutron spectrum of  $^{244}\text{Cm}$  was found to be quite similar to that from  $^{235}\text{U}$  and  $^{252}\text{Cf}$ . Thus, the spectrum for  $^{242}\text{Cm}$  was computed<sup>47</sup> from these measurements. The  $(\alpha,n)$  neutron spectra were determined by extrapolating the neutron spectrum from Po- $\alpha$ -O source measurements<sup>50</sup> to the alpha energies of  $^{242}\text{Cm}$ ,  $^{244}\text{Cm}$ , and  $^{238}\text{Pu}$ . The energy distribution of the spontaneous fission neutron spectrum is computed from the spectra for  $^{242}\text{Cm}$  and  $^{244}\text{Cm}$  described above, using the calculated concentrations of those two isotopes. This spectrum is then renormalized to include the total neutron source from all spontaneous fission isotopes. A similar calculation, using the data for all three isotopes, is performed for the  $(\alpha,n)$  neutron spectrum. The spectra are collapsed from the energy-group-structure of the data to either the group-structure input

or that of the SCALE library specified by input. The procedure assumes uniform distribution within each group and simply sums the quantities based upon energy fractions common to both groups in the two group structures. The total neutron source spectrum is then computed as the sum of the spontaneous fission and  $(\alpha,n)$  spectra.

Recently, the portion of the neutron source arising from  $(\alpha,n)$  reactions has been expanded to consider  $(\alpha,n)$  reactions with other light elements. Although no change is seen for sources from oxide fuels,  $(\alpha,n)$  sources from nuclear waste in borosilicate glass and other media can now be accurately obtained. This expansion of the  $(\alpha,n)$  neutron source will be included in the SCALE-4 version of ORIGEN-S.

### 3.2 REVIEW OF THE COUPLE FUNCTIONAL MODULE

As noted in Sect. 3.1, one of the primary objectives in developing ORIGEN-S was that the calculations be able to utilize multi-energy-group neutron flux and cross sections in any group structure. Utilization of the multigroup data is automated via the COUPLE code, which was developed in conjunction with ORIGEN-S. COUPLE uses the multigroup data to update nuclide cross sections and calculate appropriate ORIGEN-S spectral parameters (THERM, RES, FAST) to be used for nuclides where multigroup cross sections are not provided. ORIGEN-S can be run stand-alone using available card image data libraries or with one or more time-dependent binary libraries that are created with COUPLE.

As noted earlier, ORIGEN-S runs faster when binary libraries are used. COUPLE can be used to convert ORIGEN-S card-image libraries to binary libraries. The contents of a binary library can also be updated with COUPLE using user-specified data. Data that can be modified include not only cross sections, but all of the other nuclear data, such as decay constants, Q-values, effective branching fractions, spontaneous fission constants, and fission product yields.

In addition, for any given AMPX working library in the standard format of the SCALE system, the entire set of neutron cross sections in an ORIGEN-S binary library may be updated to provide either one of the following: the reaction cross section included in the AMPX working library, as the priority option; or, the cross section computed from the old library few-group data and the improved flux weight factors, updated from the AMPX library data. Note that data for a nuclide is included in an AMPX library, only when the nuclide is specified individually as part of the composition in describing the input to the code that produces the library.

The primary significance of the procedures available using COUPLE is that ORIGEN-S cross sections may be computed as a function of many of the design characteristics, operating parameters, and material compositions of a given nuclear reactor. Also, by changing the input composition at various times during a specified reactor irradiation history, several time-dependent libraries may be produced for input to a single ORIGEN-S case. In essence, once the user has produced the AMPX working library, which contains a set of cross-section constants that approximately apply to the specified problem, COUPLE will produce the updated library required by ORIGEN-S.

The remainder of the section presents and discusses the analytic methods employed by COUPLE in preparing the multigroup cross section and neutron flux information for use by ORIGEN-S.

#### 3.2.1 Flux Weight Factors

The convention used by both the ORIGEN and ORIGEN-S codes is that the input flux be thermal flux and all cross sections be normalized to only the thermal flux. This section presents the model applied by COUPLE for deriving a set of library flux weight factors that simulate the flux spectrum for the particular reactor lattice being analyzed. While these factors are required for the large bulk of nuclides in ORIGEN-S libraries, the factors are not applied to the cross sections provided by the AMPX working library.

The effective cross section,  $\sigma_{\text{eff}}$ , should be derived from data in the initial ORIGEN-S libraries as a reasonable approximation to the definition:

$$\sigma_{\text{eff}} = \int_0^{\infty} \phi(E) \sigma(E) dE / \phi_{\text{th}} , \quad (3.14)$$

where

$$\phi_{\text{th}} = \int_0^{0.5 \text{ eV}} \phi(E) dE . \quad (3.15)$$

The approximation in ORIGEN and ORIGEN-S for  $\sigma_{\text{eff}}$  is

$$\sigma_{\text{eff}} = \text{THERM} \times \sigma_0 + \text{RES} \times I + \text{FAST} \times \sigma_1 , \quad (3.16)$$

where

$\sigma_0$  = the 2200-m/s neutron-absorption cross section,

$I = \int_{0.5 \text{ eV}}^{\infty} \frac{\sigma(E)}{E} dE$ , the resonance integral,

$\sigma_1$  = the fission-spectrum-averaged cross section for all reactions with thresholds greater than 1 MeV.

Nuclide data not implicitly updated by COUPLE apply  $\sigma_1 = 0$  for thresholds less than or equal to 1 MeV and, both  $\sigma_0 = 0$  and  $I = 0$  for thresholds greater than 1 MeV.

The flux weight factors THERM, RES, and FAST, applied by the ORIGEN codes are assumed to be constant for any specified reactor (or subcase). Obviously, since all nuclides do not have the same cross-section "distribution," Eq. (3.14) cannot be derived from Eq. (3.16) for all nuclides. Thus, idealized assumptions are applied in defining the flux weight factors. Thermal reaction rates are assumed to follow that of a  $1/v$  absorber.

$$\text{THERM} = \sqrt{E_0} \int_0^{0.5 \text{ eV}} \frac{\phi(E)}{\sqrt{E}} dE / \phi_{\text{th}} . \quad (3.17)$$

Using a Maxwell-Boltzmann distribution about T for the thermal neutron population, it is known that

$$\text{THERM} = \sqrt{\frac{\pi}{4} \frac{T_0}{T}} , T_0 = 293.16 \text{ K} , \quad (3.18)$$

where T is usually considered to be the absolute temperature of the reactor moderator. If T is input to COUPLE, Eq. (3.18) is used to calculate THERM. An alternative approach is to include a  $1/v$  absorber material ( $\sigma_0 = 1$ ) in the neutronics analysis and obtain the broad group thermal value that approaches the value of Eq. (3.17) when collapsed over a sufficient number of thermal groups. This procedure is automated within SCALE sequences.

The standard computation of the resonance integral,  $I$ , implies a  $1/E$  variation in the flux, which is a common assumption for, at least, approximating an LWR flux. It has been shown<sup>30</sup> that RES can be derived from the  $1/E$  assumption and the total resonance flux,  $\phi_{res}$ . Thus, COUPLE computes RES from flux in the groups  $n+1$  through  $m$ , inclusive (for the range 0.5 eV to 1 MeV) by applying:

$$\begin{aligned} \text{RES} &= \frac{\phi_{res}}{\phi_{th} \ln(E_2/E_1)} \\ &= \frac{\sum_{j=n+1}^m \phi_j}{\ln(2 \times 10^6) \sum_{i=1}^n \phi_i} \end{aligned} \quad (3.19)$$

The factor, FAST, is applied to only the cross sections  $\sigma_1$  for reactions with thresholds greater than 1 MeV. It is assumed that  $\phi(E)$  for  $E > 1$  MeV is entirely from uncollided fission neutrons. Thus, COUPLE computes FAST from the groups  $m+1$  to  $k$ , inclusive (for the range 1 MeV to maximum energy) by applying:<sup>51</sup>

$$\text{FAST} = \frac{1.45 \sum_{j=m+1}^k \phi_j}{\sum_{i=1}^n \phi_i}, \quad (3.20)$$

where 1.45 is the ratio of the total fission neutron flux to the portion above 1 MeV.

Note in the above method that the multigroup neutron flux data should have boundaries at 0.5 eV and 1 MeV for best results. COUPLE will use the boundary nearest these values to compute THERM, RES, and FAST.

### 3.2.2 Cross-Section Collapse to ORIGEN-S Group Structure

All nuclides in the AMPX working library (for which there is a non-zero ZA number) are more completely updated by COUPLE than those simply approximated with the flux weight factors, described above. The computed  $\sigma_{eff}$ , which ultimately is applied by ORIGEN-S, more nearly equals that of the definition in Eq. (3.14). COUPLE computes  $\sigma_{eff}$  from the thermal flux groups 1 through  $n$  and all groups 1 through  $k$ , inclusive, by applying

$$\sigma_{eff} = \frac{\sum_{j=1}^k \phi_j \sigma_j}{\sum_{i=1}^n \phi_i} \quad (3.21)$$

Note that Eq. (3.21) retains the convention of ORIGEN for normalizing cross sections to thermal flux. The values produced by Eq. (3.21) are stored in an ORIGEN-S working library.

### 3.3 DEPLETION AND DECAY WITH THE SAS2 CONTROL MODULE

The Shielding Analysis Sequence 2 (SAS2) module of the SCALE code system was designed to evaluate the dose rates outside a shipping cask containing spent fuel elements from a nuclear reactor. To perform this task, it provides for the interface of data between various functional modules in the SCALE code system. SAS2 calls the functional modules in the proper sequence to (1) process resonance cross sections (BONAMI-S, NITAWL-S), (2) compute the neutron spectrum in an infinite lattice representation of a fuel assembly and collapse a multigroup set of cross sections to three groups (XSDRNPM-S), (3) update an ORIGEN-S nuclear data library with the collapsed cross sections (COUPLE), and (4) perform a depletion calculation using the updated nuclear data library (ORIGEN-S). It can repeat steps 1 through 4 as many times as requested during simulation of the operating history of a fuel assembly. The simulation of the operating history is followed by (5) a calculation of radiation sources after a specified decay period (ORIGEN-S), (6) the (1-D) transport of radiation through the cask radial walls (XSDRNPM-S), and (7) the calculation of dose rates outside the cask (XSDOSE). A flow diagram of the SAS2 sequence is provided in Fig. 3.1. The shielding analysis portion of the sequence (steps 6 and 7) will not be discussed in this paper, however. Emphasis will be on the depletion/decay portion of the sequence shown in Fig. 3.1. The sequence can be easily halted after the depletion analysis is performed and later restarted to perform a shielding analysis.

#### 3.3.1 Method and Techniques

The method applied by SAS2 starts with the data describing a fuel assembly as it is initially loaded into a particular reactor. The composition, temperatures, geometry, and time-dependent specific power of the fuel assembly are required. Then, by alternately processing cross sections based on the fuel-pin infinite-lattice representation of the assembly and applying these cross sections in a fuel burnup calculation, the nuclide densities are determined as intermediate information for use in the repeated neutronics-depletion analysis. Ultimately, the nuclide inventory is computed at discharge of the assembly.

A one-dimensional discrete-ordinates transport treatment based upon an infinite fuel-pin lattice model is used in producing the cross-section libraries coupled into the ORIGEN-S libraries for the depletion analysis of a reactor fuel assembly. Five functional modules are involved in the process of making the libraries, in addition to applying the Material Information Processor and the slightly modified data processor of the other SCALE criticality and shielding control modules.

Fundamentally, the chief function of SAS2 is to convert user input data, plus data from other sources, into the input required by functional modules and write the input on the interface units read by the codes. For example, isotopic and other material densities, required by the codes, are prepared by the Material Information Processor from both the user input (e.g., volume fractions) and the Standard Composition Library. Subsequent data processing produces the input data arrays for number densities required by the various codes. Since cross sections are developed for only the nuclides in the compositions of the problem, an arbitrary addition of trace amounts of the most significant nuclides are added by SAS2. Then, the interface data sets for input data to BONAMI-S, NITAWL-S and XSDRNPM-S are developed. After the neutronics code interfaces are completed, SAS2 produces interfaces to codes which assist in the coupling of burnup-dependent densities into the model for producing time-dependent cross sections. First, an interface data set is produced for COUPLE, which updates cross-section constants on libraries input to ORIGEN-S. Finally, the interface to ORIGEN-S is produced for a case in which computed densities of the fuel are saved in a data set.

Appropriate parameters are returned to the SCALE system driver to sequentially invoke execution of the five functional modules of this part of the SAS2 method. BONAMI-S and NITAWL-S are invoked to perform resonance self-shielding treatments for nuclides that have the appropriate data on the specified SCALE neutron cross-section library. XSDRNPM-S applies the working library output by

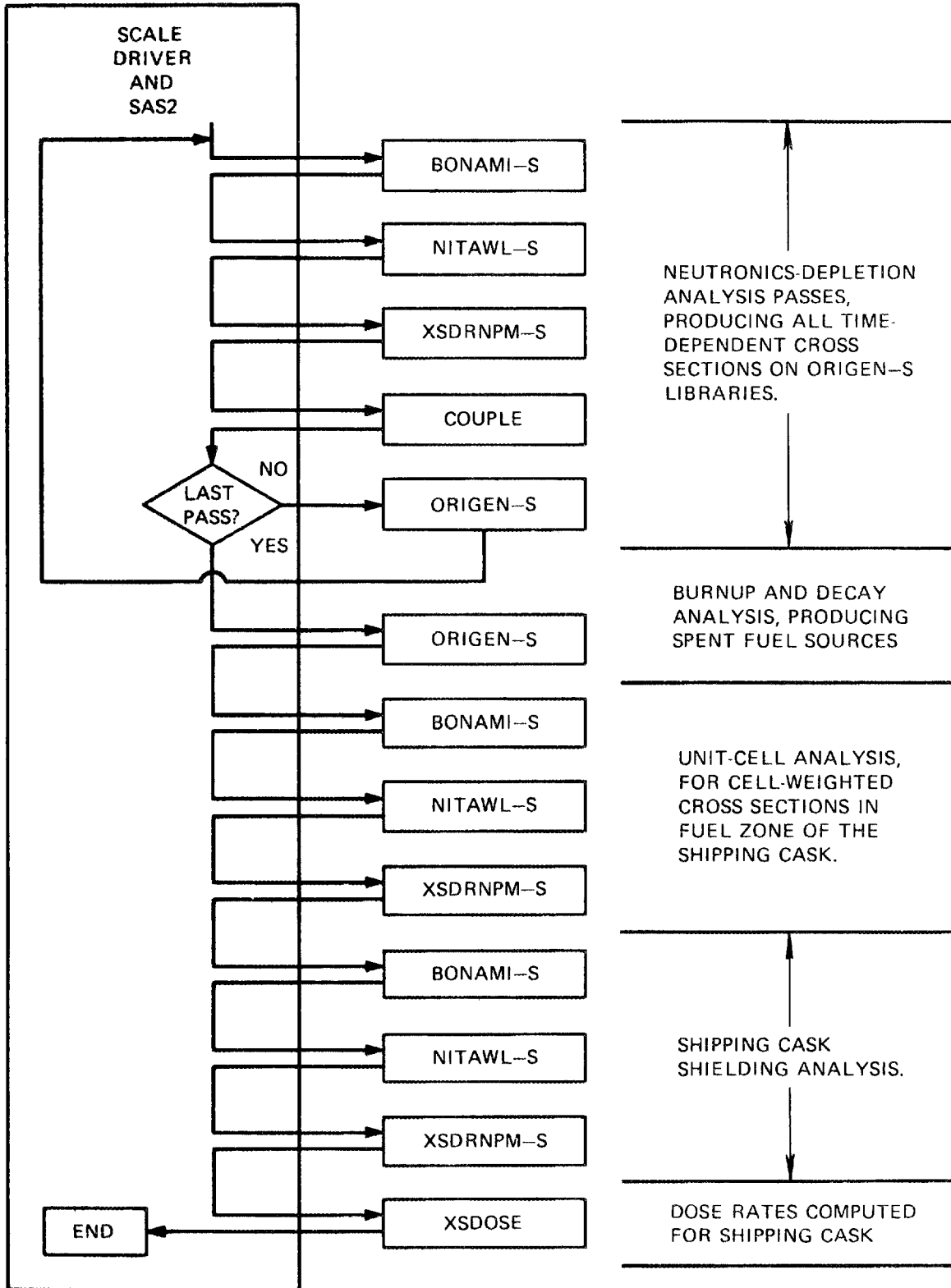


Fig. 3.1. Computation flow path invoked by SAS2 module.

NITAWL-S to produce a region-weighted working library, representing the reactor fuel cross sections for the compositions and the fuel-pin cell described by the input to the case. The compositions for the first pass through XSDRNPM-S are composed of the nuclide mixture for the new, or freshly loaded, fuel assembly. The neutronics models of these first three codes are discussed in detail in Sects. F1-F3 of the SCALE Manual <sup>4</sup> and reviewed briefly in Sect. 2 of this report. As execution continues, the driver invokes COUPLE to update an ORIGEN-S working binary library with data on the XSDRNPM-S weighted working library. The ORIGEN-S execution is invoked to compute the time-dependent densities of the nuclides in the fuel for the specified power and exposure times. This procedure is applied repeatedly to produce time-dependent cross sections that reflect the shift in the neutron energy spectrum during irradiation. The major data differences for the sequential passes through the procedure are in the nuclide densities and reactor history parameters.

The user input specifies the number of cycles (e.g., the number of years the assembly resides in the reactor), the number of libraries to make per cycle, the specific power in each cycle, and both the total operation time and downtime of each cycle. Thus, the irradiation-time interval associated with each library is derived from the input.

Then, the time-dependent cross-section libraries for ORIGEN-S are produced as follows. First the "PASS 0" ORIGEN-S library is produced from the fresh fuel densities and the power of the first cycle. It is applied to compute the densities at the midpoint time of the first, or "PASS 1", library. Note that each "pass" means the preparation of new data interfaces by SAS2, the return of control to the SCALE driver, the sequential execution of the five codes, and the return to SAS2. Next, in the procedure, SAS2: substitutes the computed midpoint densities properly, computes density-dependent parameters (i.e., those for NITAWL-S), increments required data set unit numbers, adds "PASS 1" to the ORIGEN-S library title, updates the time intervals at which ORIGEN-S saves densities to correspond to both the starting point and the midpoint of the irradiation-time interval of the second library, and rewrites all code interfaces with the new data. Then, the "PASS 1" library is produced by invoking execution of the five codes a second time with the new input interfaces. Each additional pass applies the same procedure as used for "PASS 1". The midpoint densities are applied to the neutronics analysis to produce a new library. The depletion computation applies this library and the densities for the start of the pass which were calculated in the last previous pass. A decay computation with zero power is applied for reactor downtime, if specified for the end of a cycle, before deriving densities for the next pass. All ORIGEN-S libraries are saved, starting with the "PASS 1" library.

The time-dependent densities applied in the neutronics analysis in the above procedure are obtained by different methods for the various types of materials. The heavy nuclides of the fuel, their activation products, and fission products are computed by ORIGEN-S. The densities of the clad, structural materials, moderator and fuel oxygen remain constant unless a change in the moderator densities is requested in the user input for the case. The fractional change in the water or boron density may be specified for each cycle. Also, the boron concentration is changed during the passes of a cycle if more than one library per cycle is requested. The boron density is assumed to vary linearly from 1.9 to 0.1 times its average (input) density during the time interval of the cycle. The value applied is determined from linear interpolation to the midpoints of each library time interval. This method is applied to somewhat approximate a typical decrease in the boron as a function of time for each cycle.

Up to this point, the purpose of the cross-section processing method presented above was to produce a set of burnup-dependent ORIGEN-S working libraries that apply to the specified fuel assembly during its irradiation history. Now, these libraries and the initial nuclide densities form the input to the ORIGEN-S depletion case. A separate depletion subcase is performed, in turn, for each of the input ORIGEN-S working libraries: 687 light elements, such as clad and structural materials; 101 actinides, including fuel nuclides and their decay and activation products; and 821 fission product nuclides. Ultimately, the discharge composition of the fuel assembly is determined. A decay-only subcase (six

equal-size time steps) is computed for the cooling time at which the fuel is to be loaded and shipped in the shipping cask. The calculated compositions are applied in both the final shipping cask analysis and the determination of neutron and gamma sources.

### 3.3.2 Advantages and Limitations

The SAS2 sequence was developed to be versatile, yet extremely easy to use. Within the limits of the neutronics calculation (to be discussed below), the SAS2 module allows the user to easily obtain spent fuel isotopics, radiation spectra, and decay heat for a reactor assembly and irradiation history specified by input. A complete sample input for a SAS2 case is shown in Fig. 3.2. In order, the SAS2 input consists of (1) a sequence specification (=SAS2) and title card; (2) the cross-section library specification (27GROUPSHLD) and fuel geometry type (LATTICECELL) to be used for the depletion analysis; (3) the fresh fuel, reactor moderator, and cask material specifications; (4) the lattice cell configuration (SQUAREPITCH) and geometric parameters; and (5) information for the fuel depletion and isotopic decay. The remaining input records specify the cross-section library, geometry, and fuel zones for the 1-D radial shielding analysis of the cask. However, the PARM=HALT03 on the first input card halted the SAS2 sequence after completion of the specified depletion and isotopic decay (after completion of PASS 3).

The input of Fig. 3.2 is for a Westinghouse 17 x 17 PWR assembly, with 3.2 wt %  $^{235}\text{U}$  depleted to 33 GWD/MTU. The irradiation history involved three cycles with 80% uptime and 20% downtime. A 5-year (1825 d) downtime on the last cycle represents the desired decay period for the spent fuel. The power per assembly is 17.3025 MW/assembly or 37.5 MW/MTU. Sixteen light elements are input for use by ORIGEN-S to account for activation of the assembly hardware. The first cross-section library specified in the input (27GROUPSHLD) is the basic 27 neutron group ENDF/B-IV library with a number of fission product nuclides added. Many nuclides (particularly all important actinides) have their cross sections updated automatically by SAS2 during the successive passes through NITAWL-S and XSDRNPM-S. However, the user can specify more nuclides to be updated by adding trace amounts of the nuclide to the fuel composition of the SAS2 input. The input of Fig. 3.2 shows the fission product nuclides often included as input in SAS2 cases run at ORNL.

Halting a SAS2 case after the depletion and decay provides the user with a large amount of flexibility. The user can use the restart file created by "HALT" to restart the SAS2 case using the cask specifications of the depletion case or an altered cask specification (compositions, geometry, etc.). In addition, utilizing the ORIGEN-S output file (containing isotopic data at discharge) created by the HALT case, the user can run an ORIGEN-S decay case to generate a new output file at any desired cooling time. This new ORIGEN-S output file (from the decay case) can be used in another SAS2 restart case to provide dose results at a different spent fuel cooling time.

While the basic solution scheme employed by SAS2 is excellent, it has its limitations in the 1-D neutronics treatment available with XSDRNPM-S. The neutronics analysis is performed on an infinite lattice having the uniform characteristics of the specified fuel pin cell. This idealized treatment falls short of the actual reactor environment where spatial variations within and between assemblies impact the spectral characteristics of the updated cross sections and neutron flux. The idealized neutronics model of SAS2 is its major limitation, but it also is a major factor contributing to many of the user-friendly characteristics of the module (e.g., simple input). No extensive work has been performed to show the effects that the SAS2 model limitations have on radiation source spectra and decay heat. However, the SAS2 documentation within the SCALE Manual<sup>4</sup> contains a section that has a more-detailed discussion of the limitations and uncertainties associated with using SAS2.

```

=SAS2      PARM=HALT03
PWR TYPICAL IRRADIATION HISTORY - 3.2% ENRICH - 33GWD/MTU
27GROUPSHLD  LATTICECELL
UO2  1 0.9017246 1000 92234 0.029 92235 3.2 92236 0.016 92238 96.755 END
SR-90  1 0 1-20 1000 END
Y-89   1 0 1-20 1000 END
ZR-94  1 0 1-20 1000 END
ZR-95  1 0 1-20 1000 END
NB-94  1 0 1-20 1000 END
TC-99  1 0 1-20 1000 END
RH-103 1 0 1-20 1000 END
RH-105 1 0 1-20 1000 END
XE-131 1 0 1-20 1000 END
XE-135 1 0 8.72-9 1000 END
CS-134 1 0 1-20 1000 END
CS-137 1 0 1-20 1000 END
BA-136 1 0 1-20 1000 END
LA-139 1 0 1-20 1000 END
PR-143 1 0 1-20 1000 END
ND-143 1 0 1-20 1000 END
ND-145 1 0 1-20 1000 END
PM-147 1 0 1-20 1000 END
SM-149 1 0 1-20 1000 END
SM-151 1 0 1-20 1000 END
SM-152 1 0 1-20 1000 END
EU-153 1 0 1-20 1000 END
EU-154 1 0 1-20 1000 END
ZIRCALLOY 2 1 1000 END
B-10   3 0 4.04045-6 583 END
B-11   3 0 1.75841-5 583 END
H2O    3 0.7078495 583 END
CO-59  3 0 1-20 583 END
SS304  4 2.13750-2 END
SS304  5 2.13750-2 END
SS304  6 2.17124-2 END
B4C    6 7.70660-2 END
H2O    7 1-12      END
SS304  8 1.0 END
U(.27)METAL 9 1.0 END
H2O    10 0.944 END
END COMP
SQUAREPITCH 1.25984 0.83566 1 3 0.94996 2 END
MORE DATA SZF=0.7 END
NPIN/ASSM=264 FUELNGTH=365.76 NCYCLES=3 NLIB/CYC=1
PRINTLEVEL=5 LIGHTEL=16
POWER=17.3025 BURN=293.3333 DOWN=73.33333 END
POWER=17.3025 BURN=293.3333 DOWN=73.33333 END
POWER=17.3025 BURN=293.3333 DOWN=1825 END
C 0.059993 N 0.033765 O 62.098 AL 0.045678
SI 0.065863 P 0.14216 TI 0.049832 CR 2.3398
MN 0.10963 FE 4.5991 CO 0.033443 NI 4.4021
ZR 100.83 NE 0.32753 MO 0.18156 SM 1.6518
27N-18COUPLE TEMPCASK(K)=394.27 NUMZONES=9 DRYFUEL=YES END
5 12.7532 6 21.732 4 38.0493 7 47.629 8 48.899 9 59.06 8 62.87 10 74.30 8 74.74
ZONE=1 FUELBNL=1 ZONE=3 FUELBNL=6
PRESSURE=50
END

```

Fig. 3.2. Sample input for SAS2 sequence.

### 3.3.3 New Developments for SAS2

Measured data available for spent fuel pins typically are for the actinide isotopics and total decay heat. Earlier work<sup>52</sup> reported that SAS2 provided rather good agreement with measured decay heat data but produced high results in comparison with measured actinide concentrations. Updates to SAS2 with the SCALE-3 release provided some improvements in the data libraries which further improved the comparisons with measured decay heat data. However, the problem of overestimating the actinide concentrations is due mostly to the neutronic limitations of SAS2 noted above.

Recently, development work has begun to improve the SAS2 sequence to account for the effect of guide tubes in an assembly. A substantial majority of LWR fuel assemblies contain guide tubes. These guide tubes may be used in as many as 9% of the positions for a PWR or 16% for a BWR. The guide tubes may contain the spider assemblies of (1) burnable poison rods, (2) control rods, (3) axial power shaping rods, (4) orifice rods, or others, or they may simply contain water. For all practical purposes, control rod assemblies are removed soon enough that only water should be considered within the tube for an accurate burnup calculation. The new SAS2 sequence is called SAS2H and employs a multiregion method of analysis to more nearly simulate the fraction of nonfuel rods in a given assembly. The SAS2H procedure uses two XSDRNPM-S calculations for each "PASS." The first calculation is the standard fuel pin cell calculation. The second calculation consists of the initial nonfuel unit cell (guide tubes plus inner material) surrounded by a fuel cell region with an area equal to the total fuel unit cell area per guide tube unit cell as found in the assembly.

Initial validation work with the SAS2H procedure shows a significant improvement in the calculated actinide concentrations in comparison to measured data. Table 3.3 shows the improvement that has been obtained. Current plans call for the inclusion of the SAS2H procedure within the SCALE-4 release.

Table 3.3. Comparison of measured and computed nuclide/<sup>238</sup>U atom ratios for Turkey Point assembly

| Nuclide           | SAS2, % <sup>a</sup><br>(3-Libs) <sup>b</sup> | SAS2H, %<br>(3-Libs) <sup>b</sup> |
|-------------------|---|-----------------------------------|
| <sup>234</sup> U  | 1.5   | 2.9                               |
| <sup>235</sup> U  | 3.0   | -4.9                              |
| <sup>236</sup> U  | 2.0   | 2.8                               |
| <sup>238</sup> U  | 0.0   | 0.0                               |
| <sup>238</sup> Pu | 18.2  | 3.7                               |
| <sup>239</sup> Pu | 18.9  | 2.4                               |
| <sup>240</sup> Pu | -4.4  | -8.9                              |
| <sup>241</sup> Pu | 23.1  | 6.1                               |
| <sup>242</sup> Pu | 2.2   | -2.9                              |
| U                 | 0.046   | -0.019                            |
| Pu                | 13.5  | -0.4                              |

<sup>a</sup>% difference = 100 x (calculated-measured)/measured.

<sup>b</sup>Used 3 burnup-dependent cross-section libraries, ENDF/B-IV data.

### 3.4 GRAPHICAL DISPLAY OF ORIGEN-S RESULTS

During the analyses of ORIGEN-S cases, or in the comparison of various results, the objectives may be more clearly presented through plotting of the code results. Most of the results produced by ORIGEN-S may be plotted by the PLORIGEN code which uses the DISSPLA software package.<sup>53</sup> Individual and total nuclide or element concentrations, in 15 different units, for example, may be plotted as a function of time. The various types of plots that may be made by PLORIGEN logically fall into three separate classes, briefly described as plots of dominant or selected isotopes or elements, plots of source spectra, and plots showing comparisons of similar parameters between cases.

The intent in designing the features of PLORIGEN was to permit a fairly extensive variety of plots and keep it rather easy to use. While a number of features are automatically available, at times the user may use an option that overrides the default feature. For example, the axis label used on the plot will be the built-in label for the requested units unless a label is input by the user; or, there is a provision to write out a serial-type drawing number. Furthermore, with only one exception, the data parameters may be input in any order. Also, defaults have been selected that should reduce the need to input many of the parameters. While the code always requires that the first four characters of a parameter name be given, more characters may be added to make the name more self-descriptive. The most important input to PLORIGEN is specification of the data set containing the ORIGEN-S output file.

Nuclides or elements to be plotted can be specified in three ways: (1) the symbols for those nuclides wanted may be input; (2) the code determines those with the largest quantities for the requested number to be compared; or, (3) both the dominant and the user-selected nuclides or elements may be combined on the plot. The total is also plotted, except when all of those compared are selected from the input. The dominant quantities are determined by ranking in accordance with values computed from a logarithmic numerical integration process over a requested time range. A legend on the plot identifies each nuclide or element curve. The radiation source spectra are plotted in units of  $(s\text{-MeV})^{-1}$  rather than  $s^{-1}$  as output by ORIGEN-S. This alteration allows intensities at different energies to be compared on an equal basis. For the photon source an energy intensity spectra in units of  $\text{MEV/s/MeV}$  may also be plotted. The photon spectra associated with each library (light element, fission product, actinide) can be requested or the total calculated gamma spectrum. For the neutron source the user can request the total, spontaneous fission, or  $(\alpha,n)$  sources be plotted. All spectral plots are logarithmic in intensity through a maximum of seven decades.

Case comparison-type plots are available to compare time-dependent totals of similar data (e.g., thermal power, from two or more different ORIGEN-S cases). The differences in the cases may be from variation in burnup,  $^{235}\text{U}$  initial enrichment, or reactor assembly types, as examples. Also, the plot may compare an ORIGEN-S case result with user input data from possibly another calculation or measurement. A legend line may be input to identify each curve. Instead of comparing totals, the plots may compare individual nuclides from different cases. While these plots may compare the totals for nuclides from all three libraries, they may be made to compare the totals from only one of the three types of libraries or the totals from the combination of actinide and fission product libraries.

Examples of each of the three types of plots are shown in Figs. 3.3-3.5.

PWR - 33 GWD/MTU - 3.3% U-235

# ORIGEN-S

ORNL DWG 85-13078

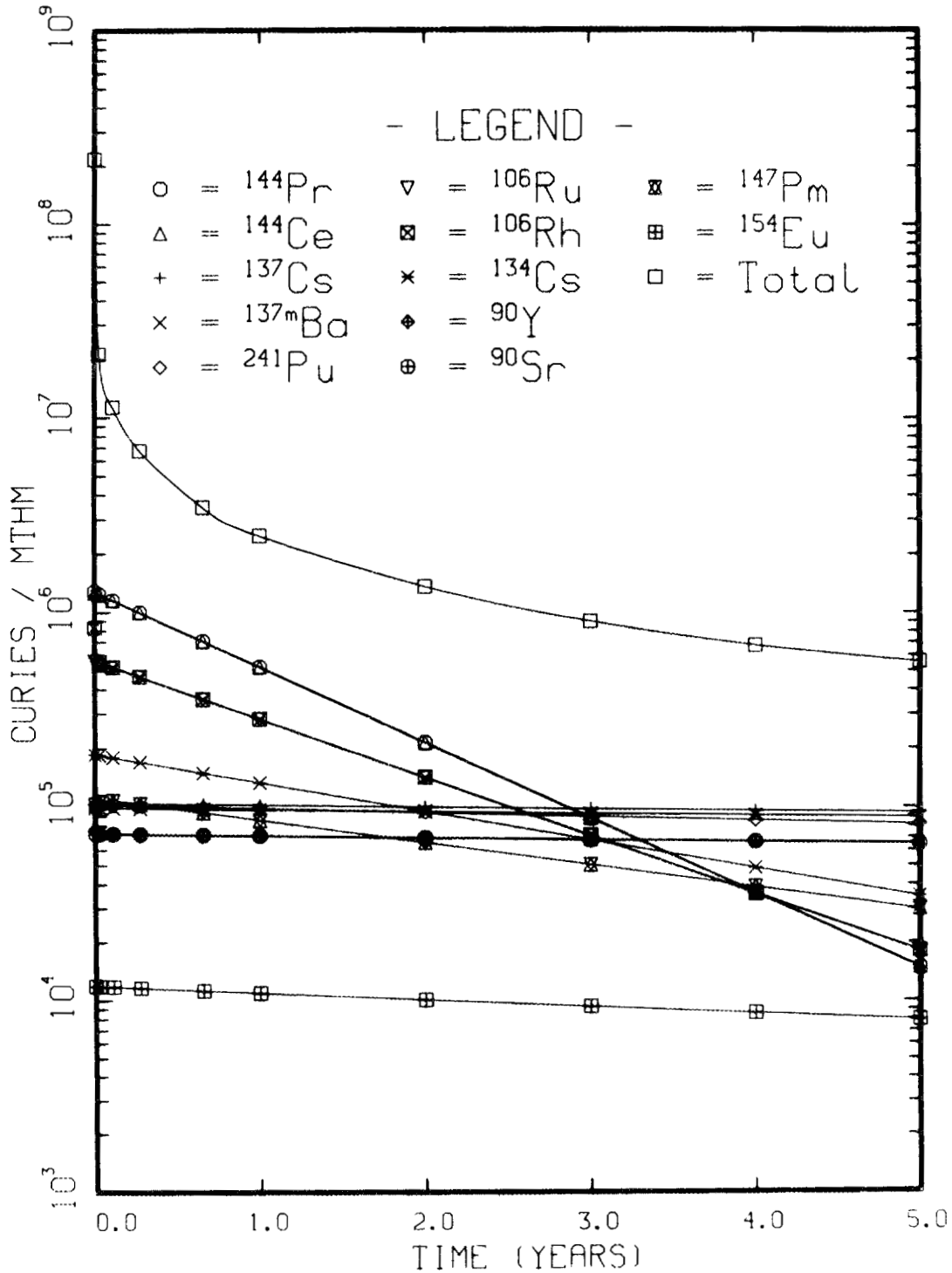


Fig. 3.3. Example of PLORIGEN plot of important nuclides.

# GAMMA SPECTRUM AT 1 YEAR ORIGEN-S

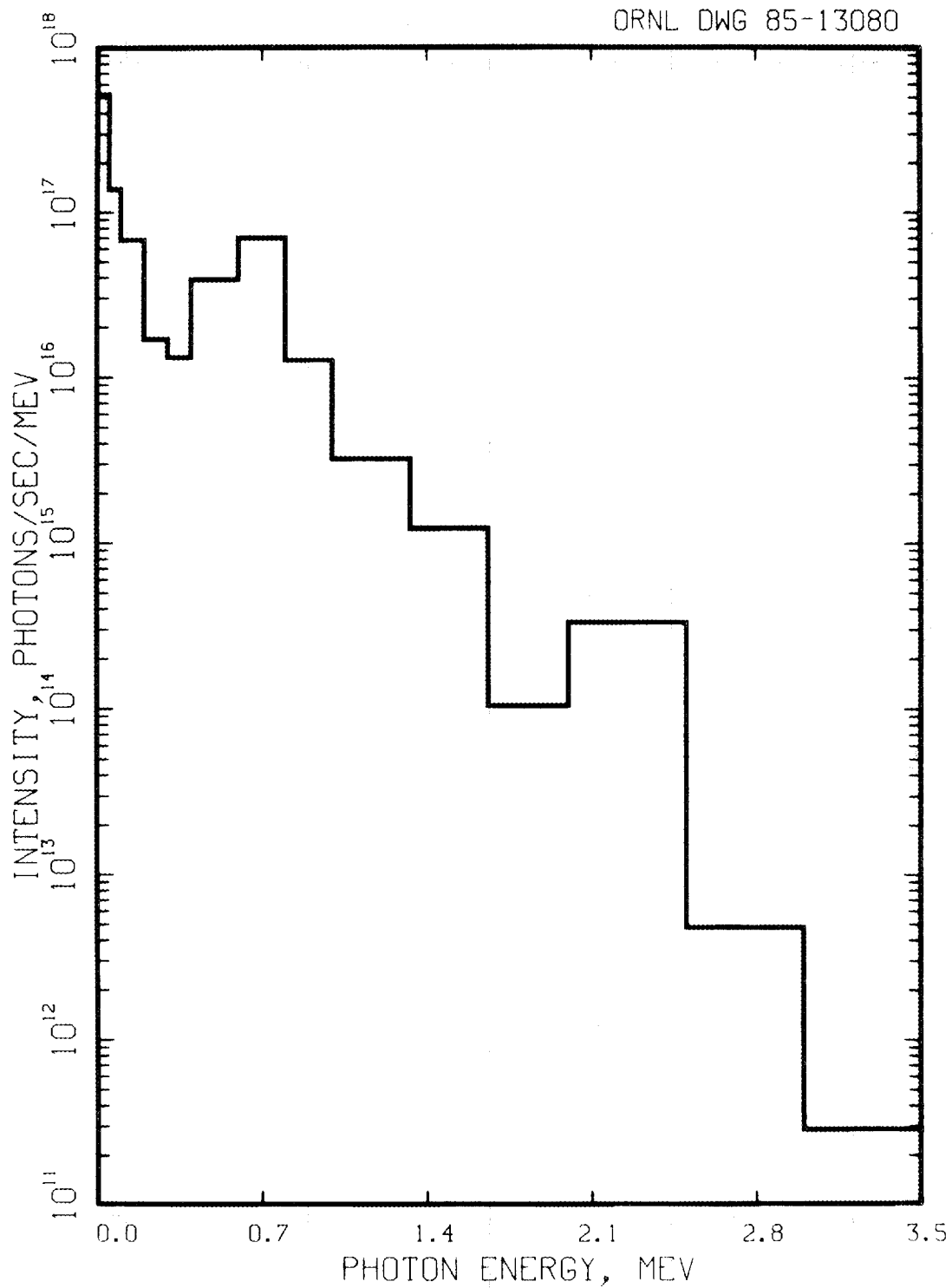


Fig. 3.4. Example of PLORIGEN plot of gamma spectrum.

# AFTERHEATS FOR 3 BURNUPS

## ORIGEN-S

ORNL DWG 85-13082

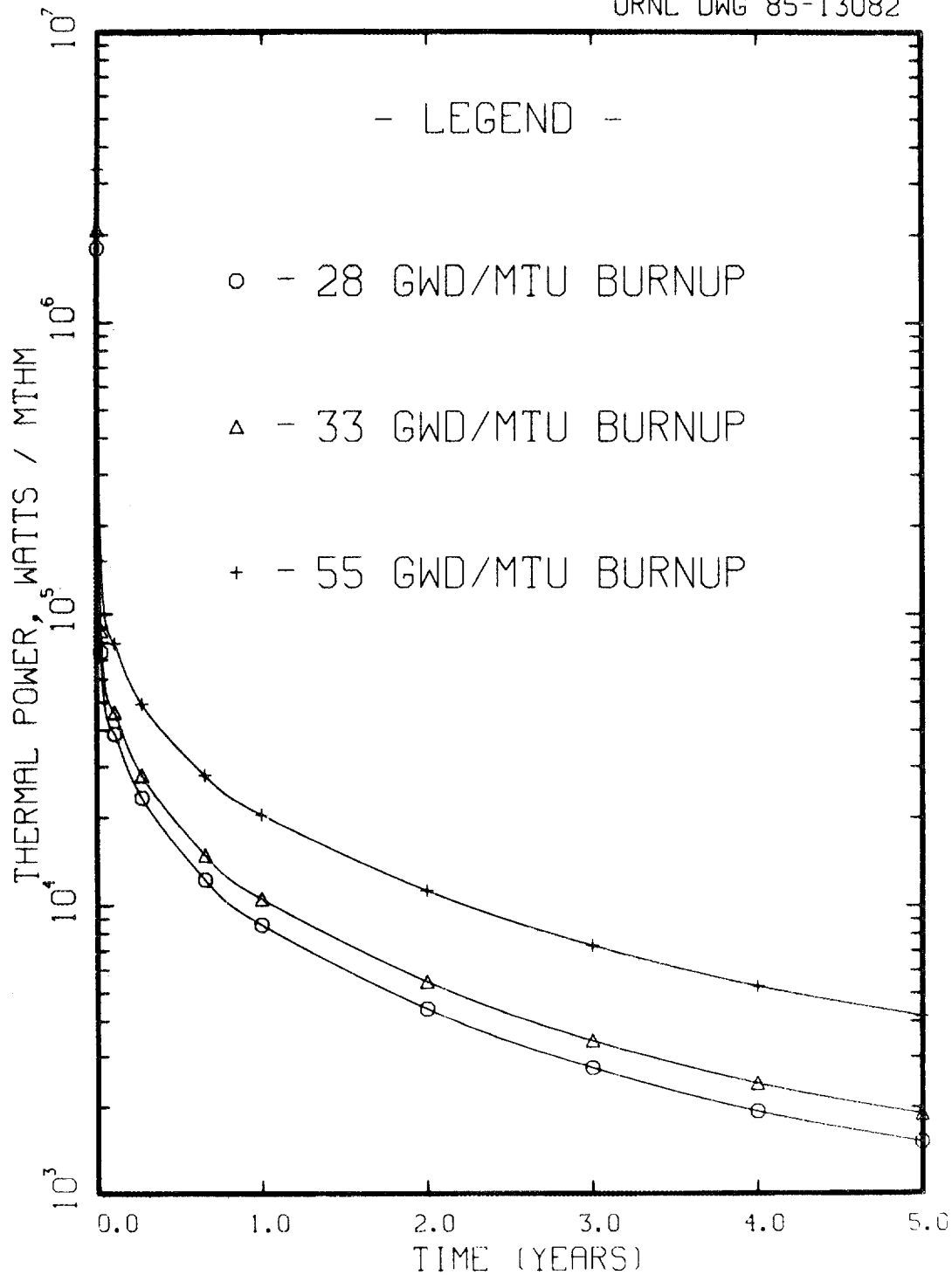


Fig. 3.5. Example of PLORIGEN plot comparing decay heat from three separate burnups.

### 3.5 SUMMARY

Computational tools for depletion and decay analysis of spent fuel have been included in the SCALE system to facilitate evaluation of radiation sources and decay heat. The depletion and decay technique is principally dependent on the well-known ORIGEN code, which has been updated for the SCALE system. One major benefit of ORIGEN-S is its capability to interface with multigroup cross sections and neutron fluxes via the COUPLE code. Gamma and neutron source strengths and spectra are also evaluated by ORIGEN-S in the multigroup format input by the user. Burnup-dependent binary libraries for use by ORIGEN-S can be created in SCALE via the SAS2 module or directly by the COUPLE code from burnup-dependent neutronic data on an AMPX working library. Recent modifications to the SAS2 sequence have been made in-house to improve the neutronics calculations within the current SAS2 procedure.

The overall goal of developing the SCALE modules was to provide an easy-to-use, yet versatile, tool. The modules described in this section are designed to allow a user to quickly and accurately obtain the spent fuel data needed for subsequent shielding and heat transfer analyses. Graphical display of isotopic data, decay heat, or radiation spectra is also easily obtained with the PLORIGEN code.

## 4. COMPUTATIONAL METHODS FOR CRITICALITY SAFETY ANALYSIS

The initial emphasis for the SCALE computational system was on developing the cross-section libraries and tools to enable automated cross-section processing and accurate criticality safety analysis with a user-friendly, free-form input format. Work on development of the cross-section libraries and processing techniques has been reviewed in Sect. 2. This paper will review the functional modules and analytic sequences used in SCALE to calculate effective multiplication factors ( $k_{\text{eff}}$ ).

The XSDRNPM-S module is one of the major computational tools within SCALE. For criticality analyses, XSDRNPM-S is used to obtain  $k_{\text{eff}}$  for one-dimensional (1-D) systems. For multidimensional systems, the KENO IV and KENO V.a codes have been included in SCALE. The reason for including both of these KENO versions in SCALE should be explained. When work began in the late 1970s on the first Criticality Safety Analysis Sequences (CSAS) for SCALE, KENO IV was the established code<sup>54</sup> in use by analysts. The development of KENO V was still in progress. Thus, in order to meet development goals the first criticality safety analysis sequence for multidimensional systems (CSAS2) used the KENO IV code. The completion of KENO V, and later KENO V.a, and their inclusion in the CSAS4 control module rendered the analysis capabilities of KENO IV and CSAS2 redundant. However, it was determined that many established users of KENO IV were not willing to shift to KENO V. Also, the CSAS2 sequence had been heavily used in cross-section validation efforts for the SCALE project and was being widely used by safety analysts. Thus, to date, both KENO IV and KENO V.a are maintained within the SCALE system. However, current plans call for KENO IV and CSAS2 to be removed from SCALE-4. All three of these functional modules (XSDRNPM-S, KENO IV, and KENO V.a) will be reviewed briefly in this paper, although emphasis will be placed on the KENO V.a module. The major differences between the two KENO versions will be highlighted. More detailed information can be obtained from Sects. F3, F5, and F11 of the SCALE Manual.<sup>4</sup>

Two control module programs have been developed in SCALE for criticality safety analysis. However, these two programs allow many different sequences to be run. The initial control module was released with the SCALE-0 package and contains Criticality Safety Analysis Sequence No. 1 (CSAS1) and Criticality Safety Analysis Sequence No. 2 (CSAS2). The CSAS1 sequence uses the XSDRNPM-S module to obtain  $k_{\text{eff}}$  for one-dimensional unit cells or "multiregion" systems in slab, cylindrical, or spherical geometry. Infinite homogeneous media calculations can also be performed. The CSAS2 sequence calculates  $k_{\text{eff}}$  for multidimensional systems using the KENO IV module. These sequences are documented in detail in Sects. C1 and C2 of the SCALE Manual.<sup>4</sup>

The second criticality analysis control module was released with SCALE-2 and updated with the SCALE-3 release. This program is typically designated as Criticality Safety Analysis Sequence No. 4 (CSAS4), but it provides for eight different sequences that can be executed. These sequences are all basically subsets of the CSAS4X sequence which does resonance cross-section processing, cell weights cross sections via XSDRNPM-S, performs a multidimensional  $k_{\text{eff}}$  calculation with KENO V.a, and then modifies the geometry and iterates until the specified value of  $k_{\text{eff}}$  is obtained. All the analysis capabilities of the CSAS1/CSAS2 control module are within the CSAS4 control module. However, many analysts still use the CSAS2 sequence in particular because of their familiarity with KENO IV. This paper will concentrate on the features of the CSAS4 control module (documented as Sect. C4 of ref. 4), although the differences between the two control module programs will be presented.

### 4.1 REVIEW OF FUNCTIONAL MODULES FOR CRITICALITY SAFETY ANALYSIS

#### 4.1.1 One-Dimensional Analyses

Because of their high importance in system safety, criticality analyses are typically done with extreme detail and rigor. Although truly one-dimensional (1-D) systems are difficult to find in practice,

criticality safety analyses of 1-D models are often performed for scoping work and/or studies where the reactivity effects (i.e., the change in  $k_{\text{eff}}$ , are evaluated). The XSDRNPM-S module is employed in SCALE to obtain  $k_{\text{eff}}$  values for 1-D systems.

XSDRNPM-S is a highly evolved discrete ordinates transport program which has a wide variety of features. Its origins trace back to the popular ANISN program, which pioneered the treatment of anisotropic scattering in discrete ordinates calculations. With sufficient angular quadrature and spatial mesh specifications, highly precise solutions to one-dimensional transport problems are obtained. The preciseness of the solutions are what make the XSDRNPM-S module desirable for studying system changes that provide only a small reactivity change.

The finite differencing in XSDRNPM-S is done with the weighted diamond-difference model with weighting parameters chosen on the basis of experience with the DOT IV code.<sup>26</sup> As default, angular quadrature sets are calculated in an automatic fashion for the appropriate one-dimensional geometry. Scattering expansion can be treated to whatever order is provided in the cross-section sets. Boundary conditions on the angular fluxes can be specified as vacuum, reflected, periodic, white, or user-supplied albedos. Also, transport in the transverse direction can be approximated with geometric buckling losses or with void streaming corrections.

A number of search options are available in XSDRNPM-S. For a specified system multiplication factor, one can perform a zone width search, an outer boundary search, or a buckling loss search. Also, direct searches can be performed to determine alpha, the coefficient of the exponential variation of the flux, or a direct determination of buckling losses.

Convergence in XSDRNPM-S is determined by tests on several quantities. The point values of the scalar fluxes must vary by less than a prescribed amount between outer iterations. Also, the ratio of source terms and scattering rates (up and down in energy) between outer iterations must converge. Provision is made for banding thermal groups and thereby accelerating upscatter convergence.

#### 4.1.2 Multidimensional Analysis

The KENO family of Monte Carlo codes have become perhaps the most-used computational tools for detailed criticality analysis. The original KENO code was developed in the late 1960s at Oak Ridge National Laboratory.<sup>1</sup> In 1975, a significantly improved version of the code was released as KENO IV,<sup>54</sup> which subsequently was included in the original SCALE system release (SCALE-0) in 1980. In 1982, the KENO V version of the family was released with the SCALE-1 release. Work to enhance the geometry modeling features led to the replacement of KENO V with KENO V.a in the SCALE-3 release. This section will review the basic theory and modeling techniques used in all of these codes and highlight the differences between the various SCALE versions.

The KENO codes all solve a multi-energy-group form of the Boltzmann transport equation. Monte Carlo techniques are employed to iteratively solve the equation for the largest eigenvalue ( $k_{\text{eff}}$ ) of the homogeneous integral equations. The definition of  $k_{\text{eff}}$  may be given as the ratio of the number of neutrons in the  $(n+1)$ th generation to the number of neutrons in the  $n$ th generation. Other quantities that are calculated include lifetime and generation time, energy-dependent leakages, energy- and region-dependent absorptions, fissions, fluxes, and fission densities.

Like other neutronic Monte Carlo codes, KENO tracks particle "histories" through the specified geometry to obtain such information as the space- and energy-dependent scattering source, fission source, and collision density. A collision occurs in a geometrical region when a history exhausts its mean free path length within the boundaries of the region. For each collision, the absorbed weight and the fission weight are tabulated, then the weight is modified by the nonabsorption probability. This new

weight is checked for splitting and Russian roulette,<sup>55</sup> and if it survives, the history is scattered. A new energy group is selected from the cumulative transfer probability distribution.

Anisotropic scattering is treated by using discrete scattering angles. The angles and associated probabilities are generated in a manner that preserves the moments of the angular scattering distribution for the selected group-to-group transfer. These moments can be derived from the coefficients of a  $P_n$  Legendre polynomial expansion. All moments through the  $2n-1$  moment are preserved for  $n$  discrete scattering angles. A one-to-one correspondence exists such that  $n$  Legendre coefficients yield  $n$  moments. The cases of zero and one scattering angle are treated in a special manner. KENO V can recognize that the distribution is isotropic even if the user specifies multiple scattering angles, and therefore selects from a continuous isotropic distribution. If the user specifies one scattering angle, the code performs semicontinuous scattering by picking scattering angle cosines uniformly over some range (range selected such that first moment is preserved) between  $-1$  and  $+1$ . The probability is zero over the rest of the range.

In order to minimize the statistical deviation of  $k_{\text{eff}}$  per unit computer time, weighted tracking is utilized rather than analog tracking. Weighted tracking accounts for absorption by reducing the neutron weight, rather than allowing the neutron history to be terminated by absorption. To prevent expending excessive computer time tracking low-weight neutrons, Russian roulette is played when the weight of the neutron drops below a preset value, WTLOW. Neutrons which survive Russian roulette are assigned a weight, WTAVG. The value of WTLOW and WTAVG can be assigned as a function of position and energy. The values used are the following:

DWTAV = 0.5, the default value of WTAVG;

WTAVG = DWTAV, the weight given a neutron that survives Russian roulette; and

WTLOW = WTAVG/3.0, the value of weight at which Russian roulette is played.

A study by Hoffman<sup>55</sup> shows these default values to be reasonable for bare critical assemblies.

Inside a fissile core, the importance of a neutron is a slowly varying function in terms of energy and position. Hence, for many systems, the standard defaults for WTLOW and WTAVG are good values to use. For reflectors, however, the worth of a neutron varies both as a function of distance from the fissile material and as a function of energy. As a neutron in the reflector becomes less important relative to a neutron in the fissile region, it becomes desirable to spend less time tracking it. Therefore, a space- and energy-dependent weighting or biasing function is used to allow the user to minimize the variance in  $k_{\text{eff}}$  per unit tracking time. When a biasing function is used in a reflector, it becomes possible for a neutron to move from one importance region into another whose WTLOW is greater than the weight of the neutron. When this occurs, Russian roulette is played to reduce the number of neutrons tracked. When the reverse occurs, that is, the neutron moves to a region of higher importance, its weight may be much higher than WTAVG for that region. When the weight of the neutron is greater than a preset value, WTHI, the neutron is split into two neutrons, each having a weight equal to one-half the weight of the original neutron. This procedure is repeated until the weight of the split neutron is less than WTHI. The default value for WTHI is WTAVG\*3.0. WTHI is the weight at which splitting occurs.

The weighting or biasing function for a given core material and reflector material can be obtained by using the adjoint solution from  $S_n$ -type programs for a similar (usually simplified) problem. This adjoint flux gives the relative contribution of a neutron at a given energy and position to the total fissions in the system. The weighting function for KENO is thus proportional to the reciprocal of the adjoint flux. Although such a function can be difficult to obtain, the savings gained makes the effort worthwhile for many of the materials that are frequently used as reflectors. Biasing functions have been prepared for several reflector materials commonly used in KENO calculations. The use of biasing to minimize the

variance in  $k_{\text{eff}}$  per unit computer time will usually increase the variance in other parameters such as leakage or absorption in the reflector.

Arrays reflected by thick layers of material having a small absorption to scattering ratio may require large amounts of computer time to determine  $k_{\text{eff}}$  because of the relatively long time a history may spend in the reflector. A differential albedo technique was developed for use with the KENO codes to eliminate tracking in the reflector. This technique involves returning a history at the point it impinges on the reflector and selecting an emergent energy and polar angle from a joint density function dependent upon the incident energy and polar angle. The weight of the history is adjusted by the fractional return from the reflector, which is also based on the incident energy and angle.

Because differential albedos are expensive and time-consuming to generate, those corresponding to the Hansen-Roach 16-energy-group structure are the only differential albedos currently available for use with KENO. In the past, their use was limited to problems utilizing cross sections having the Hansen-Roach 16-energy-group structure. KENO V extends the use of differential albedos to other energy group structures by allowing appropriate energy transfers. This extension is accomplished by creating lethargy boundary tables for the albedo group structure and the cross-section group structure and determining the lethargy interval corresponding to the desired transfer (cross-section group structure to albedo group structure or vice versa) based on a uniform lethargy distribution over the interval. When the energy group boundaries of the cross sections and albedos are different, the results should be scrutinized by the user to evaluate the effects of the approximations.

A new feature incorporated in KENO V is the capability of supergrouping energy-dependent information, which includes the cross sections, albedos, pointer arrays, weights, leakages, absorptions, fissions, and fluxes. If the available computer memory is too small to hold all the problem data at once, KENO V automatically determines the number of supergroups necessary to allow execution of the problem. Thus, larger problems can be run on smaller computers.

KENO V incorporates a versatile and convenient restart capability. Certain changes can be made when a problem is restarted, including the use of a different random sequence and turning off certain print options such as fluxes or the fissions and absorptions by region.

One major reason for the success of KENO IV as a popular analytic tool is its efficient and easy-to-use geometry package. In light of the recent geometry enhancements of KENO V.a, this standard KENO IV geometry is often referred to as the "simple geometry." The simple geometry is three-dimensional and allows for the simultaneous use of cuboids, spheres, hemispheres, cylinders, hemicylinders, and an embedded array of such bodies. Each geometry shape defines a region, and each shape is input via keywords (SPHERE, CUBE, etc.) and appropriate dimensions. The regions can be nested one outside another to construct a desired object. Each region must be completely enclosed by the next larger region (tangency and common faces are allowed, but intersecting regions are not). This procedure is used to describe box types, each of which may contain a different geometry configuration. The box types can then be stacked together to form a three-dimensional array of units. When stacking box types, the outermost region must be a cube or cuboid, and the adjacent faces of adjacent box types must be the same size. Once an array has been described, a reflector can be built around the array by using the automatic reflector option, building it of geometry keywords enclosing the entire array, or using the albedo feature.

The original KENO V version made only one change to the simple geometry by allowing a user to specify the origins for cylinders, hemicylinders, spheres, and hemispheres. This modification allows the use of nonconcentric cylindrical and spherical shapes and provides a great deal of freedom in positioning them. The major modeling extensions to the KENO geometry came with the KENO V.a version, which

replaced the KENO V version with the SCALE-3 release. Cylindrical and spherical vessels that are partially filled in the radial direction can now be easily modeled because the cut surface for hemicylinders and hemispheres can be placed at any distance between the radius and the origin (rather than at the origin only).

However, the most outstanding KENO V.a geometry advancement is the addition of the "array of arrays" and "holes" capabilities. The array-of-arrays option allows the construction of arrays from other arrays. The depth of nesting is limited only by computer space restrictions. This option greatly simplifies the setup for arrays involving different units at different spacings. The hole option allows placing a unit or an array at any desired location within a geometry region. The emplaced unit or array cannot intersect any geometry region and must be wholly contained within a region. As many holes as will snugly fit without intersecting can be placed in a region. This option is especially useful for describing transport/storage casks, storage pools, and reflectors that have gaps or other geometrical features. Any number of holes can be described in a problem, and holes can be nested to any depth. With the exception of holes, each geometry region in a unit must completely enclose each interior unit.

These new features in KENO V.a allow the modeling of complex geometry configurations not possible with KENO IV. As an example, consider a typical shipping cask model illustrated by Fig. 4.1. Note that a very detailed model of the shipping cask can be obtained. The shipping cask contains seven 17 x 17 PWR fuel assemblies, with each pin in each assembly modeled. The rods placed between the fuel assemblies are B<sub>4</sub>C rods with stainless steel cladding. The geometry input consisted of only 53 statements. The stand-alone KENO V.a calculation took 8 min of IBM 3033 cpu time for 30,000 histories and yielded a  $k_{\text{eff}}$  of  $0.954 \pm 0.004$ .

In order to confirm the accuracy of the geometry description, KENO V.a provides an option to generate two-dimensional printer plots at any given slice through the geometry. The value plotted may be specified to be either the material (mixture number) by location, or the unit number by location. Any number of plots can be made. KENO V.a will allow generation of the plots with or without executing the problem.

The KENO V.a geometry package does have two major restrictions: (1) intersections are not allowed, and (2) the geometric shapes must be oriented along orthogonal axes and cannot be rotated. Although a hindrance for some problems, these limitations allow particle tracking to be done in a much faster and more efficient manner than could be done otherwise. Given some time and patience, a clever and/or experienced user can model many complex geometries that wouldn't seem possible with the above restrictions and/or available body types.

The above review has provided some information on the similarities and differences between KENO IV and KENO V.a. Other differences that have not been noted are listed below.

1. KENO IV allows the user to select one fission spectrum, but KENO V and KENO V.a provide for mixed fission spectrums based on the fissile content.
2. KENO V and KENO V.a added a periodic boundary condition option.
3. KENO IV uses the 16-group KENO formatted library or an AMPX working library format. KENO V and KENO V.a allow only an AMPX working library format.
4. KENO IV allows specified  $k_{\text{eff}}$  searches to be made on the dimensions of a unit, the spacing between units, or on the number of units in an array. An improved search technique using KENO V.a is currently automated in SCALE with the CSAS4 control module, but is not allowed in the stand-alone KENO V.a module.

ORNL - DWG 83 - 12797

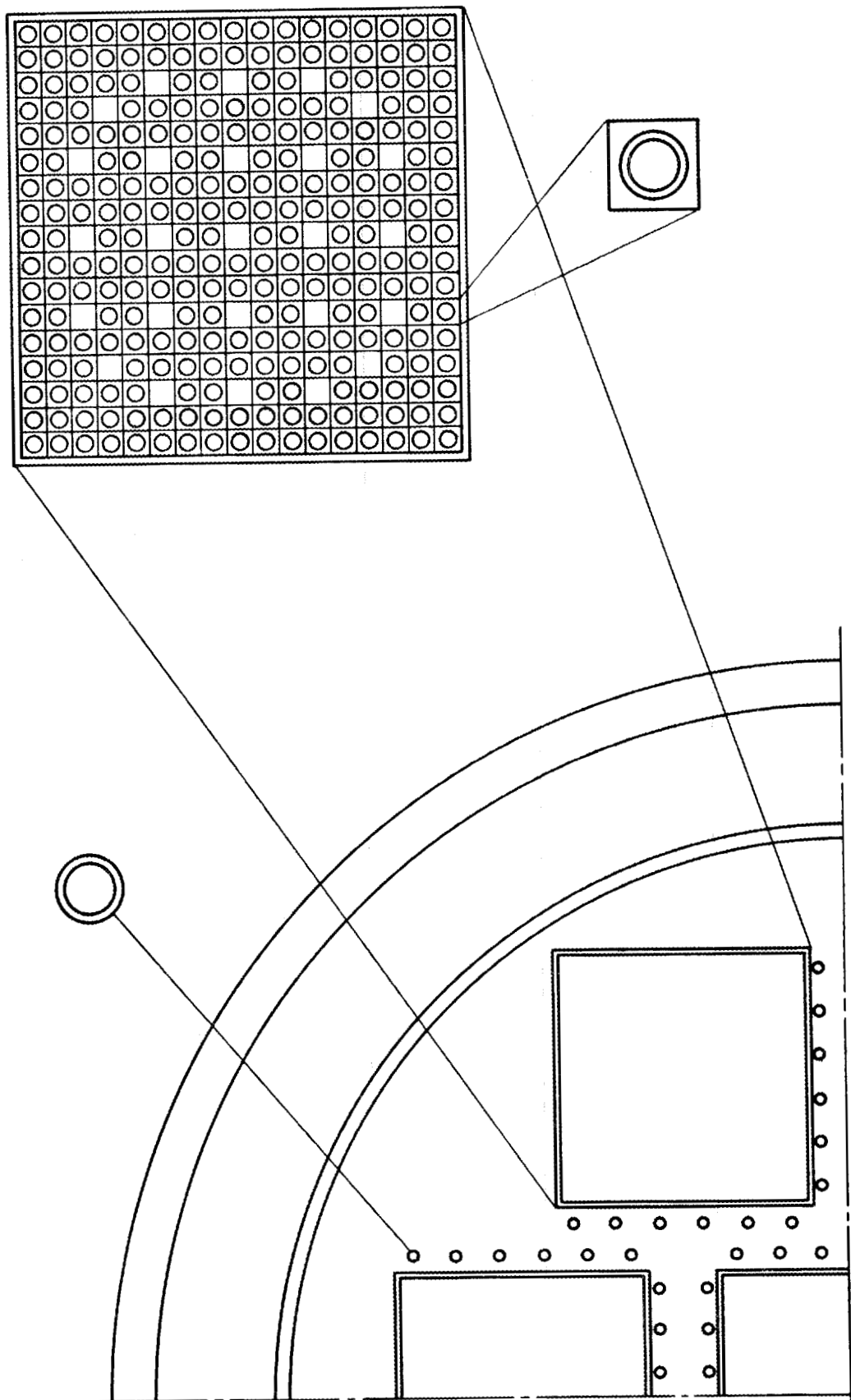


Fig. 4.1. Cross section of a typical PWR shipping cask model for KENO V.a.

5. The KENO V data input features flexibility in the order of input. The single restriction is that the title must be entered first and the parameter data, if any, must follow immediately. A large portion of the data has been assigned default values that have been found to be adequate for many problems. This enables the user to run a problem with a minimum of input data. Blocks of input data are entered in the form:

READ XXXX input data END XXXX

where XXXX is the keyword for the type of data being entered. The types of data entered include parameters, geometry region data, array definition data, biasing or weighting data, albedo boundary conditions, starting distribution information, the cross-section mixing table, extra 1-D (reaction rate) cross-section IDs for special applications, and printer plot information. A block of data can be omitted unless it is needed or desired for the problem. Within the blocks of data, most of the input is activated by using keywords to override the default values.

## 4.2 REVIEW OF THE CRITICALITY SAFETY ANALYSIS SEQUENCES

### 4.2.1 Description of Sequences

The Criticality Safety Analysis Sequences (CSAS) available in SCALE-3 are shown in Table 4.1, together with the functional modules that each accesses. All the sequences perform the automated cross-section processing and material composition setup as described in Sect. 2. The first two sequences in Table 4.1 make up the CSAS1/CSAS2 control module program while the last eight sequences are provided in the CSAS4 control module program.

The CSAS1 sequence basically provides an easy-to-use tool for calculating  $k_{\text{eff}}$  for one-dimensional systems via the XSDRNPM-S code. Calculations for unit cell geometries, large multiregion geometries or infinite homogeneous mediums can be performed in slab, cylindrical, or spherical geometries. An automatic mesh generator is incorporated to provide the spatial mesh for XSDRNPM-S (see Sect. C1.2.5 of the SCALE Manual<sup>4</sup>). The CSAS2 sequence was developed to obtain  $k_{\text{eff}}$  for multidimensional systems using the KENO IV code. As noted in Table 4.1, the execution path for CSAS2 actually includes XSDRNPM only when one specifically uses mixture 500 in the multidimensional problem description. If mixture 500 is not used anywhere, the XSDRNPM step is skipped and the cross-section data produced by NITAWL are used in KENO IV directly.

Table 4.1. Functional modules executed by the Criticality Safety Analysis Sequences

| Analytic sequence | Search function | Functional modules executed by the control module |          |                        |       |          |
|-------------------|-----------------|---|----------|------------------------|-------|----------|
|                   |                 | BONAMI-S  | NITAWL-S | XSDRNPM-S              | ICE-S | KENO V.a |
| CSAS1             | No search       | BONAMI-S  | NITAWL-S | XSDRNPM-S              |       |          |
| CSAS2             | No search       | BONAMI-S  | NITAWL-S | XSDRNPM-S <sup>a</sup> |       | KENO IV  |
| CSASN             | No search       | BONAMI-S  | NITAWL-S |                        |       |          |
| CSAS1X            | No search       | BONAMI-S  | NITAWL-S | XSDRNPM-S              |       |          |
| CSASI             | No search       | BONAMI-S  | NITAWL-S |                        | ICE-S |          |
| CSASIX            | No search       | BONAMI-S  | NITAWL-S | XSDRNPM-S              | ICE-S |          |
| CSAS25            | No search       | BONAMI-S  | NITAWL-S |                        |       | KENO V.a |
| CSAS2X            | No search       | BONAMI-S  | NITAWL-S | XSDRNPM-S              |       | KENO V.a |
| CSAS4             | Search          | BONAMI-S  | NITAWL-S |                        |       | KENO V.a |
| CSAS4X            | Search          | BONAMI-S  | NITAWL-S | XSDRNPM-S              |       | KENO V.a |
|                   |                 |   |          |                        |       | MODIFY   |
|                   |                 |   |          |                        |       | MODIFY   |

<sup>a</sup>Optionally accessed if mixture 500 used.

The last eight sequences listed in Table 4.1 are contained within the CSAS4 control module program. An X at the end of a sequence name (e.g., CSAS1X) always denotes that XSDRNPM-S is used to create a cell-weighted mixture. The automatic mesh generator developed for the CSAS1 sequence is used to generate a spatial mesh for XSDRNPM-S. The sequences CSASN through CSASIX of Table 4.1 provide a convenient scheme for generating cross-section libraries for use in stand-alone modules. The last four sequences of Table 4.1 are available for multidimensional  $k_{\text{eff}}$  calculations and searches using the KENO V.a module.

Table 4.2 provides a description of the primary product from each analytic sequence and the cross-section libraries available for future use. In reviewing the sequences available in the CSAS4 control module, it should be evident that (1) CSAS1X is like the CSAS1 sequence **except** a cell-weighted library is produced, and (2) the CSAS25 and CSAS2X sequences are functionally the same as the CSAS2 sequence **except** CSAS25 and CSAS2X use KENO V.a rather than KENO IV.

Table 4.2. Primary products from sequences in CSAS4 control module

| Module name | Primary product  | Unit numbers of generated cross-section libraries |                |                |                 |
|-------------|--|---|----------------|----------------|-----------------|
|             |  | 2 <sup>a</sup>                                    | 3 <sup>b</sup> | 4 <sup>c</sup> | 14 <sup>d</sup> |
| CSASN       | Resonance-corrected working library                          |   |                | X              |                 |
| CSAS1X      | XSDRNPM eigenvalue calculation                               |   | X              | X              |                 |
| CSASI       | Resonance-corrected mixture cross-section MORSE/KENO library | X   |                | X              | X               |
| CSASIX      | Resonance-corrected cell-weighted mixed cross-section        | X   | X              | X              | X               |
| CSAS25      | KENO V $k_{\text{eff}}$                                      | X   |                | X              | X               |
| CSAS2X      | KENO V $k_{\text{eff}}$ using homogenized cell               | X   | X              | X              | X               |
| CSAS4       | Dimension alterations  | X   |                | X              | X               |
| CSAS4X      | Dimension alterations using homogenized cell                 | X   | X              | X              | X               |

<sup>a</sup>Resonance-corrected mixed working library from ICE-S.

<sup>b</sup>Resonance-corrected cell-weighted working library from XSDRNPM-S.

<sup>c</sup>Resonance-corrected working library from NITAWL-S.

<sup>d</sup>Resonance-corrected mixed cross-section MORSE/KENO library from ICE-S.

The search capability developed for the CSAS4 and CSAS4X sequences are controlled by the MODIFY module. As released in SCALE-1, the search capabilities of CSAS4 and CSAS4X were limited to an optimum pitch search for the maximum  $k_{\text{eff}}$  value. When the CSAS4 program was updated (SCALE-3) to use KENO V.a, the search capabilities were expanded to allow searches for the geometry associated with the maximum, the minimum, or a specified  $k_{\text{eff}}$  value. The user specifies whether the pitch (center-to-center spacing) or the dimensions of one or more geometry regions will be varied to obtain the desired  $k_{\text{eff}}$ . Because only an initial value of  $k_{\text{eff}}$  and a set of boundary constraints are available, four initial points are generated as nearly equally spaced as possible within the parameter constraints. The search package identifies the type of cubic equation [i.e., a cubic with no local extrema (type A), or a cubic with two local extrema (type B)], and utilizes this knowledge in determining the

pitch corresponding to the required  $k_{\text{eff}}$  value. The solution scheme is an iterative procedure that makes use of all previous information to modify the geometry and determine when the desired  $k_{\text{eff}}$  value has been achieved.<sup>56</sup> The number of iterations and the convergence criteria for the search can be optionally input.

The input data for the CSAS sequences of Table 4.2 are composed of three broad categories of data. The first (Material Information Processor, including Standard Compositions Data and Geometry Specification) specifies the cross-section library and defines the composition of each mixture and the cell geometry that is used to process the cross sections (see Fig. 2.3). This data block is all that is necessary for CSASN, CSASIX, CSASI, and CSASIX. The second category of data is the KENO V.a input data, which are used to specify the geometric model and boundary conditions that represent the physical configuration of the problem. Both data blocks are required for CSAS25 and CSAS2X. The last category of data is the search data. All three data blocks are required for CSAS4 and CSAS4X. Table 4.3 indicates the basic input data requirements of these CSAS sequences. To check the input data without actually processing the cross sections, the words "PARM=CHECK" or "PARM=CHK" should be entered, starting in column 11 of the analytical sequence specification for IBM versions. For example, =CSAS4 PARM=CHK would cause the input data for CSAS4 to be checked and appropriate error messages to be printed. If plots are specified in the data, they will be printed. This feature allows the user to debug and verify the input data using a minimum of computer time. Many problems can be checked (including plots) in ten seconds or less (IBM 3033). The CSAS1/CSAS2 control module requires data block input similar to the first two blocks noted above except KENO IV rather than KENO V.a input data are needed. The PARM=CHECK and plot features noted above are not available in CSAS1/CSAS2.

Table 4.3. Table of input data requirements for sequences in CSAS4 control module program

| Summary of data input requirements (see Sect. C4.4.2) |                     |         |         |         |         |         |        |        |
|---|---------------------|---------|---------|---------|---------|---------|--------|--------|
| Type of Data  | Analytical Sequence |         |         |         |         |         |        |        |
|   | =CSAS4              | =CSAS4X | =CSAS25 | =CSAS2X | =CSAS1X | =CSASIX | =CSASN | =CSASI |
| 1 Analytical sequence specification (IBM versions)    |                     |         |         |         |         |         |        |        |
| 2 Material information processor data                 | yes                 | yes     | yes     | yes     | yes     | yes     | yes    | yes    |
| 3 KENO V data   | yes                 | yes     | yes     | yes     | no      | no      | no     | no     |
| 4 Search data   | yes                 | yes     | no      | no      | no      | no      | no     | no     |
| 5 END for the analytical sequence (IBM versions)      | yes                 | yes     | yes     | yes     | yes     | yes     | yes    | yes    |

The data input required to obtain the optimum pitch for an array of fuel bundles in a square aluminum cask is shown in Fig. 4.2. The input utilizes a cell-weighted mixture (500) to represent a PWR-like fuel bundle. The cask contains a 2 x 2 x 1 array of fuel bundles. Each fuel bundle consists of a 17 x 17 x 1 array of zirconium clad, 2.35% enriched UO<sub>2</sub> fuel pins arranged in a square pitch. The pin diameter is 0.823 cm, and its length is 366 cm. The clad is 0.1393 cm thick, and the pitch is 1.275 cm. Each fuel bundle is contained in a 0.6615-cm-thick boral sheath. The bundles are separated by 1 cm of water, representing a flooded cask. The square aluminum cask is 10 cm thick on all faces and is reflected by 15 cm of water. The input consists of a sequence keyword, title, cross-section library specification (HANSEN-ROACH), MIPLIB geometry keyword (LATTICECELL), standard composition input, fuel pin cell specification, KENO V data, and search data (OPTIMUM PITCH). The output from the above sample problem indicated a maximum  $k_{\text{eff}}$  value of  $0.754 \pm 0.048$  when the fuel bundles were touching (i.e., at the minimum constraint).

ORNL DWG. 87-13387

```

=CSAS4X
SAMPLE FUEL CASK
HANSEN-ROACH LATTICECELL
UO2  1 .84 293. 92235 2.35 92238 97.65 END
ZR   2 1 END
H2O  3 1 END
B4C  4 0.367 END
AL   4 0.636 END
H2O  5 1 END
AL   6 1 END
END COMP
SQUAREPITCH  1.2751 .823 1 3 .9627 2 END
SAMPLE SQUARE FUEL CASK
READ PARAM  TME=5.0  NUB=YES  FAR=YES  GEN=53
END PARAM
READ ARRAY  NUX=2  NUY=2  NUZ=1  END ARRAY
READ GEOM
CUBOID 500 1 10.8385 -10.8385 10.8385 -10.8385 183.1 -183.1
CUBOID 4 1 11.5 -11.5 11.5 -11.5 183.1 -183.1
CUBOID 5 1 12.0 -12.0 12.0 -12.0 184.0 -184.0
CORE      0 1 3*0
REFLECTOR 6 1 6*10.0 1
REFLECTOR 5 2 6*3 5
END GEOM
READ BIAS  ID=500 2 6  END BIAS
END DATA
READ SEARCH  OPTIMUM PITCH  END SEARCH
END

```

Fig. 4.2. CSAS4X input for PWR assemblies in square aluminum cask.

### 4.3 VALIDATION EXPERIENCE

Criticality safety analyses are of extreme importance in environments where fissile materials are processed, handled, or stored. For this reason, the SCALE system analytic tools and data libraries have been employed in a number of studies in order to determine the effectiveness of the system in calculating  $k_{\text{eff}}$  for critical systems. A discussion of the initial effort to validate the cross-section libraries employed in SCALE for criticality analyses is provided in Sect. 2. However, a number of independent studies have also been performed which concentrated on the use of KENO IV and/or KENO V.a in conjunction with the SCALE libraries for various classes of critical systems.<sup>57-63</sup> The studies provide a basis for a user to verify the adequacy of using the SCALE system and available libraries for the intended calculation. The SCALE system has also been utilized in analyzing a series of international standard problems developed under the auspices of the Organization for Economic Cooperation and Development (OECD). An international working group analyzed the results submitted by participating countries and published final reports.<sup>64,65</sup>

Experience gained from the validation studies together with participation in the OECD standard problem exercise have provided the SCALE developers with a large amount of feedback needed to further improve the performance of the SCALE system for criticality safety analysis.

### 4.4 SUMMARY

This paper has provided an overview of the criticality safety analysis tools available in the SCALE system. Updated versions of the well-established KENO codes (KENO IV and KENO V.a) are provided in SCALE to enable a user to obtain  $k_{\text{eff}}$  for multidimensional systems. The XSDRNPM-S code is used for evaluating  $k_{\text{eff}}$  for one-dimensional models. These basic tools have been combined with the resonance processing codes (NITAWL-S and BONAMI-S) to produce a number of easy-to-use analytic sequences. These Criticality Safety Analysis Sequences (CSAS) have been developed to be highly flexible and general in their application. The KENO codes in SCALE and the CSAS sequences are being widely used for research, operational safety analyses, design, and safety review. The broad range of experience with these analytic tools, together with extensive validation efforts provides users with a significant degree of confidence in applying the SCALE system for criticality safety analyses. Also, the easy-to-use features and extensive error/warning messages available with the SCALE sequences hopefully reduce the misuse of the system. However, like any computational tool, SCALE can be used or applied improperly. Therefore, the user is encouraged to read and understand the relevant sections of the SCALE Manual<sup>4</sup> and review the literature (e.g., refs. 57-65) for actual validation relevant to the intended applications.

## 5. SHIELDING ANALYSIS METHODS

In SCALE, the primary functional tools for simulating radiation transport through shields are the XSDRNPM-S module and the MORSE-SGC/S module. XSDRNPM-S is a well-established discrete ordinates program for one-dimensional (1-D) analysis; MORSE-SGC/S is a super-grouped version of the well-known MORSE-CG program.<sup>66</sup> In addition, the MARS geometry package was developed for MORSE-SGC/S to allow easy input of geometric models with multiple rectangular arrays. With these two functional modules situated in the SCALE system, a series of control modules were developed to provide easy-to-use analytic sequences for cross-section processing, radiation transport, and dose evaluation.

The first shielding control module was released with the SCALE-1 package (January 1982) and was called the Shielding Analysis Sequence No. 3 (SAS3). This sequence provides automated data processing, but basically relies on the user's expertise with MORSE (or Monte Carlo techniques) to ensure reliable dose results. With the SCALE-2 package release in 1983, the SAS2 control module was provided for public use. This analytic sequence automates the following analyses: (1) a depletion and decay analysis for a specified assembly geometry and irradiation history, (2) generation of gamma and neutron source strength and spectra (in any desired multi-energy-group format), and (3) a one-dimensional radial shielding calculation (XSDRNPM-S) and dose evaluation (XSDOSE) for a transport/storage cask. The first two steps of the SAS2 sequence noted above are discussed in more detail in Sect. 3.3. This section will concentrate on the shielding analysis portion of the SAS2 sequence although there will be discussion on utilizing the sources generated by the sequence.

Two new sequences have recently been developed for future use in SCALE. Both modules have been extensively tested and used at ORNL over the past 2 years. The first new sequence is called SAS1 and is basically a user-friendly tool for cross-section processing and subsequent 1-D shielding analysis using XSDRNPM-S and XSDOSE. The second new sequence is called SAS4 and provides an easy-to-use, automated procedure to obtain radiation doses exterior to a transport/storage cask via a three-dimensional Monte Carlo analysis.

This paper provides a brief review of the functional modules XSDRNPM-S, MORSE-SGC/S, and XSDOSE, along with a more-detailed discussion of the four shielding analysis sequences. Also, the features of the MARS combinatorial geometry will be briefly presented along with the plotting tools PICTURE and JUNEBUG which are available for verifying the input geometric model.

### 5.1 REVIEW OF THE FUNCTIONAL MODULES

#### 5.1.1 One-Dimensional Radiation Transport and Dose Evaluation

As noted, the XSDRNPM-S code is the available module in SCALE for evaluating one-dimensional radiation transport through a shield. XSDRNPM-S is used for several purposes within the SCALE system. The shielding analysis sequences employ XSDRNPM-S to (1) cell-weight cross sections, (2) collapse cross sections to fewer energy groups, (3) produce particle importance functions — via an adjoint calculation — for generation of Monte Carlo biasing factors, and (4) simulate radiation transport through a shield.

XSDRNPM-S is a highly evolved one-dimensional discrete-ordinates transport program that has a wide variety of features. Its origins trace back to the popular ANISN program that pioneered the treatment of anisotropic scattering in discrete-ordinates calculations. XSDRNPM-S is capable of performing neutron or coupled neutron-gamma calculations with the scattering anisotropy represented to any arbitrary order. The primary emphasis in the solution algorithm is on the accurate calculation of detailed

spectral variations. However, with sufficient angular quadrature and spatial mesh specifications, highly precise solutions to the Boltzmann transport equation are obtained for one-dimensional slab, cylindrical, or spherical problems.

The finite-differencing in XSDRNPM-S is done with the weighted diamond difference model with weighting parameters chosen on the basis of experience with the DOT-IV code.<sup>25</sup> As default, angular quadrature sets are calculated in an automatic fashion for the appropriate one-dimensional geometry. Scattering expansion can be treated to whatever order is provided in the cross-section sets.

Boundary conditions on the angular fluxes can be specified as vacuum, reflected, periodic, white or user-supplied albedos. Also, transport in the transverse direction can be approximated with geometric buckling losses or with void streaming corrections. Two types of fixed sources can be specified. Boundary sources are angle- and group-dependent. Volumetric sources specified by spatial interval are group-dependent and isotropic in angular variation.

Convergence in XSDRNPM-S is determined by tests on several quantities. The point values of the scalar fluxes must vary by less than a prescribed amount between outer iterations. Also, the ratio of source terms and scattering rates (up and down in energy) between outer iterations must converge. Provision is made for banding thermal groups and thereby accelerating upscatter convergence.

The XSDOSE module was developed to be used in conjunction with XSDRNPM-S. This module eliminates the disadvantages of using XSDRNPM-S for calculating a dose in an external void beyond a finite shield.<sup>67</sup> XSDOSE is a code used in conjunction with XSDRNPM to compute the  $n/\gamma$  flux and the resulting dose at various points outside a finite cylinder or sphere. It may also be used to compute the flux and/or dose at various points due to a finite rectangular surface source or a circular disc. The code assumes that the outgoing angular flux distribution on the rectangle, cylinder, sphere, or disc is independent of position and that the surrounding media is a void. The numerical technique employed in XSDOSE is suitable for points on, close to, or far from the source.

XSDOSE is typically used in conjunction with a fixed-source XSDRNPM calculation for an infinite slab, cylinder, or sphere. XSDOSE then reads the angular flux file produced by XSDRNPM and performs the required numerical integration over a finite surface to obtain the actual scalar flux at those points specified by the user. To the extent that the XSDRNPM angular flux distribution on the surface of the body represents the actual angular flux distribution, XSDOSE will yield an exact solution.

### 5.1.2 Multidimensional Radiation Transport and Dose Evaluation

Multidimensional shielding analyses are performed within the SCALE modular code system using the MORSE-SGC/S code which is a member of the MORSE family of codes. The MORSE code versions all employ multi-energy-group Monte Carlo techniques to solve problems in neutron and gamma-ray transport. The original MORSE code<sup>68</sup> was written at ORNL in 1970 and used the general geometry package of the O5R code. Notable improvements have been a general analysis package, improved cross-section handling capabilities, and easy-to-use geometry packages. The combinatorial geometry version of MORSE (MORSE-CG) was used to develop a new version called MORSE-SGC which was designed to make more efficient use of a computer core size requirements. The MORSE-SGC code version was included in SCALE along with the MARS combinatorial geometry system, which was developed for MORSE-SGC to allow the ability to model complex lattice geometries efficiently and quickly with a minimum of geometric approximation and a minimum of computer memory requirements.

MORSE-SGC/S solves the multigroup integral form of the Boltzmann transport equation with the detailed geometry modeling feature available with MARS. Fixed source problems, as well as eigenvalue problems, can be solved, but it has been used mainly for shielding analyses. MORSE-SGC/S can

operate in either forward or adjoint mode for neutron, photon, or coupled calculations. Particle kinetic energy is divided into discrete groups, and materials are treated macroscopically whereby particles interact with an entire material, not an individual nuclide in the material. The details of the collision mechanics have been absorbed into the multigroup cross-section processing. Radiation doses are typically the Monte Carlo responses calculated by MORSE-SGC/S as part of the analysis. Surface- or volume-averaged doses and/or point detector results can be obtained by a variety of estimation procedures. The code can operate in a static or time-dependent mode. For time-dependent problems, neutron speed corresponds to the averaged energy of an energy group, and gamma rays travel at the speed of light.

The MORSE-SGC/S code exists only in the SCALE code system and is used in the SAS3 and SAS4 shielding control modules, although it is capable of running "stand alone." The major features of MORSE-SGC/S which distinguish it from other versions are listed below:

1. Cross-section storage is supergrouped. MORSE-SGC/S does not store all cross sections in memory at any given time. Cross sections are stored in available computer memory and are transferred to and from online storage as needed. This feature allows MORSE-SGC/S to run fine group calculations with many different media and high-order Legendre expansions for the scattering cross sections.
2. Particle tracking is supergrouped. Individual particles are tracked through one supergroup at a time. If a particle survives the supergroup and enters the next supergroup, the particle is banked for later processing and retrieval.
3. The Multiple ArRay System (MARS) geometry package in MORSE-SGC/S allows complicated rectangular arrays to be modeled with a minimum of computer memory requirements and a minimum of user input. This feature greatly enhances the lattice modeling capabilities of the code.
4. Combinatorial geometry is integrated into the MARS geometry system, thereby giving the user a great deal of flexibility in modeling irregular geometric shapes. It simplifies user input descriptions by using combinatorial logic to describe material and shapes.
5. FIDO free-form input eases input effort and reduces the chance of making input error.
6. The AMPX working format is used for cross sections instead of the less-flexible ANISN format.
7. User flexibility is enhanced by a general volumetric source sampling subroutine, a generalized array flux editing capability, a point detector flux option, and several problem-independent biasing schemes.

As implied by the above discussion, the MARS combinatorial geometry package allows representation of extremely complex models. Graphical verification of the input MARS geometry is available via the JUNEBUG-II and PICTURE programs. JUNEBUG-II is a three-dimensional graphics module within SCALE which uses the DISSPLA software package<sup>53</sup> to produce report-quality drawings. A more economical tool for model verification is the PICTURE module which displays, as printed output, two-dimensional (2-D) slices through the specified MARS geometry. Specification of various 2-D slices allows the user to graphically verify the accuracy of the input.

## 5.2 REVIEW OF THE SHIELDING ANALYSIS SEQUENCES

### 5.2.1 Common Features of the Sequences

All the shielding analysis sequences within the SCALE computational system use free-form input. The first step activated by each sequence is the Data Preprocessor and Material Information Library which were developed to centralize the procedure for automated cross-section processing (see Sect. 2.4).

The other common feature of the shielding modules involves the flux-to-dose conversion factors that are available in SCALE. The designated dose factors specified in the calculation are provided and read from the available SCALE cross-section libraries. The available dose factors are shown in Table 2.1. The shielding sequences use the ANSI standard dose factors as the default conversion factors.

### 5.2.2 The SAS3 Sequence

Shielding Analysis Sequence No. 3 (SAS3) was first released with the SCALE-1 package. The sequence performs a shielding analysis with the MORSE-SGC/S module. Complex geometries are easily input using the MARS combinatorial geometry package. The ICE-S module of SCALE is used to automatically mix the cross sections processed by the Material Information Processor into the proper format for use by MORSE-SGC/S. Cell-weighting of cross sections via XSDRNPM-S is requested by the input sequence keyword =SAS3X rather than =SAS3, which skips the XSDRNPM-S call.

Execution of SAS3 requires the following input:

1. data for Material Information Processor,
2. combinatorial MARS geometry input,
3. a fixed source strength for each energy group,
4. an energy importance parameter for each group if running a coupled neutron/gamma problem,
5. splitting and Russian roulette parameters by importance region and energy group, and
6. MORSE-SGC/S control parameters.

Criticality problems may be run for models containing fissile material, but it is not possible to run a criticality calculation simultaneously with a shielding calculation. SAS3 runs MORSE-SGC/S in a "fully coupled" mode for neutron gamma problems. This mode treats the gamma production as an energy transfer, as opposed to a true secondary particle. To enhance neutron transport and encourage gamma production, energy biasing is invoked to bias selection of the scattered particle energy.

The following analysis systems are available in SAS3:

1. point detector response, and
2. array collision edits by location and media.

The source description in SAS3 is composed of:

1. defining the source volume, ZMIN, XMAX, YMIN, YMAX, ZMIN, ZMAX;
2. defining the source in each energy group; and
3. optionally defining the source media.

As evidenced from the above description, Monte Carlo biasing parameters suitable for the problem must be input by the user. Default biasing parameters are provided for problems very similar to the sample problem — a fissile solution in a thin-walled tank. The user should be aware of the values and limits of the default biasing parameters.

### 5.2.3 The SAS2 Sequence

The Shielding Analysis Sequence No. 2 (SAS2) processes fuel assembly cross sections, computes photon and neutron source spectra, and evaluates dose rates from shipping casks by a one-dimensional transport shielding analysis. The execution includes: repeated passes through BONAMI-S, NITAWL-S,

XSDRNPM-S, COUPLE, and ORIGEN-S for cross-section processing and fuel burnup; radiation source computations; the radial shipping cask shielding analysis applying the calculated spent-fuel composition and sources; and the final determination of dose rates by XSDOSE from the angular flux leakage. See Fig. 3.1 for a flow diagram of this sequence. This section will review only that portion of the SAS2 sequence which performs the cask shielding analysis. The depletion and radiation source portion of the module was discussed in detail in Sect. 3.3.

Nuclide compositions are computed for a specified reactor assembly, which is allowed to decay for a given cooling time after discharge. The subsequent gamma source includes radiation from fission products, activation products of both the fuel and structural materials, and  $(n,\gamma)$  reactions resulting from neutrons produced by some of the heavy isotopes. The neutron source includes neutrons from spontaneous fission and  $(\alpha,n)$  reactions with oxygen isotopes. The final dose rates are calculated in the shielding analysis, applying these sources in a specific shipping cask.

SAS2 computes the gamma and neutron dose rates at various distances from a specified shipping cask, which contains fuel assemblies having a prescribed reactor history and cooling time. Only basic data are required to perform the SAS2 evaluation of a shipping cask. These data, briefly, include:

1. The material zone dimensions of both the shipping cask and the unit cell representation of the fuel assembly.
2. The material densities of the fresh fuel assembly and the shipping cask.
3. The material temperatures.
4. The specific power, exposure time and shutdown time of the fuel assembly in each appropriate cycle of the reactor history.
5. Various control parameters used to select libraries, nondefault options, the level of printout, or modifications to the transport computations (e.g., the fineness of mesh intervals or the problem convergence criteria).
6. Other optional data such as dose detector distances that differ from default values or light element weights per assembly.

Figure 3.2 shows an example of the SAS2 input.

The SAS2 control module converts the user input to data required by the functional modules, which are used in the execution of the case. The SCALE system driver invokes the execution of the various codes requested by SAS2 and, then, returns control to SAS2. Pertinent results computed by one functional module are used in generating input data for other codes. Passes through the functional modules are repeated until the case is completed.

Two additional passes through SAS2 are required after the final burnup and decay analysis via ORIGEN-S is performed. These passes prepare data for the shielding analysis and the computation of dose rates outside the spent fuel shipping cask. The purpose of the first pass is the cell-weighted calculation of the fuel-pin lattice cross sections within fuel zones in the cask. During the second pass, the cross sections for other zones of the shipping cask are processed and the transport calculation for the entire shipping cask is performed to get the neutron and photon angular flux at the surface of the cask. Then, gamma and neutron dose rates are computed at either specified or default detector locations outside of the shipping cask using XSDOSE.

The cell-weighted cross-section calculation is required in order to correct cross sections by a self-shielding resonance treatment (BONAMI-S and NITAWL-S) and to weight them in accordance with flux magnitudes of the unit-cell zones (XSDRNPM-S). The fuel zone nuclide densities of the unit cell are those calculated by the last ORIGEN-S case (i.e., that of the cooled spent fuel).

The final pass through SAS2 performs the cross-section processing and final shielding analysis for the cask. Cross sections from the cask zones are merged with those that have been cell-weighted. The XSDRNPM-S case performs the transport shielding analysis for the fixed volumetric sources and the multiregion geometry of the shipping cask. Since fission cross sections of fuel nuclides are supplied, both neutron multiplication and attenuation are computed. Secondary gamma production is computed from  $(n,\gamma)$  transfer data on the neutron-photon library. The attenuated neutron and photon flux is ultimately calculated, producing the angular flux at the shipping cask surface required by XSDOSE. The final functional module executed in the last pass through SAS2 is XSDOSE. It performs the required numerical integration of the angular flux over the finite surface of the cylindrical shipping cask to compute the scalar flux at specified detector locations. The dose rates that are automatically evaluated by SAS2 are at locations on the midplane of the shipping cask at distances of 0, 1, 2, and 4 m from the surface, unless specified differently in the user input.

The material mixtures 4–10 and the last three data records prior to the END card are the only portion of the SAS2 input of Fig. 3.2 that deals exclusively with the shielding portion of the sequence. Mixtures 4 and 5 specify material (SS304) that will be added to the smeared fuel zones in the specified volume fraction (2.1357-2). The keyword 27N-18COUPLE specifies the cross-section library for the shielding analysis (this keyword determines the multi-energy group format for the source spectra generated by ORIGEN-S). The specification DRYFUEL=YES indicates that the cask is dry and all water existing in the spent fuel composition should be removed. The mixture and radius of each of the nine zones are then specified followed by specification of the source zones and number of assemblies per zone. SAS2 automatically converts the radiation source per assembly that is generated by the last ORIGEN-S case to the correct source for the source zones and also generates the correct material composition (homogenized spent fuel plus added mixture material) for the source zones. The same source spectra is used in both source zones. The finite mesh used by XSDRNPM-S is automatically generated within SAS2 for both the pin cell calculations and the cask radiation transport calculation. The generated mesh has been found suitably conservative for pin cell and 1-D radial cask geometries, although the mesh spacing can be altered by input of an optional scaling factor. Other parameters used by SAS2 in the radiation transport calculation can also be overridden (e.g., the angular quadrature and convergence criteria).

One very attractive feature of SAS2 is its HALT and RESTART features. In a typical application, specification of PARM=HALT*i* (*i* = number of libraries/cycle) stops the SAS2 calculation with the final ORIGEN-S case and provides source spectra and concentrations at discharge and the specified SAS2 decay time on an ORIGEN-S output file. Then the SAS2 case can be restarted to produce the cask dose rates from the cooled spent fuel. Different decay times for the spent fuel can be considered by generating a new ORIGEN-S output file from the discharge concentrations on the old file. A different cask geometry or material composition can also be allowed in the restart. Thus, dose rates for a variety of cooling times and different cask designs or models can be easily obtained with maximum efficiency (depletion portion of SAS2 not repeated) and minimal user effort.

#### 5.2.4 The SAS1 Sequence

Since the SAS2 sequence limits the shielding analyst to considering only spent fuel assemblies in a 1-D cylindrical cask model, a more flexible 1-D shielding sequence has been developed with the Shielding Analysis Sequence No. 1 (SAS1). The SAS1 sequence will be made available with the SCALE-4 release.

The SAS1 module has been designed to enable general one-dimensional shielding analyses to be performed without requiring the user to be experienced in the use of such functional modules as NITAWL-S, BONAMI-S, XSDRNPM-S, or XSDOSE. Radiation transport through slabs, spheres, or cylinders is computed with XSDRNPM-S, and XSDOSE obtains the dose rate based on leakage from a

finite portion of the shield. The calculational flow of SAS1 is shown in Fig. 5.1. The basic scheme uses the Material Information Processor for the cross-section processing with cell-weighting specified by the keyword =SAS1X rather than =SAS1.

The SAS1 control module allows source spectra to be input from cards and/or an ORIGEN-S binary output file. The latter option was added to allow easy input of the neutron and gamma source spectra calculated by ORIGEN-S for spent fuel assemblies and/or other radiation sources. Neutron, gamma, or coupled neutron-gamma libraries and sources may be used. Note that the ORIGEN-S source spectra must have the same energy group structure used in SAS1. Depending on the cross-section library type (neutron only, gamma only, or coupled) used in the calculation, SAS1 will employ the appropriate portion of the coupled source located on the ORIGEN-S output file. Source spectra from cards or the ORIGEN-S output file can be specified for more than one zone. The input spectra must be normalized to the unit volume source strength. For applications involving spent nuclear fuel, the SAS2 module within SCALE could also be used to simulate the fuel depletion and generate the fuel source spectra on an ORIGEN-S output file.

The SAS1 control module has the feature of allowing several different shielding calculations to be run using the same cross-section working library. This adaptation is achieved by separating data for the cross-section processing and data for the shielding analysis by a Problem Control Card. If the Problem Control Card in the input data is left blank, additional shielding problems following the current problem will be solved using the same cross-section set and mixing table. If this card contains LAST, the program terminates on completion of the current problem. Generation of the cross-section working library can also be skipped by saving the working library from a previous SAS1 case and using the PARM=RESTART option on the module specification card. For the restart case, the working library is read, and the Material Information Processor portion of the data must be the same as that used in preparation of the working library (to ensure a valid mixing table is generated). Generation of a working library without execution of the shielding analysis can also be done by using the PARM=HALT option on the module specification card. These features for using the same working library with multiple shielding calculations may be very beneficial for design analyses where only the geometry or source specification differs between problems.

Another attractive feature of the SAS1 module is the optional COLLAPSE parameter. This keyword parameter is available as an option in the MORE DATA section of data for the Material Information Processor. Engaging the COLLAPSE parameter causes the thermal neutron groups available on the cross-section set to be collapsed to one group. The collapse is done using a typical thermal reactor flux spectrum (Maxwellian to 1/E to fission). The sources read from an ORIGEN-S file are also collapsed to remove multiple thermal neutron groups. **However, sources input from cards are assumed to be collapsed by the user prior to input.** In shielding problems where the neutron thermal group structure is not needed, the COLLAPSE option can significantly enhance the calculational efficiency with little or no impact on the final dose rates. In particular, this option is aimed at the 27-group neutron and 27n-18 $\gamma$  group libraries available in SCALE which contain 13 thermal neutron groups. The COLLAPSE option can prove very beneficial in reducing cpu time with minimal effect on the neutron dose results (2 to 4%).

Default dose factor identifiers (IDs) and detector locations for use by XSDOSE are also provided in SAS1. The default dose factors are the ANSI standard neutron and gamma flux-to-dose-rate factors. The default detector locations are at 0, 1, 2, and 4 m from the center of the outer shield surface. Besides the dose rates available from the XSDOSE output of SAS1, the dose rates internal to the shield are always provided in the activity tables at the end of the XSDRNPM-S output. Activity No. 1 is the neutron dose (mrem/h) based on the ANSI neutron dose conversion factors while Activity No. 2 is the gamma dose (mrem/h) based on the ANSI gamma dose conversion factors. An example of a SAS1 input is shown in Fig. 5.2. The SAS1 input specifies (1) the sequence specification and title card, (2) the cross-section library and geometry (infinite homogeneous medium) for the resonance treatment,

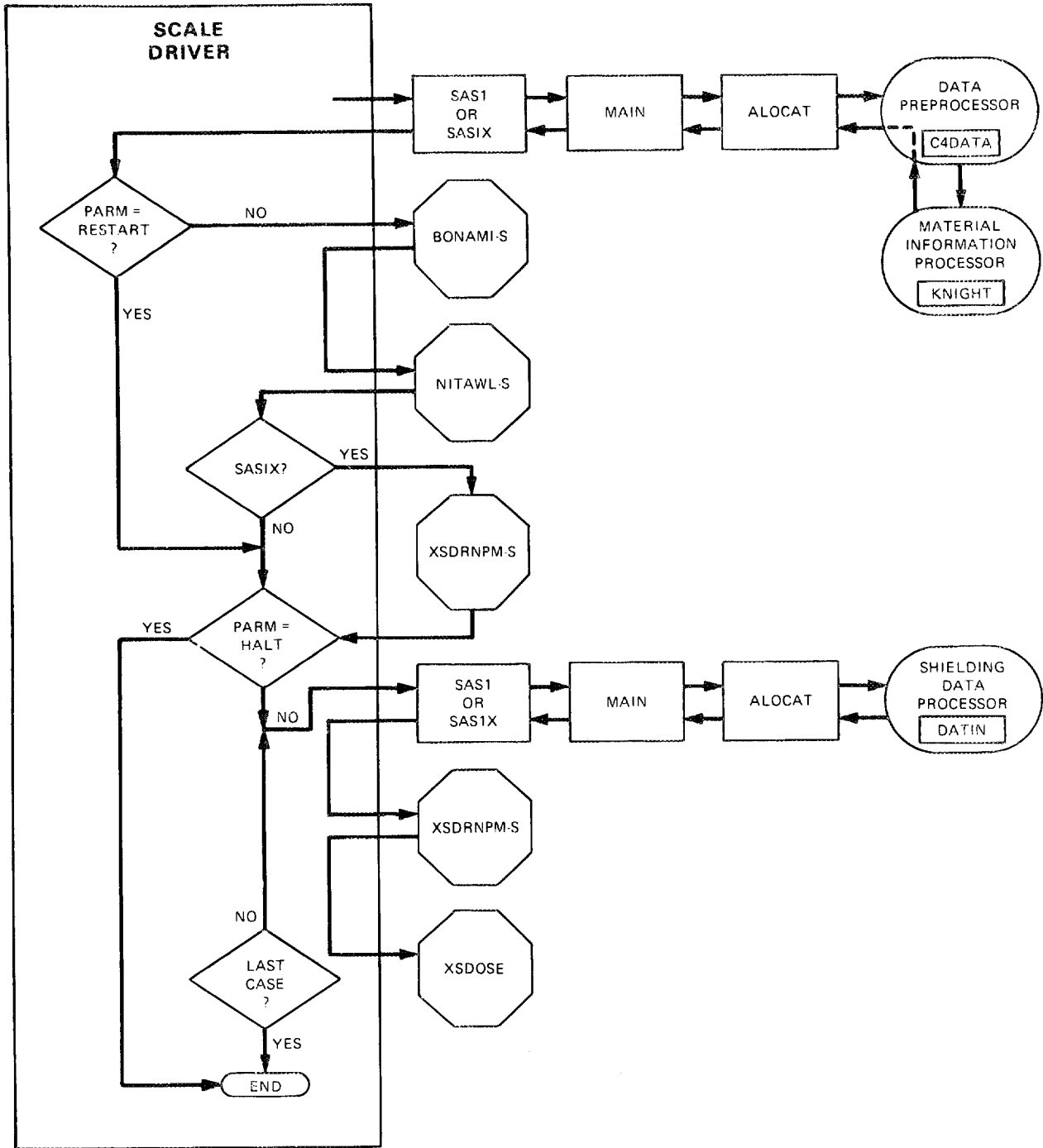


Fig. 5.1. General SAS1 flow diagram.

ORNL DWG. 87-13388

```

-SAS1
PWR CASK - 22 AT 11.5 GWD/MTU & 18 AT 9.7 GWD/MTU, 13 YR. COOLED
27N-18COUPLE INFHOMMEDIUM
U-238 1 0 6.104-3 END
U-235 1 0 2.229-4 END
O 1 0 1.265-2 END
ZR 1 0 3.577-3 END
FE 2 0 5.804-2 END
CR 2 0 1.658-2 END
NI 2 0 1.064-2 END
B-10 2 0 1.484-3 END
N 4 0 5.4-5 END
CARBONSTEEL 5 1 END
END COMP
END
LAST
PWR CASK - 22 AT 11.5 GWD/MTU & 18 AT 9.7 GWD/MTU, 13 YR. COOLED
CYLINDRICAL
1 54.1 60 1 0 0 60 2 3.36311+6 22
2 54.8 1 0
1 73.4 25 2 0 0 61 2 2.74352+6 18
2 74.1 1 0
4 91.1 17 0
5 114.6 45 0 END ZONE
READ XSDOSE
457.2
END

```

Fig. 5.2. Example of SAS1 input used for ferritic steel cask analysis.

(3) material specifications, and (4) geometric specifications for the shielding analysis. Just prior to the READ XSDOSE card are six zone specification cards. The first and third are source zones (fourth entry = 1) which use SAS2 output source spectra from designated units (60 and 61). The conversion of the ORIGEN-S output source from per assembly units to per  $\text{cm}^3$  units and/or normalization is accomplished with an input zone volume and number of assemblies (last two entries on card). Note that the mesh intervals/zone must be input for each zone.

### 5.2.5 The SAS4 Sequence

In a Monte Carlo shielding analysis of a deep-penetration problem such as a shipping cask, variance reduction techniques must be employed in order to calculate reasonably good results at an affordable cost. Generation of biasing parameters and application of the parameters to solve a particular problem are no trivial tasks. Nevertheless, a systematic approach has been developed recently for biasing a Monte Carlo transport calculation of a shipping cask.<sup>69</sup> This approach uses adjoint fluxes from a one-dimensional discrete ordinates calculation with the XSDRNPM-S code to generate the biasing parameters for a Monte Carlo analysis by the MORSE-SGC/S code. The entire procedure for cross-section preparation, adjoint flux calculation, automatic generation of Monte Carlo biasing parameters, and a Monte Carlo calculation has been implemented in the new Shielding Analysis Sequence No. 4 (SAS4) to provide calculated radiation dose levels exterior to a cask at a reasonable computational cost. This new sequence (with slight modifications to that described here) will be made available with the SCALE-4 release.

An outline of the SAS4 calculational sequence is shown in Fig. 5.3. Preparation of the cross-section data is done using the method and input common to all the shielding sequences. Then XSDRNPM-S is executed in the adjoint mode with a slab geometry to calculate adjoint fluxes that are used to generate biasing parameters for the Monte Carlo analysis. Finally, MORSE-SGC/S performs a Monte Carlo fixed-source analysis that calculates dose rates outside a shipping cask. Most of the standard biasing options in the MORSE code, including source biasing, splitting, Russian roulette, path-length stretching, and collision energy biasing, are invoked. All the required biasing parameters are derived from results of the adjoint XSDRNPM-S calculation and automatically input to MORSE so that the user is rid of this difficult input task. A simplified input option is also allowed for the geometry input.

In generating the biasing parameters, a one-to-one correspondence is made between the zones, IZ, of XSDRNPM-S and the importance regions, IR, in MORSE-SGC/S. The energy-dependent and zone-averaged adjoint flux,  $\phi^*(IG,IZ)$ , is then used directly as the importance function for selection of the emergent particle energy and the source energy. The Russian roulette survival weights are set equal to  $\lambda/\phi^*(IG,IZ)$ , where  $\lambda$  is the effect of interest (dose rate) approximated with the 1-D adjoint calculation. Similarly, the weight above which splitting occurs and the weight below which Russian roulette is played are determined respectively by the lowest and highest adjoint flux in IZ. The path length biasing is performed by (1) fitting the event-value function (obtained from the adjoint calculation) of the most important direction to an exponential function, and (2) using the exponential function to bias the transport kernel. In order to further conserve computational time, estimation probabilities are implemented to the next-event estimation to the point detectors. Reference 69 provides a detailed discussion of the automatic biasing techniques and their implementation.

A great deal of consideration has been given to the development of the SAS4 cask model. A cask model has been developed for SAS4 in order to implement the automated biasing procedure and the simplified geometry input option. The simplified input is used to generate MARS input for the MORSE-SGC/S module. The cask model, shown in Fig. 5.4, has the following common features found in many shipping and storage casks: a neutron shield liner, neutron shielding, axial impact limiters, corner coolant holes, and a fuel basket (or insert). The cask model is symmetrical about the cask mid-plane. Since most nuclear fuel casks are tall cylinders, more than 4 m in height, this assumption on

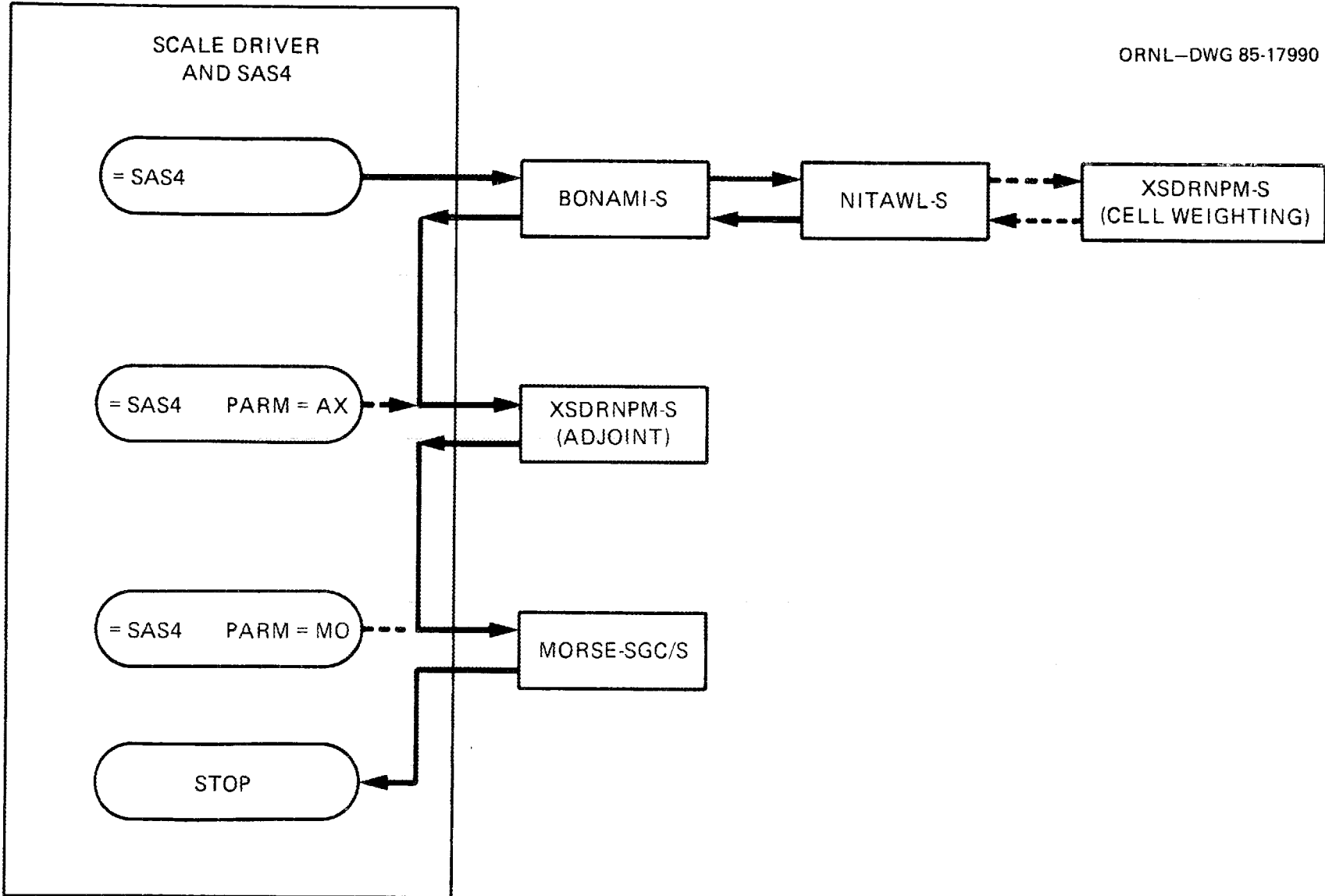


Fig. 5.3. Outline of the SAS4 analytic sequence.

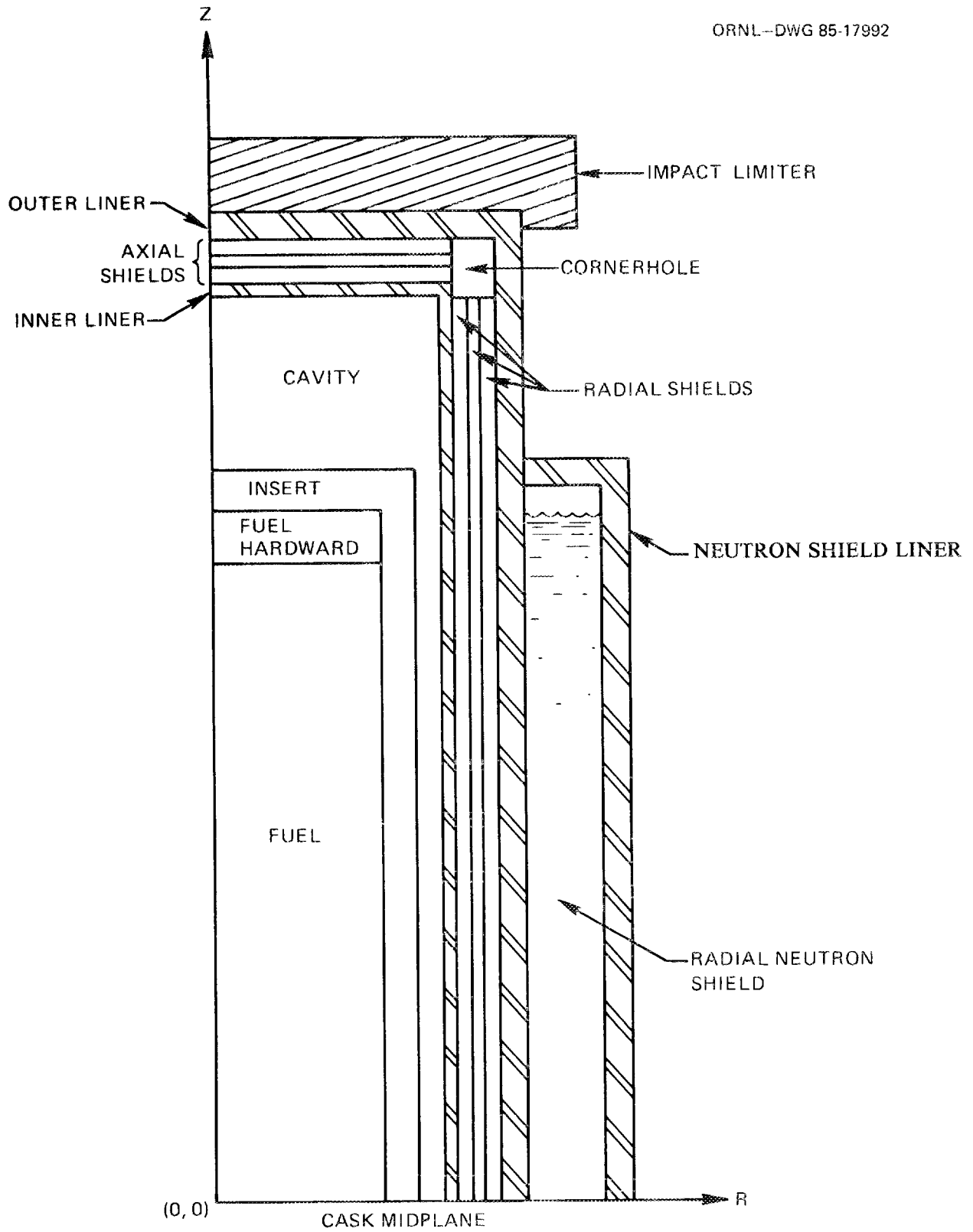


Fig. 5.4. SAS4 shipping cask model for IGO=0.

symmetry should not introduce significant error to the results of the calculation. There are two reasons for applying symmetry to this model: (1) symmetry improves the calculational efficiency, and (2) more importantly, the symmetry is necessary in order to implement the automated biasing procedure in the Monte Carlo analysis. In the Monte Carlo analysis, the entire cask is modeled in the geometry.

The fuel materials within the SAS4 cask model can be easily input in the homogeneous or heterogeneous configurations shown in Fig. 5.5. For the IGO=2 option, the assemblies are placed in the cask in set arrangements that vary according to the number of assemblies that are specified. The cask model of Fig. 5.4, in combination with the fuel region models of Fig. 5.5, should allow a broad class of casks to be modeled with very simple input specifications. However, as a last resort, an option is provided for the user to input the cask and fuel region geometry using MARS input. In either case, the user has the option of saving the detailed MARS input generated by SAS4. Then the PICTURE module or JUNEBUG-II can be used to graphically verify the input geometry or produce report-quality geometry plots.

In a Monte Carlo shielding calculation, the user must define the source parameters (position, energy, and direction), and the detector conditions (location, geometric shape, and response function) of the problem. SAS4 assumes source particles start isotropically and uniformly in the source region (consisting of the active fuel and fuel hardware) with an energy spectrum specified by the user, and provides four surface detectors in addition to the point detectors input by the user. The source energy spectrum is supplied to SAS4 either by direct input or from a file generated by ORIGEN-S. When the source energy spectrum is input via an ORIGEN-S file, it is imperative that the input file contain the appropriate neutron and/or gamma-ray spectrum represented in the same multigroup structure used in the calculation.

Note that when a neutron response is desired, only the neutron source spectrum is input. However, both neutron and gamma-ray source spectra must be input when a gamma-ray response is to be calculated. Clearly, if the user wishes to calculate only the primary gamma-ray dose (dose due to gamma-ray source), the neutron source spectrum should be set to zero. On the other hand, if the secondary gamma-ray dose (dose due to neutron-captured gamma ray) is desired, the gamma-ray source spectrum should be set to zero.

Two types of detectors are used in the Monte Carlo calculation: surface detectors and point detectors. The surface detectors are analog detectors that calculate averaged responses based on particles crossing the detector surfaces. The accuracy and precision of the responses depend on the number of particles and their respective weights crossing the detector surfaces. Four surface detectors are automatically implemented in the SAS4 Monte Carlo calculation. Depending on the direction of the transport calculation indicated by the IDR parameter in the adjoint discrete ordinates input data ( $IDR = 0$  for a radial calculation, and  $IDR > 0$  for an axial calculation), the surface detectors are located radially or axially on the outermost surface of the cask and 1, 2, and 3 m from this outermost surface.

The point detectors are input by the user. The user indicates the number of point detectors and their coordinates in the Monte Carlo input data. It is important that the positions of the point detectors (radial or axial) are consistent with the direction of the transport calculation indicated by the IDR parameter. For point detectors that lie within the axial projection of the cask cylinder, IDR should be set greater than zero to indicate a calculation with axial biasing. For point detectors located outside this projection, IDR should be zero, indicating a calculation with radial biasing. In a radial biasing calculation, next-event estimations are made from all collision and source points to the point detectors. In an axial biasing calculation, next-event estimations are made only from points that lie in the half (top or bottom half) of the cask nearest to the detectors. This procedure assumes that for an axial calculation the contributions from collision and source points in the other half of the cask are negligible. In a next-event estimation, tracking is made from a source or collision point to point detectors that are many

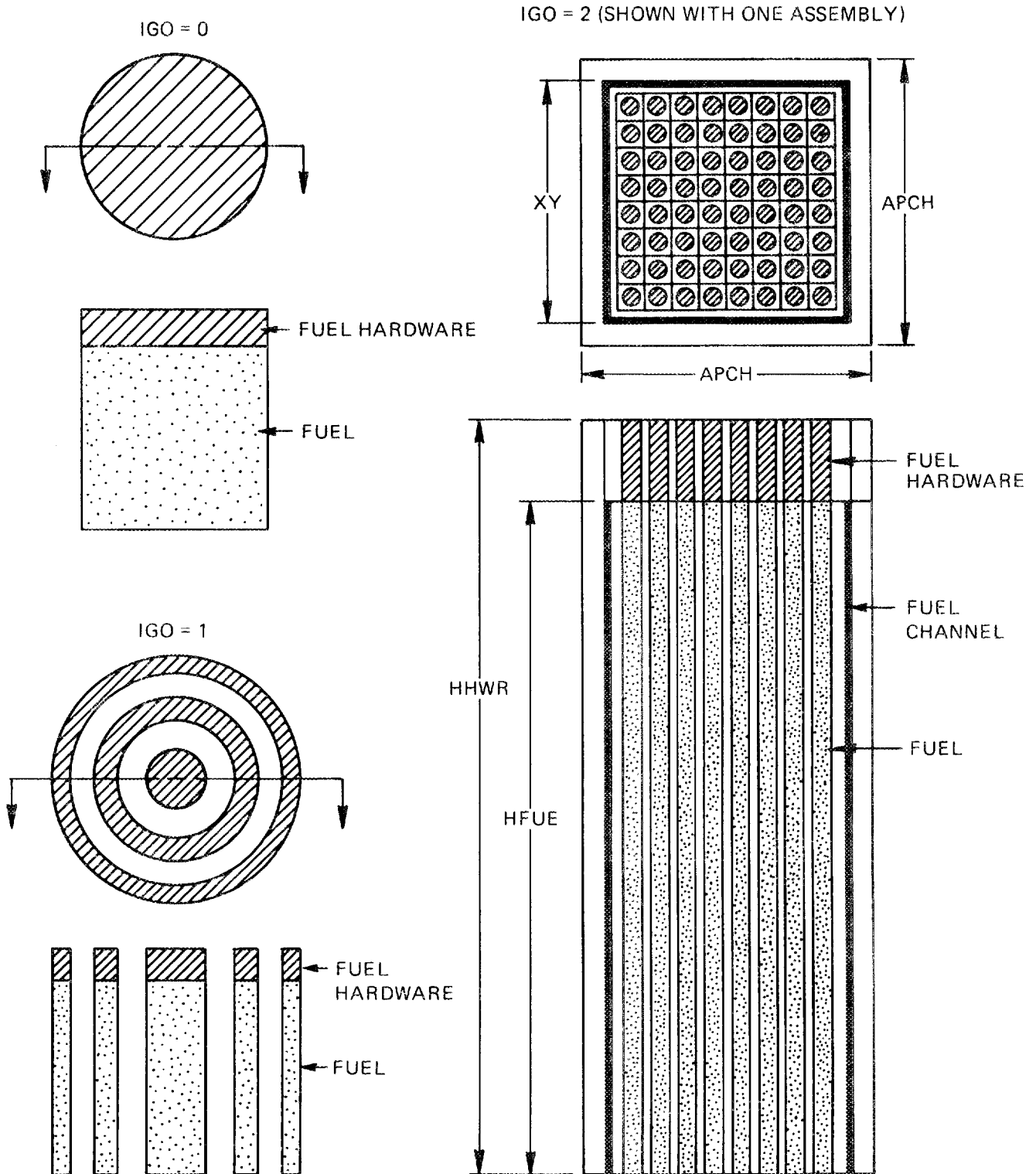


Fig. 5.5. Geometry options of source region for simplified geometry input. Only the top halves of the source regions are shown.

mean-free paths away. Since tracking is the most time-consuming portion of Monte Carlo transport analysis, next-event estimation will add significantly to the cost of a calculation.

Because of the automated biasing procedure in SAS4, neutron and gamma doses are computed in separate calculations. Therefore, to obtain a full characterization of a shipping cask by SAS4, the user must perform at least four calculations. And two more are needed if gamma doses due to the fuel hardware material are desired. Finally, the normal results output by MORSE-SGC/S are in response per source particle per second. To obtain the total response, the user must multiply MORSE's results by the total source strength in source particle per second. For source particles originating from the active fuel, the total source strength is the source intensity in the full length of the fuel. For source particles originating from the fuel hardware, the total source strength is two times the source intensity in one end (top or bottom) of the fuel hardware being analyzed. In SAS4 a source strength factor, SFA, is included in the parameter card of the Monte Carlo input data. The MORSE-SGC/S results are automatically multiplied by this factor. Therefore, if SFA is set equal to the total source strength in particles per second, all of the results output by MORSE-SGC/S are per total source strength.

Testing and verification of the biasing techniques and procedures used in SAS4 have been ongoing for several years. The biasing techniques were initially tested using the dry shipping cask model of Fig. 5.6 and five detectors. Excellent agreement was obtained between the biased MORSE-SGC calculation and a DOT-IV<sup>26</sup> calculation of neutron dose.<sup>69</sup> Other comparisons have been made between DOT-IV and SAS4 that show good agreement in the calculated dose rates.<sup>22,70</sup>

A sample input for SAS4, corresponding to the cask of Fig. 5.6, is shown in Fig. 5.7. Radial neutron doses were calculated in this problem. The cask wall is composed of a layer of depleted uranium sandwiched between steel inner and outer liners. The source is made up of 7 PWR fuel assemblies, but the source region is modeled as two concentric cylinders. The inner cylinder represents one fuel assembly, and the outer cylinder represents six fuel assemblies. The fuel hardware at the ends of the assemblies has been ignored. Each assembly has 17 x 17 unit cells of which 25 are vacant cells. The pitch dimension between the cells is 1.2598 cm. The diameter of each fuel pin is 0.83566 cm, and the diameter of the clad is 0.94996 cm. No gap exists between the fuel and the clad. The outside dimension of an assembly is 21.4493 cm. The height of the fuel is 365.76 cm (12 feet). Three point detectors are located outside the cask: two radial detectors on the midplane of the cask 91.4 cm (3 feet) and 182.8 cm (6 feet) away from the cask surface, and a corner detector 91.4 cm from the rim of the cask on a 45° plane. The material information data were followed by five lines of discrete ordinates input data and 17 lines of Monte Carlo input data. Note that mixtures 4, 5, and 12, representing the materials outside the source region, were used in both the adjoint discrete ordinates calculation and the Monte Carlo calculation. The input values of FR1, FR2, FR3, and FR4 in the parameter card of Monte Carlo input determine the height of the radial surface detectors to be 182.88 cm from the midplane of the cask.

### 5.3 SUMMARY

The shielding analysis capabilities developed for the SCALE system center around the one-dimensional (1-D) discrete-ordinates code XSDRNPM-S and the multidimensional Monte Carlo code MORSE-SGC/S which uses the MARS combinatorial geometry package for easy modeling of complex geometries. These radiation transport codes along with other SCALE modules for cross-section processing (BONAMI-S, NITAWL-S, ICE-S), spent fuel source generation (ORIGEN-S), and dose evaluation (XSDOSE) are incorporated into four **Shielding Analysis Sequences** — SAS1, SAS2, SAS3, and SAS4. The SAS1 and SAS3 module essentially provide automated cross-section processing and simplified input for running an XSDRNPM-S or MORSE-SGC/S calculation, respectively. The SAS2 module provides an automated, easy-to-use scheme for generating the source spectra required for the other shielding

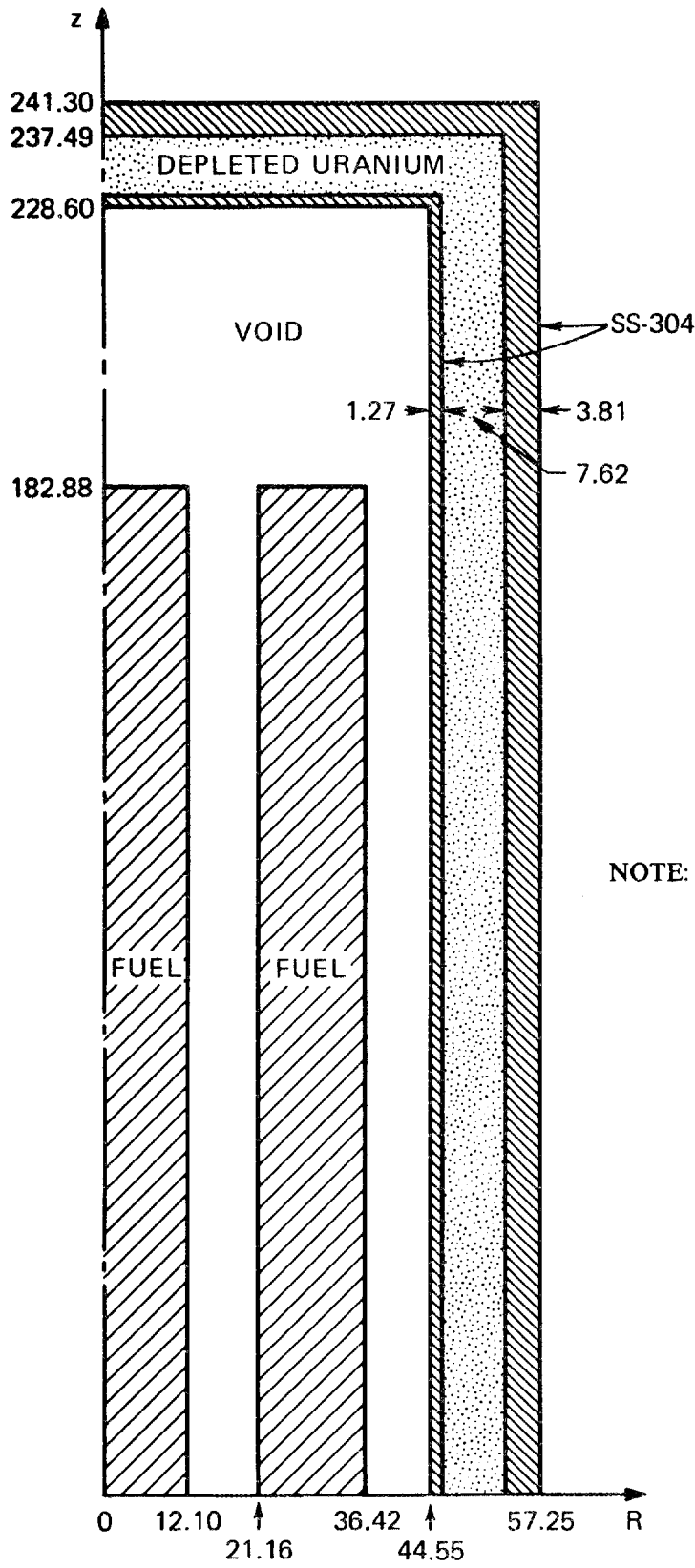


Fig. 5.6. Upper half of depleted uranium cask model.

```

-SAS4
SAMPLE PROBLEM 1, RADIAL NEUTRON DOSES OF DRY DEPLETED URANIUM CASK
22N-18COUPLE LATTICECELL
U-235 1 0.0 1.6736-4 END
U-238 1 0.0 1.9602-2 END
PU-239 1 0.0 1.0409-4 END
PU-240 1 0.0 4.7534-5 END
O 1 0.0 3.9877-2 END
ZR 2 0.0 1.9350-2 END
O 3 0.0 1.000-20 END
CR 4 0.0 1.662-2 END
MN 4 0.0 1.200-3 END
FE 4 0.0 5.775-2 END
NI 4 0.0 7.520-3 END
MO 4 0.0 1.100-4 END
U-235 5 0.0 1.070-4 END
U-238 5 0.0 4.770-2 END
O 6 0.0 1.00-20 END
O 7 0.0 1.00-20 END
O 8 0.0 1.000-20 END
O 9 0.0 1.000-20 END
O 10 0.0 1.00-20 END
O 11 0.0 1.00-20 END
O 12 0.0 1.00-20 END
END COMP
SQUAREPITCH 1.25984 0.83566 1 3 0.94996 2 END
TY-1 IZM-5 MHW-6 FRD-36.42 END
7 17 25 7 8 9 10 11 0.01 21.4493 END
36.42 44.55 45.82 53.44 57.27 END
14 12 4 5 4 END
XEND
TIM-20.0 NST-100 NIT-80 NOD-3 IGO-1 RAN-F2AE3EBFB1EB FR1-1. FR2-0.6465
FR3-0.6465 FR4-0.6465 END
SOE 2.474-13 2.096-12 5.766-12 2.899-11 7.228-11 1.457-10 6.099-10
4.542-10 9.070-11 3.824-10 4.990-10 3.982-10 1.836-10 1.761-14
8Z END
DET 148.69 0.0 0.0 240.13 0.0 0.0
121.91 0.0 305.96 END
GEND
SAMPLE PROBLEM 1, 2 HOMOGENIZED FUEL ZONES
FU1 0.0 12.10 182.88 182.89 END
FU2 21.16 36.42 182.88 182.89 END
FEND
CAV 12 44.55 228.60 END
INN 4 45.82 229.87 END
RS1 5 53.44 237.49 END
OUR 4 57.25 241.30 END
AS1 5 45.82 237.49 END
CEND
END

```

*Material information input data*

*Adjoint discrete ordinates input data*

*Monte Carlo input data*

*Neutron doses are calculated*

*IDR not input, radial calculation by default*

*22 entries required*

Fig. 5.7. SAS4 input listing for simple cask model.

sequences and its own 1-D radial cask analysis. Finally, the SAS4 sequence provides a user-friendly procedure that includes automated biasing for doing multidimensional Monte Carlo shielding analyses for cask geometries.

Taken altogether, the shielding sequences provided in SCALE provide excellent tools to be used for source generation, preliminary shield design, final safety analyses, and review calculations.

## 6. HEAT TRANSFER ANALYSIS CAPABILITIES

The heat transfer analysis capabilities within the SCALE computational system are centered around the HEATING6 functional module that was made available with the SCALE-1 release in 1982. This functional module is a general-use tool for solving multidimensional, steady-state, and/or transient heat conduction problems using finite-difference techniques. HEATING6 is the latest version of the HEATING (Heat Engineering and Transfer in Nine Geometries) series of programs developed and maintained at Oak Ridge since the 1960s. When the SCALE development began, the HEATING5 version<sup>71</sup> was just being publicly released. This code was selected for further modification and subsequent inclusion in the SCALE system. The other modules in SCALE used in heat transfer analysis are (1) REGPLOT6 and HEATPLOT-S for obtaining HEATING6 region geometry plots and temperature profile plots, respectively, and (2) HTAS1, which is a control module that prepares HEATING6 input data and then accesses HEATING6 to analyze a transport cask under the normal and accident thermal conditions of the established USNRC and IAEA regulations. Much of the information is taken directly from Sects. F10, F13, F14, and H1 of the SCALE Manual.<sup>4</sup> Emphasis is placed on the modeling capabilities in HEATING6 and HTAS1. The paper also provides some discussion of recent HEATING6 verification efforts and the new radiation modeling capabilities developed for HEATING6.1.

### 6.1 REVIEW OF THE HEATING6 FUNCTIONAL MODULE

HEATING6 solves steady-state and/or transient heat conduction problems in one-, two-, or three-dimensional Cartesian or cylindrical coordinates or in one-dimensional spherical coordinates. The thermal conductivity, density, and specific heat may be both time- and temperature-dependent. In addition, the thermal conductivity may be anisotropic. Selected materials may undergo a change of phase for transient calculations involving one of the explicit procedures. The heat generation rates may be dependent on time, temperature, and position; and boundary temperatures may be dependent on time and position. Boundary conditions which may be applied along surfaces of a model include specified temperatures or any combination of prescribed heat flux, forced convection, natural convection, and radiation. Models are available to simulate the thermal fin efficiency of certain finned surfaces. In addition, one may specify radiative heat transfer across gaps or regions embedded in the model. The boundary condition parameters may be time- and/or temperature-dependent. The mesh spacing may be variable along each axis.

#### 6.1.1 Modeling Techniques

The following paragraphs provide a brief review of the problem and numerical model solved by HEATING6. The physical problem is approximated by a system of nodes each associated with a small volume. In order to define the nodes, a system of orthogonal planes is superimposed on the problem. The planes may be unequally spaced, but they must extend to the outer boundaries of the problem. A typical, internal node, which is defined by the intersection of any three planes, is depicted in Fig. 6.1. Heat may flow from a node to each adjacent node along paths that are parallel to each axis. Thus for a three-dimensional problem, heat may flow from an internal node to each of its six neighboring nodes. The system of equations describing the temperature distribution is derived by performing a heat balance about each node.

The finite difference heat balance equation for node  $o$  in Fig. 6.1 is

$$C_o \frac{T_o^{n+1} - T_o^n}{\Delta t} = P_o^n + \sum_{m=1}^6 {}_oK_m (T_m^n - T_o^n), \quad (6.1)$$

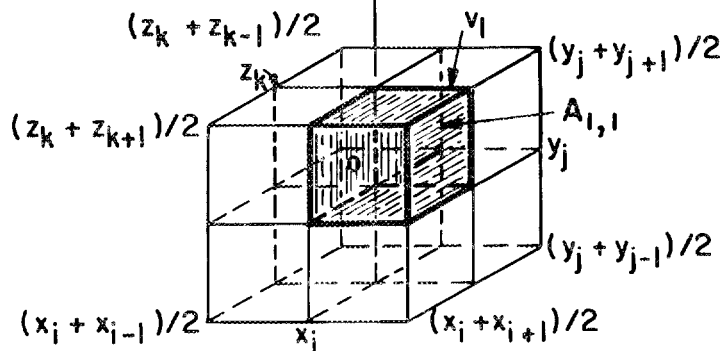
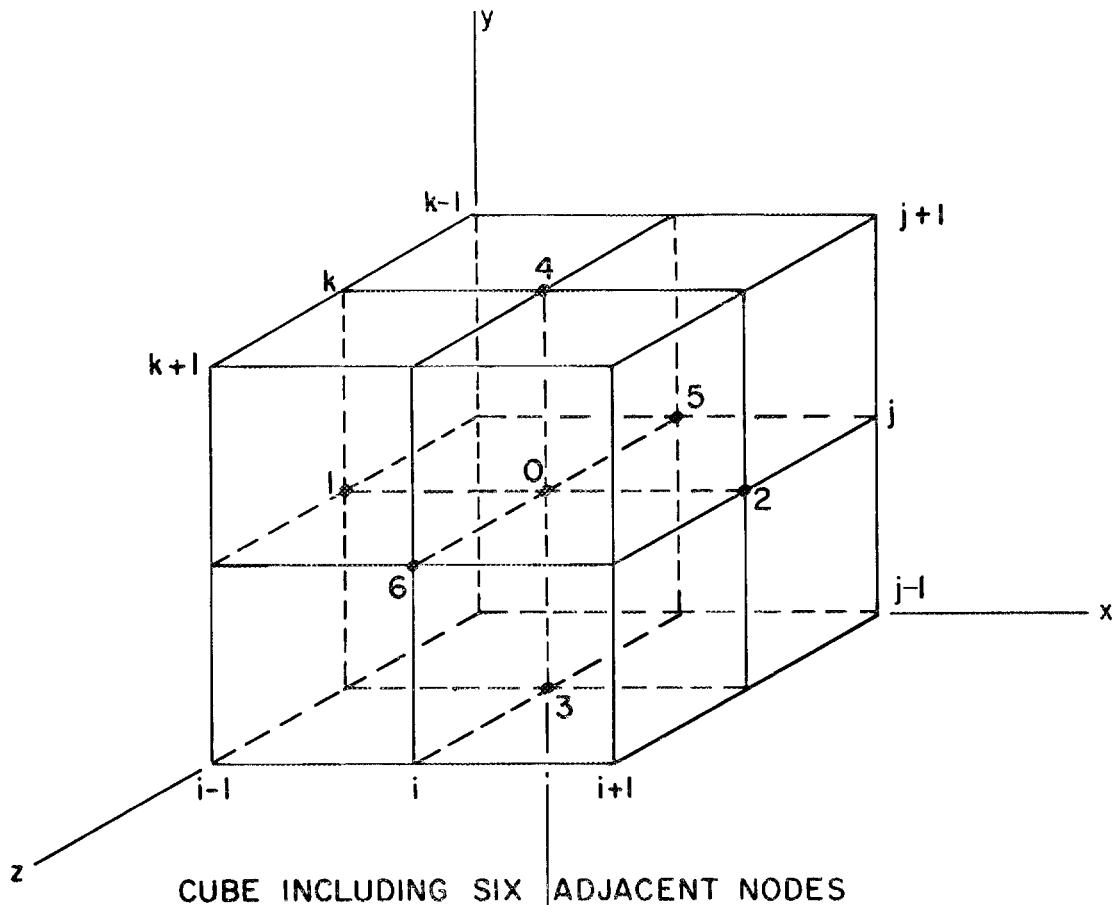


Fig. 6.1. Nodal description for three-dimensional problem.

where  $T_m^n$  is the temperature of the  $m$ th node adjacent to node  $o$  at time  $t_n$ ,  ${}_oK_m$  is the conductance between nodes  $o$  and  $m$ ,  $C_o$  is the heat capacitance of the material associated with node  $o$ , and  $P_o^n$  is the heat generation rate in the latter material at time  $t_n$ . Since planes go through the nodes and the material is homogeneous between any two successive planes along any axis, a node may be composed of as many as eight different materials, and the heat flow path between adjacent nodes may be composed of as many as four different materials positioned in parallel. The parameters  $C$ ,  $P$ , and  $K$ , associated with each internal node at a particular time,  $t_n$ , are calculated based on the heat capacity, density, and conductivity of the material in the regions surrounding the node. Perfect thermal contact is assumed between regions of different materials.

Since nodes lying on a surface or nodes from one- or two-dimensional problems will not necessarily have six neighbors, the general heat balance equation for node  $i$  having  $M_i$  neighbors can be written as

$$C_i \frac{T_i^{n+1} - T_i^n}{\Delta t} = P_i^n + \sum_{m=1}^{M_i} {}_iK_{\alpha_m} (T_{\alpha_m}^n - T_i^n), \quad (6.2)$$

where  $\alpha_m$  is the  $m$ th neighbor of the  $i$ th node. By choosing the increments between lattice lines small enough, the solution to the system of equations yields a practical approximation to the appropriate differential equation.

For a steady-state heat conduction problem, the heat balance reduces to

$$P_i + \sum_{m=1}^{M_i} {}_iK_{\alpha_m} (T_{\alpha_m} - T_i) = 0 \quad (6.3)$$

For  $I$  nodal points, there will be a system of  $I$  equations with  $I$  unknowns. HEATING6 contains two techniques for solving the resulting system of equations. The first technique involves point successive overrelaxation (SOR) iteration<sup>72</sup> combined with a modification of the "Aitken  $\delta^2$  extrapolation process." This method can be used for any steady-state problem modeled with HEATING6. However, for certain classes of problems, convergence may be slow or the convergence criterion may be unreliable since it only requires that the maximum relative change in temperature from one iteration to the next be less than the specified value. In other words, the steady-state temperature distribution could change significantly as the convergence criterion is decreased in magnitude. Such difficulties can arise in problems with widely varying parameters such as thermal conductivity, grid spacing along an axis, or nonlinear boundary conditions. Thus, a second technique is available to HEATING6 to solve the steady-state system of equations using a direct solution technique. The direct solution technique is available only for one- and two-dimensional problems, and even then it is not always more efficient than the successive overrelaxation method since it can require a large amount of core. This can occur for two-dimensional calculations when the problem requires a large number of lattice lines along the  $X$  (or  $R$ ) axis, or when the problem requires heat transfer across a gap along the  $Y$  (or  $\theta$ ) or  $Z$  axes. However, it can be much faster and more reliable than the successive overrelaxation technique for many problems.

The recommended procedure for using point successive overrelaxation iteration to solve a steady-state problem is to obtain several solutions using different convergence criteria (e.g.,  $10^{-5}$ ,  $10^{-6}$ , and  $10^{-7}$ ). These solutions must be compared, and the differences that are noted at points of interest must be acceptable. For questionable steady-state profiles, one could perform a transient calculation using the steady-state boundary conditions and heat generation rates. The steady-state temperature distribution would serve as the initial temperature distribution. A change in the temperature distribution during the transient indicates the steady-state solution has not converged.

The direct solution method involves representing Eq. (6.3) in a linear matrix form and solving for the vector of unknown temperatures via subroutines from the LINPACK software library.<sup>73</sup> For non-linear problems where  $P_i$  and  ${}_iK_{\alpha_n}$  are functions of the unknown temperature, an estimate of the temperatures is used to evaluate  $P_i$  and  ${}_iK_{\alpha_n}$ , and the solution vector is evaluated. Then the process is repeated using successive iterations of the temperature vector until a specified convergence criterion is satisfied. It is advised that the user start with a fairly lax criterion such as  $10^{-6}$  and then make one or two runs, tightening the criterion for each run until the code cannot satisfy the given criterion. By comparing the converged temperature distribution from these runs, the user can determine whether the calculated temperature distribution is sufficiently converged.

HEATING6 is designed to solve a transient problem by any one of several numerical schemes. The first is the Classical Explicit Procedure (CEP) which involves the first forward difference with respect to time and is thus stable only when the time step is smaller than the stability criterion. Levy's modification to the CEP is the second scheme, and it requires the temperature distribution at two times to calculate the temperatures at the new time level. The technique is stable for a time step of any size. The third procedure, which is written quite generally, actually contains several implicit techniques which are stable for a time step of any size. One can use the Crank-Nicolson heat balance equations, the Classical Implicit Procedure (CIP) (or backwards Euler) heat balance equations, or a linear combination of the two. The resulting system of equations is solved by point successive overrelaxation iteration. Techniques have been included in the code to approximate the optimum acceleration parameter for problems involving constant thermal parameters as well as those whose effective thermal conductances and capacitances vary with time or temperature. The time step size for implicit transient calculations may be varied as a function of the maximum temperature change at a node. The implicit procedure in HEATING6 has not been designed to solve problems involving materials which are allowed to undergo a change of phase. The implicit procedure using the Crank-Nicolson heat balance equation is the recommended technique for solving transient problems.

Levy's modification to the CEP can be a useful tool for obtaining the solution to problems. However, one must experiment with the time step size before accepting the resulting solution. The stability criterion for the CEP is a function of a temperature-dependent heat generation rate or heat flux. This fact is not accounted for in HEATING6. Also, Levy's modification to the CEP is based on a heat generation rate or heat flux with respect to temperature. If one attempts to use one of the explicit transient algorithms along with a temperature-dependent source or heat flux, then the code will write out a warning message indicating that the time step allowed by HEATING6 may not yield a stable solution.

As implied above, one of the explicit procedures must be used for problems involving change of phase. The following technique is used in calculating the temperatures of nodes composed of materials which can have a change of phase. Let the melting ratio,  $X1_i$ , be the ratio of heat that has been absorbed after the transition temperature has been reached to the total heat needed to complete the phase change for a material in node  $i$ . Unless an input value is specified, the initial melting ratio is calculated as

$$X1_i = \begin{cases} 0.0, & T_i^0 < T_{\text{melt},i} \\ 1.0, & T_i^0 \geq T_{\text{melt},i} \end{cases} \quad (6.4)$$

where

$T_i^0$  = the initial temperature of node i,

$T_{\text{melt},i}$  = the smallest phase-change or transition temperature associated with node i.

If the melting ratio of a node is zero, its temperature is allowed to increase until it reaches the transition temperature of the material associated with it. Then, the temperature of the node is held at the transition temperature, and the material is allowed to change phase in the following manner. The incremental melting ratio over the nth time step is calculated as

$$\Delta X1_i^n = \frac{\Delta q_i^n}{\rho_{i,m}^n H_m V_{i,m}}, \quad (6.5)$$

where

$\Delta q_i^n$  = the net heat into node i during the nth time step,

$\rho_{i,m}^n$  = the density of material m evaluated at  $T_i^n$ ,

$H_m$  = the latent heat of material m,

$V_{i,m}$  = the volume of material m associated with node i.

This incremental ratio is added to the current value of  $X1_i$  at each time step until  $X1_i$  exceeds unity. Any excess heat remaining after a change of phase is used to change the temperature of the node as follows:

$$\Delta T_i^n = (X1_i^n - 1.0) \rho_{i,m}^n H_m V_{i,m} / C_i^n, \quad (6.6)$$

for  $X1_i^n > 1.0$ , where  $C_i^n$  is the heat capacitance of node i during the nth time step. Then the melting ratio is set to unity, and the temperature of the node is allowed to increase. The above logic works in a similar manner for the reverse phase change from a melting ratio of 1.0 to a melting ratio of 0.

If a node is associated with more than one material that can change phase, then each material is allowed to change phase independently by following the above process for each material transition temperature associated with the node. It must be emphasized that this technique will allow changes of phase in both directions for as many times as it may be needed.

HEATING6 possesses a variety of boundary conditions to enable the user to model his physical problem as accurately as possible. In general, a boundary condition is applied along a surface of a region, and heat is transferred from a surface node to a boundary node or to the corresponding node on the opposing parallel surface. Surface nodes are actually internal nodes that are located on the edge of a region. Boundary nodes are dummy nodes, and their temperatures are not calculated by the code but are specified as input to the code. These temperatures are only used to calculate the heat flow across a boundary surface. The boundary conditions that can be applied over the surface of a region in the current version of HEATING6 are listed below.

1. The temperature on the surface of a region can be specified as a constant or a function of time and/or position.

2. The heat flux across the surface of a region can be specified directly as a constant or a function of time and/or surface temperature.
3. The heat flux across the surface of a region can be specified indirectly by defining the heat transfer mechanism to be forced convection, radiation, and/or natural convection.

The numerical techniques used in calculating the temperatures of surface nodes associated with a boundary condition are discussed below. The temperatures of nodes on surfaces whose temperatures are specified are not calculated from Eq. (6.2). Instead, the surface node temperature is set equal to the specified value. When a heat flux is specified across a surface, then for each node on that surface, the specified heat flux is multiplied by the node's surface area normal to the heat flow path associated with the boundary condition, and the result is added to the heat generation term,  $P_i^p$ , in Eq. (6.2). If the heat flux is temperature-dependent, then it is evaluated at the average temperature of the related surface node and boundary node for surface-to-boundary boundary conditions and the average temperature of opposing surface-nodes for surface-to-surface boundary conditions. Simulation is not required for insulated boundaries; heat is simply not allowed to cross the surface.

The boundary conditions are classed as either surface-to-boundary (type 1), isothermal (type 2), or surface-to-surface (type 3). Boundary conditions of the surface-to-boundary type are used to define heat transfer between a surface node and a boundary node. The temperature of the boundary node is specified and can be a function of time and/or position. Surface-to-surface boundary conditions are used to define heat transfer between parallel surfaces. In this case, heat is transferred between a node on one surface to the corresponding node on the opposing surface. In other words, in Fig. 6.2, surface-to-surface boundary conditions could be utilized to describe the heat transfer process between nodes 1 and 2, nodes 3 and 4, and nodes 5 and 6.

ORNL DWG. 87-13390

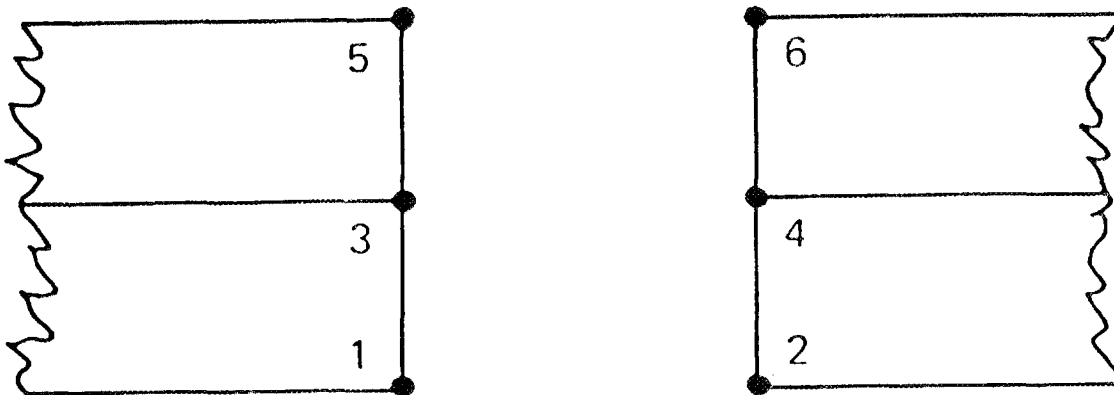


Fig. 6.2. Surface-to-surface heat transfer.

For both surface-to-boundary and surface-to-surface boundary conditions, the leakage term in Eq. (6.2) is calculated as follows:

$$[{}_iK_{\alpha_n}(T_{\alpha_n}^n - T_i^n)] = {}_iK_b(T_b^n - T_i^n) , \quad (6.7)$$

where  ${}_iK_b$  is the effective conductance from surface node  $i$  to boundary node  $b$  or the opposing surface node  $b$ , and  $T_b^n$  is either the temperature of boundary node  $b$  or the opposing surface node  $b$  at time  $t_n$ . The effective conductance is calculated as

$${}_iK_b = hA , \quad (6.8)$$

where  $h$  is the effective heat transfer coefficient, and  $A$  is the surface area, normal to the heat flow path, of node  $i$  associated with the boundary condition.

The effective heat transfer coefficient is defined as

$$h = h_c + h_r[(T_i^n)^2 + (T_b^n)^2][T_i^n + T_b^n] + h_n|T_i^n - T_b^n|^{h_e} , \quad (6.9)$$

where

- $h_c$  = the heat transfer coefficient for forced convection,
- $h_r$  = a coefficient (product of the gray body shape factor and Stefan-Boltzmann constant) for radiative heat transfer,
- $h_n$  and  $h_e$  = the coefficient and exponent, respectively, for the term simulating the effects of natural convective heat transfer or some other heat transfer process such as boiling.

HEATING6 is designed so that, simultaneously, one may consider surface-to-surface heat transfer across a region as well as conduction through the region. This capability is accomplished by defining the region to contain a material as well as by defining surface-to-surface boundary conditions across parallel surfaces of the region. Also, one may consider surface-to-surface heat transfer across a gap as well as surface-to-boundary heat transfer along the edge of the gap. To provide both heat transfer mechanisms, the gap is defined as a gap region (i.e., it does not have a material associated with it) with surface-to-surface boundary conditions applied across parallel surfaces of the region. Then surface-to-boundary boundary conditions are defined on the adjacent material regions at the surfaces defining the edges of the gap. Note: A surface-to-boundary boundary condition can be applied along the surface of a region only if there is no region adjacent to it or the adjacent region is defined as a gap region.

A fin effectiveness technique based on simple geometric descriptions and well-known fin effectiveness relations (refs. 74-76) is contained in HEATING6 to simplify the modeling of finned surfaces. The fin effectiveness,  $\eta_f$ , is the ratio of the heat transfer from the fin to that from the base area of the fin, assuming convection to the fluid at the same temperature and convective heat transfer coefficient. The fluid temperature and heat transfer coefficient and fin material thermal properties are assumed constant along the length of the fin. This concept is extended to finned surface effectiveness,  $\eta_s$ . The finned surface effectiveness is the ratio of the heat transferred by the fin surface and the surface between the fins to that transferred by the surface if the fins were removed. In HEATING6, the fin effectiveness is used

to modify the effective conductance for the boundary condition on the right side of Eq. (6.7) by adjusting the effective heat transfer coefficient in Eq. (6.9) as follows:

$$h = h_c \eta + h_r [(T_i^a)^2 + (T_b^a)^2] [T_i^a + T_b^a] + h_n \eta [T_i^a - T_b^a] h_c \quad (6.10)$$

where

$\eta = \eta_s =$  finned surface effectiveness for that boundary condition and will be the same for both natural or forced convection.

Table 6.1 shows the fin effectiveness models implemented in HEATING6. Fin effectiveness models not included in Table 6.1 can be supplied in a user-supplied subroutine, FINUSR. The fin effectiveness is determined from simple geometric input and the material properties of the surface node. If the surface node's material properties or the boundary heat transfer coefficient are temperature-dependent, the fin effectiveness is updated whenever the temperature-dependent properties are updated. A similar approximation was utilized to allow transient analysis of finned surfaces even though the models were developed for steady-state applications only. The fin heat capacity was added to the heat capacity of the node to approximate the transient effect of the fin on the surface node. In general, the transient response of the surface node's temperature is a very complex calculation and could not be included in this technique. If this heat capacity modification is not desired, it can be easily eliminated. The specific heat and density can be temperature-dependent and will cause the updating of the fin effectiveness and fin heat capacity.

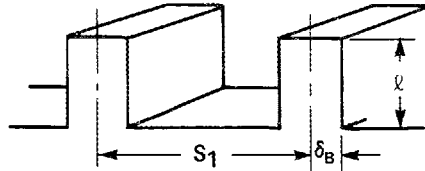
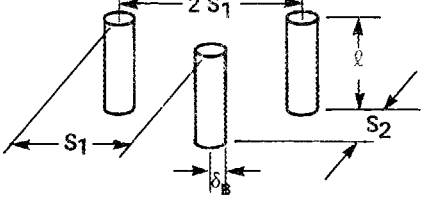
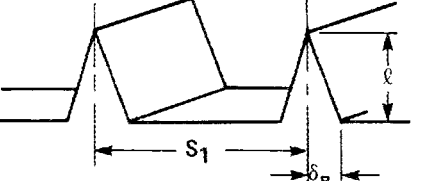
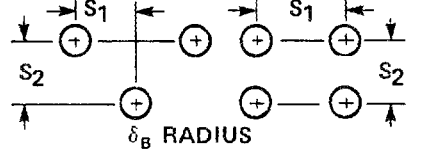
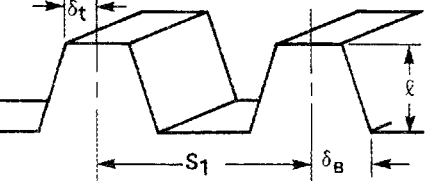
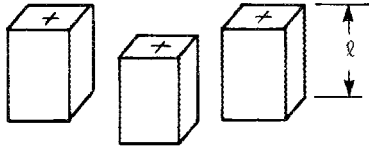
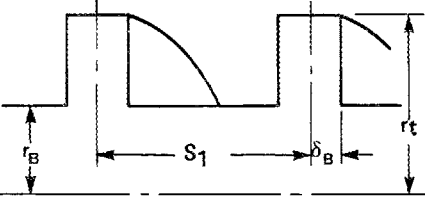
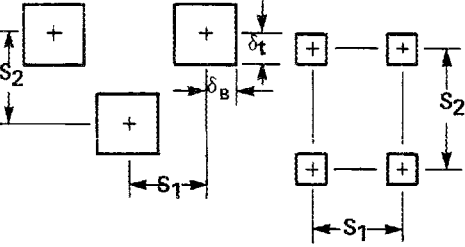
The fin effectiveness technique implemented does not check for inconsistent geometric definitions (e.g., width of fin greater than the fin spacing, fin length greater than space between surfaces for surface-to-surface boundary) or if the node spacing is smaller than the fin spacing. Modeling errors can result from these problems but checking was not implemented because of the complexity and the desire not to restrict the freedom of the user. Such inconsistencies may constitute a valid model if applied properly. If the node spacing is much smaller than the fin spacing or if the fin volume is significant compared to the node volume, an accurate geometric model of the fins is recommended rather than utilizing the fin effectiveness technique. Fin models 1-5 are two-dimensional in nature and conduction along the third dimension is neglected. The code also does not allow for thermal growth of fins.

## 6.2 USER INTERFACE AND MODELING CAPABILITIES

The input data for HEATING6 uses SCALE's free-form reading subroutines and is subdivided into data blocks identifiable by keywords. Data items or blocks may be added, modified, or deleted from the input data stream for the current model or from the previously defined model, making parametric studies easy. HEATING6 will read the input data for a case until it encounters an end-of-case indicator. It checks the input data for errors and inconsistencies and issues messages clearly identifying any data problems that may be encountered. Some data errors are fatal and cause processing to be terminated immediately. However, most errors will allow the input data processing to continue for the case but will not allow the case to be executed. This procedure allows the code to locate all or most of the input data errors with one execution. If no input data errors are encountered, HEATING6 will proceed with the specified calculations for the case. If input data errors are encountered or if the calculations for the case are completed, the code starts reading input data for the next case. If a case relies on data from the previous case, the new case will not be executed unless the previous case terminated successfully. Most of HEATING6's diagnostic messages have been improved (over that of HEATING5) by directing the user to remedial actions.

Table 6.1. Fin effectiveness models, pictorial.

DWG. NO. K/G-80-2687  
(u)

| FIN TYPE NO. | DESCRIPTION   | FIGURE   | FIN TYPE NO. | DESCRIPTION   | FIGURE  |
|--------------|---|--|--------------|---|---|
| 1            | STRAIGHT (LONGITUDINAL) RECTANGULAR CROSS SECTION         |    | 7            | SPINE RIGHT CIRCULAR CYLINDER TRIANGULAR PATTERN    |    |
| 2            | STRAIGHT (LONGITUDINAL) TRIANGULAR CROSS SECTION          |    | 8            | SPINE RIGHT CIRCULAR CYLINDER RECTANGULAR PATTERN   |    |
| 3            | STRAIGHT (LONGITUDINAL) TRAPEZOIDAL CROSS SECTION         |   | 9            | SPINE RECTANGULAR CROSS SECTION TRIANGULAR PATTERN  |   |
| 5            | CIRCULAR (ANNULAR) RECTANGULAR CROSS SECTION EXTERNAL FIN |  | 10           | SPINE RECTANGULAR CROSS SECTION RECTANGULAR PATTERN |  |

The remainder of this section will discuss the geometry models used by HEATING6, methodology for placing the lattice of nodes, user flexibility allowed via built-in functions and user-supplied routines, and availability of a material properties library.

First, the configuration of a problem is approximated by dividing it into regions, depending on the shape, material structure, indentations, cutouts, and other deviations from the allowed geometry types. In some cases, zoning into regions must be done in order to describe a specific boundary condition or a material whose thermal conductivity, density, or specific heat is a function of position. All boundaries must be parallel to the axes. There are three basic rules governing region division:

1. Boundary lines or planes must be parallel to the coordinate axes (two points, four lines, or six planes are required to enclose a region in one-, two-, or three-dimensional geometry, respectively).
2. A region may contain one material, at most (however, many regions may contain the same material). A gap region does not contain a material.
3. When a boundary condition is defined along the boundary of a region, it must apply along the full length of the boundary line for two-dimensional problems and over all of the boundary plane for three-dimensional problems.

Consider, for example, a case consisting of a simple rectangle in x-y geometry — half of which contains one material, and the other half a second material — as depicted in Fig. 6.3. This elementary case would require two regions (as indicated), one for each material. If the upper right corner of the rectangle is omitted as in Fig. 6.4, three regions are required as shown. The division of the right half of the rectangle into two regions accounts for the indented or cutout upper right corner. Note that regions 2 and 3 of Fig. 6.4 contain the same material.

Now consider the case of Fig. 6.4, introducing boundary conditions as in Fig. 6.5. The left boundary of the left-most rectangle now contains two different boundary types. Thus, in accordance with the third basic rule, region zoning is performed to account for the different boundary conditions, and an additional region is required.

To specify heat transfer between parallel surfaces, one defines a region whose boundaries include the two parallel surfaces. Then, the boundary condition describing the heat transfer process (type 3) is applied along both of the surfaces of this region. Although the regions adjoining the parallel surfaces involving the surface-to-surface heat transfer may be composed of more than one material, they must be defined and must contain a material. The region itself may or may not contain a material. In Fig. 6.6, surface-to-surface heat transfer cannot be defined between the left and right boundaries of Region 3 since part of the area adjoining the right boundary is undefined. In Fig. 6.7 surface-to-surface boundary conditions can be applied along the left and right sides of Region 3.

If a surface-to-surface (type 3) boundary condition has been defined along a surface of a region and a surface-to-boundary (type 1) boundary condition is desired along the same surface, then the type 1 boundary condition must be applied along the surface of the adjoining region. In Fig. 6.7, surface-to-surface boundary conditions can be applied along the left and right sides of Region 3, while a surface-to-boundary boundary condition can be applied along the left side of Region 4. Again, boundary condition specifications can be done only if Region 3 is a gap region.

The second requirement for describing the overall problem configuration is to construct a set of lattice lines perpendicular to each axis and extending the entire length of the remaining coordinates. The lattice lines are really points, lines, or planes for a one-, two-, or three-dimensional problem, respectively. However, the phrase, lattice line, will be used for illustrative purposes. The lattice is defined in the following manner. The lattice lines are divided into two classes: gross lattice lines and fine lattice lines. A

ORNL-DWG 76-10916

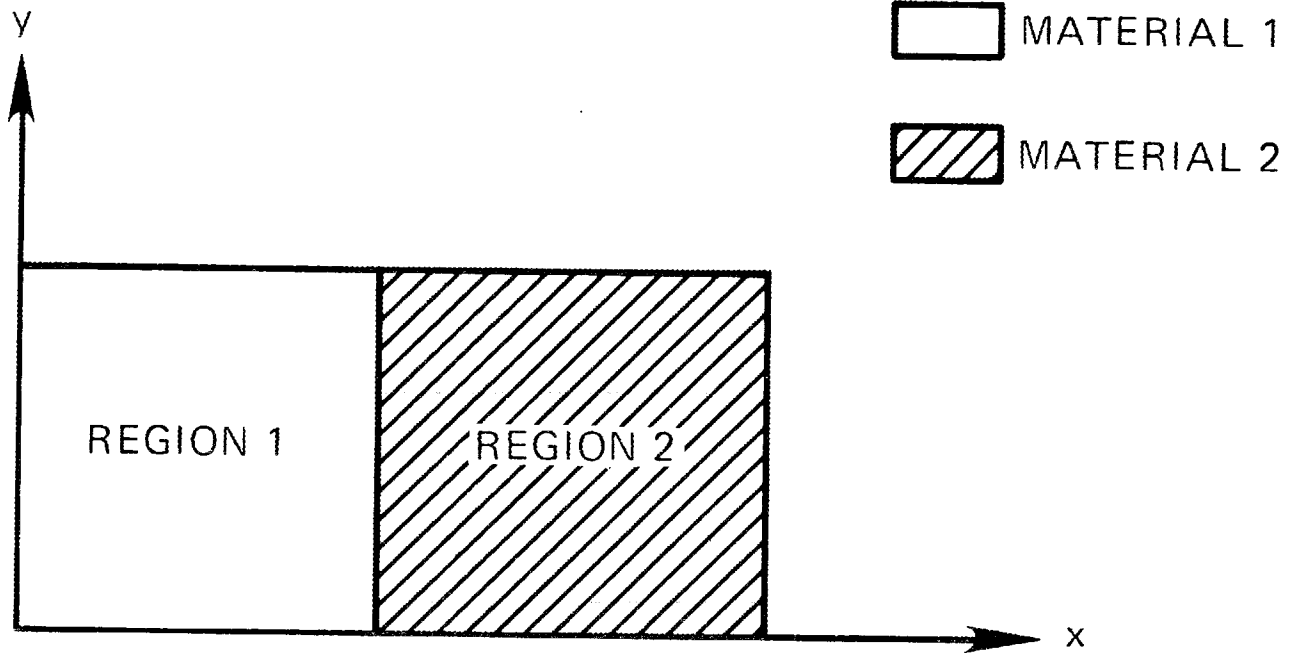


Fig. 6.3. HEATING6 region description for two-dimensional, rectangular model composed of two materials.

ORNL-DWG 76-10915

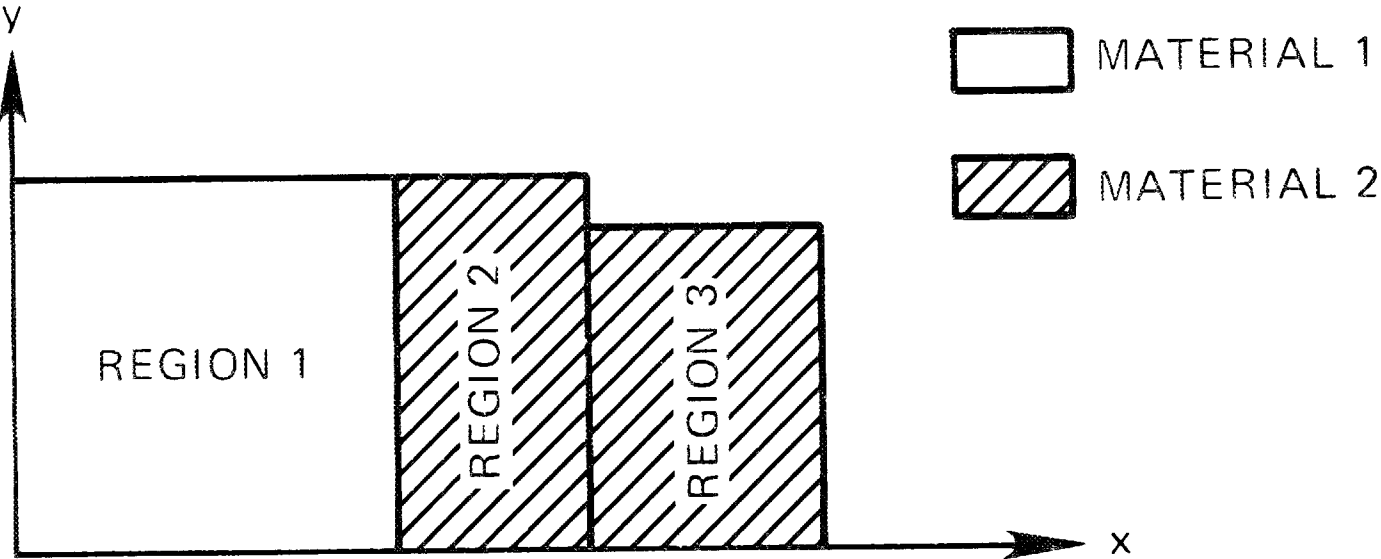


Fig. 6.4. HEATING6 region description for two-dimensional, rectangular model with indentation.

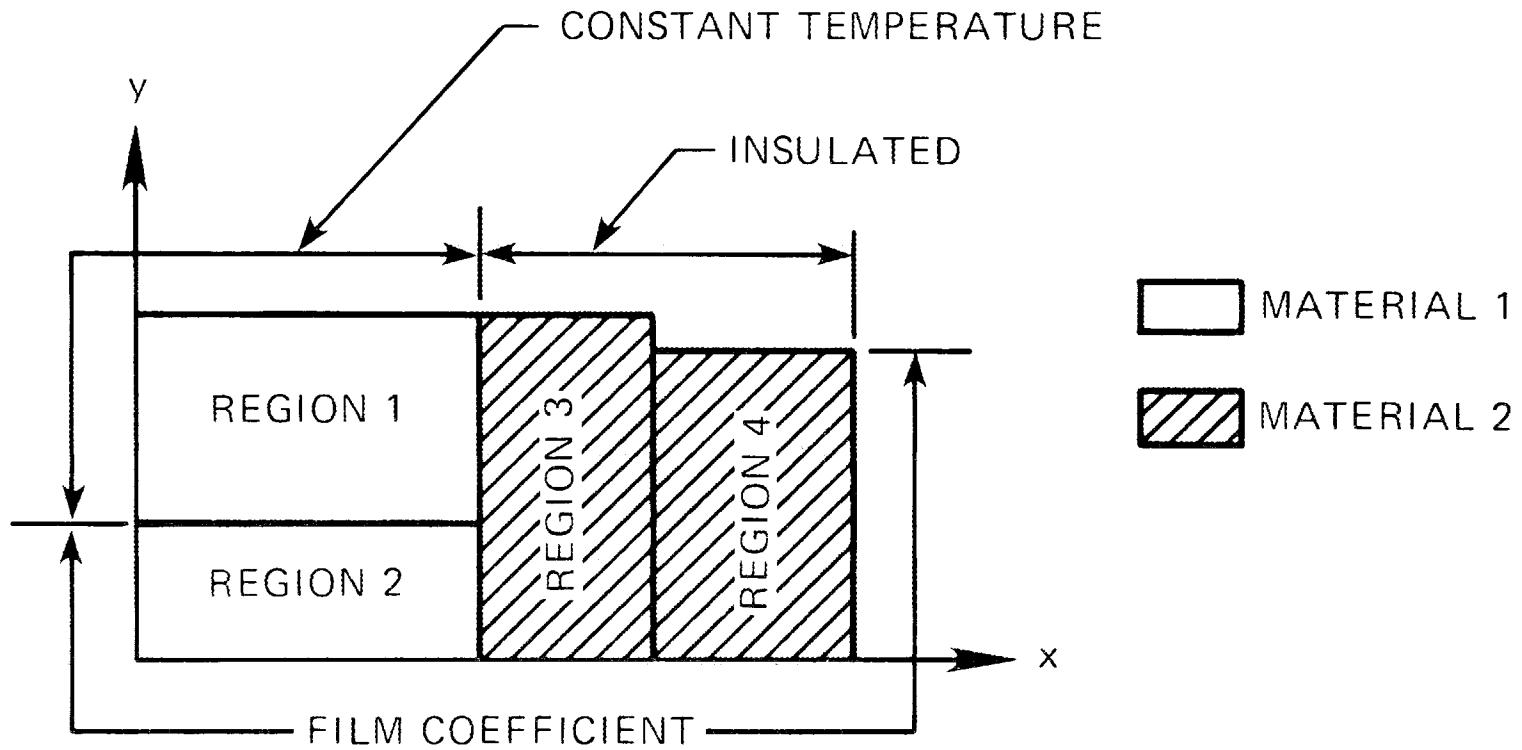
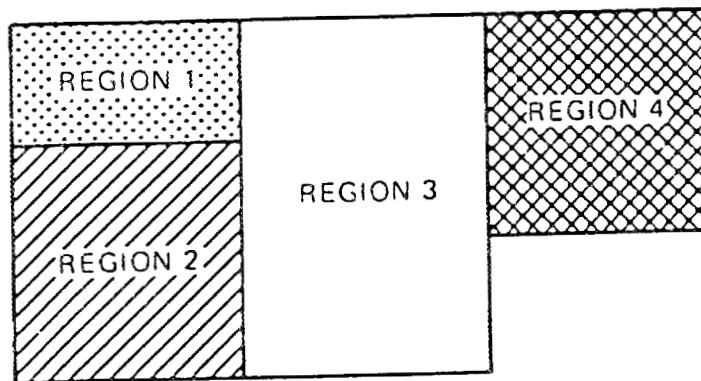


Fig. 6.5. HEATING6 region description for two-dimensional, rectangular model with various boundary conditions.



ORNL DWG 76 10918

-  MATERIAL 1
-  MATERIAL 2
-  MATERIAL 3
-  GAP

Fig. 6.6. Region description for two-dimensional, rectangular model involving surface-to-surface boundary conditions, incompatible with HEATING6.

ORNL-DWG 76-10919

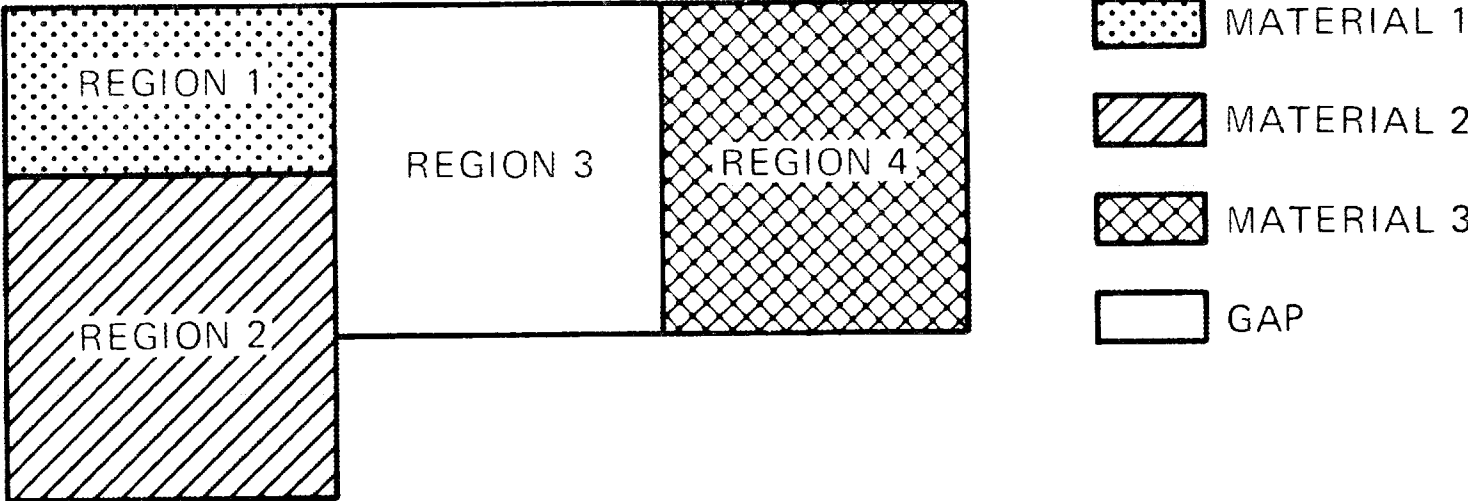


Fig. 6.7. HEATING6 region description for two-dimensional rectangular model involving surface-to-surface boundary conditions.

gross lattice line must be specified at both region boundaries along each axis. Fine lattice lines, equally spaced, may appear between two consecutive gross lattice lines to create a finer mesh. If unequal mesh spacing is desired within a particular region, then gross lattice lines may appear within that region. A nodal point is defined by each lattice point in one-dimensional problems, by each intersection of two lattice lines appearing in a material region or on its boundary in two-dimensional problems, and by every intersection of three lattice planes appearing in a material region or on its boundary in three-dimensional problems. The points are numbered consecutively by the program at the intersection of each X- (or R-), Y- (or  $\theta$ -), and Z-plane starting with the planes nearest the origin and changing the X- (or R-) plane most rapidly and the Z-plane least. Temperatures are calculated at each such nodal point.

The nodal temperature output from HEATING6 is a map-type presentation of two-dimensional slices. Figure 6.8 shows an example of the map-type output for a HEATING6 sample problem. The horizontal dashed lines and "I's" in the decimal location serve to denote different materials. The number of significant figures, material marking characters, and format of the map output can be controlled via the input. An additional user-supplied routine is available to obtain special output desired by the user.

Specification of the time, space, and temperature dependency of various input parameters is another step in the HEATING6 input. Built-in analytical and tabular functions are provided to aid in the description of these input parameters. An analytical function is defined by

$$F(v) = A_1 + A_2v + A_3v^2 + A_4\cos(A_5v) + A_6\exp(A_7v) \\ + A_8\sin(A_9v) + A_{10}\ln(A_{11}v) \quad (6.11)$$

A tabular function is defined by a set of ordered pairs,  $(v_1, G(v_1)), (v_2, G(v_2)), \dots, (v_n, G(v_n))$ , where the first element of a pair is the independent variable and the second is the corresponding value of the function. In order to evaluate the tabular function at some point, the program uses linear interpolation in the interval containing the point. The set of ordered pairs must be chosen so that the independent variables are arranged in ascending order. Extrapolation beyond the end points is not done; instead, the respective end-point values are used.

The input parameters included in Table 6.2 must be defined by a function having the following form:

$$P(x,y,z,t,T) = P_0 \cdot f(x,y,z,t,T) , \quad (6.12)$$

where  $P_0$  is a constant factor and  $f(x,y,z,t,T)$  may be a product of analytical and tabular functions. Note that only the volumetric heat generation rate is a function of all the independent variables. Thus, if any variable is omitted from the definition of the parameter, then the corresponding factor is set equal to unity. The constant factor,  $P_0$ , is part of the input data, and its value appears on the data card, which is used to define the parameter.

If the parameter cannot be defined by a product of analytical and tabular functions, then the user may supply his own subroutine to evaluate Eq. (6.11). Table 6.2 contains each input parameter and the name of the corresponding subroutine that must be supplied if the user wishes to create his own function. Table 6.2 also includes the independent variables which may be used to define each parameter.

The HEATING6 program gives the user the option of supplying the material properties data for a problem on the material input cards or of allowing the program to extract the properties from one of the

HEATING6 10/30/80  
WDTHEAT6

TEST PROBLEM #3 FOR HEATING6

STEADY STATE TEMPERATURE DISTRIBUTION AFTER 10 ITERATIONS, TIME = 6.000000+01

| GROSS GRID |    | 1    | 2       | 3       | 4       | 5       | 6       | 7       |         |         |
|------------|----|------|---------|---------|---------|---------|---------|---------|---------|---------|
| FINE GRID  |    | 1    | 2       | 3       | 4       | 5       | 6       | 7       |         |         |
| DISTANCE   |    | 1.00 | 1.50    | 2.00    | 2.75    | 3.25    | 3.75    | 4.50    | 5.50    |         |
| 1          | 1  | 1.50 | 600I00  | 600.00  | 600I00  | 600I00  | 237I60  | 228I55  | 0.0     | 0I0     |
| 2          | 2  | 2.25 | 670I11  | 663.85  | 643I08  | 544I21  | 251I61  | 246I09  | 0.0     | 0I0     |
| 3          | 3  | 3.00 | 745I57  | 737.58  | 711I56  | 592I62  | 281I10  | 280I99  | 274.96  | 255I96  |
| 4          | 4  | 3.50 | 803I12  | 796.60  | 775I36  | 675I55  | 294I68  | 292.62  | 284.83  | 274I76  |
| 5          | 5  | 4.00 | 863I52  | 860.21  | 851I00  | 831I58  | 907I40  | 934.41  | 942.25  | 949I40  |
| 6          | 6  | 4.75 | 947I14  | 947.41  | 949I94  | 957.98  | 974.64  | 984.83  | 985.78  | 962I00  |
|            | 7  | 5.25 | 988I99  | 989.58  | 991.71  | 998.15  | 1005.42 | 1009.88 | 1007.12 | 983I21  |
|            | 8  | 5.75 | 1018I84 | 1019.35 | 1020.93 | 1025.08 | 1028.08 | 1028.99 | 1023.23 | 998I29  |
|            | 9  | 6.25 | 1036I66 | 1037.06 | 1038.21 | 1040.79 | 1041.80 | 1040.82 | 1033.21 | 1007I37 |
| 7          | 10 | 6.75 | 1042I58 | 1042.94 | 1043.92 | 1045.97 | 1046.38 | 1044.84 | 1036.59 | 1040I41 |

TEMPERATURES ON NUMBERED BOUNDARIES

| BOUNDARY NUMBER | TEMPERATURE |
|-----------------|-------------|
| 1               | 600.000000  |
| 2               | 0.0         |
| 3               | 68.000000   |
| 4               | 0.0         |
| 5               | 100.000000  |

ELAPSED CPU TIME IS 14.32 SECONDS

THE MAXIMUM TEMPERATURE IS - 1.046380+03 (+-0.1 PERCENT)

MAX. TEMP. APPEARS AT NODES - 72 73

THE MINIMUM TEMPERATURE IS - 2.285500+02 (+-0.1 PERCENT)

MIN. TEMP. APPEARS AT NODES - 6

THE STEADY STATE CALCULATIONS HAVE BEEN COMPLETED.

NUMBER OF ITERATIONS COMPLETED = 10

Fig. 6.8 Example of map-type temperature edit from HEATING6.

Table 6.2. Dependence of input parameters<sup>a</sup>

| Parameter      | Function of |     |     |     |   | Related user-supplied subroutine |
|----------------|-------------|-----|-----|-----|---|----------------------------------|
|                | x           | y   | z   | t   | T |                                  |
| k              |             |     |     | (x) | x | CONDTN                           |
| $\rho$         |             |     |     | (x) | x | DNSITY                           |
| C <sub>p</sub> |             |     |     | (x) | x | CPHEAT                           |
| T <sub>o</sub> | x           | x   | x   | (x) |   | INITTP                           |
| Q              | x           | x   | x   | x   | x | HEATGN                           |
| T <sub>b</sub> | x           | x   | x   | x   |   | BNDTMP                           |
| h <sub>c</sub> | (x)         | (x) | (x) | x   | x | CONVTN                           |
| h <sub>r</sub> | (x)         | (x) | (x) | x   | x | RADITN                           |
| h <sub>n</sub> | (x)         | (x) | (x) | x   | x | NATCON                           |
| h <sub>e</sub> | (x)         | (x) | (x) | x   | x | NCONEX                           |
| h <sub>f</sub> | (x)         | (x) | (x) | x   | x | BNFLUX                           |

<sup>a</sup>The x enclosed in parentheses, (x), indicates that although the parameter cannot be an explicit function of the indicated variable using normal input data, this variable is initialized in the respective user-supplied subroutine. Thus, the parameter can be a function of the indicated variable if it is so defined in its respective user-supplied subroutine.

three available material properties libraries which differ only in the unit systems of the material properties (cgs-calorie-°C, mks-J-°C, mks-J-°K).<sup>11</sup> The material properties given in the libraries are density, thermal conductivity, specific heat, transition temperature, and latent heat. The density of the material is typically either the value at or near room temperature, or the lowest temperature for which specific heat or conductivity is tabulated, whichever is highest. The thermal conductivity of the material is given if it is constant or if the temperature dependence is unknown. When a table of conductivity vs temperature is listed, the table will be stored and used as a tabular function. The specific heat of a material is given if it is constant or if the temperature dependence is unknown. When a table of specific heat vs temperature is listed in the library, the table will be stored and used as a tabular function. The transition temperature is the temperature at which either a phase change or a solid-state transition occurs. The latent heat is the amount of heat absorbed by the material when the temperature is increased past the transition temperature. The transition temperature and the latent heat of a material will be stored only if a phase change is specified.

Finally, the user is cautioned that, like most sophisticated analysis codes, HEATING6 is not a black box that digests the input data and automatically yields the correct solution to the physical problem. Care must be exercised in correctly simulating the physical problem as well as in interpreting the results from the code. For steady-state problems, one must experiment with the mesh spacing in order to gain confidence in the numerical solution to a model of a physical problem. For instance, numerical solutions must be obtained for several different mesh spacings, then these solutions must be compared and the differences that are noted at points of interest must be acceptable. As noted earlier, one must also experiment with the convergence criterion. When the criterion is satisfied, it only guarantees that the temperatures did not change more than a specified amount over the previous iteration. This is sufficient for many problems, but it is possible to have a problem that is converging so slowly that the convergence criterion is satisfied even though the last iterate is a very poor estimate of the true solution to the model. Again, one must make several calculations with different convergence criteria and compare the results before obtaining confidence in the solution. For transient problems, one must often experiment with the size of the time increment as well as study the effects of varying the mesh spacing and convergence criteria.

### 6.3 NEW FEATURES OF HEATING6.1

Recent development work on HEATING6 has produced a new version denoted as HEATING6.1 which will be released as part of the SCALE-4 package.update. The major improvements to the new version include addition of node-to-node connectors, two- and three-dimensional spherical geometries, and a shared nodal location philosophy.

The current public release version of HEATING6 (January 22, 1985) models radiation within an enclosure as strictly one-dimensional (i.e., a node can only exchange heat by radiation with the node that is directly across a region from itself). This approximation is accurate only for narrow gaps. A more realistic model would include radiant exchange between a node and all other nodes in the enclosure that it can "see." The HEATING6.1 version allows this more general radiation modeling capability by including user-defined heat flow paths (node-to-node connectors) between any two nodes in the mesh. The number of connections that can be included in the model is limited only by the size of the computer being used. These heat flow paths are added to those produced by the normal HEATING6 technique. This technique is presently not as automated as the normal HEATING6 techniques in that it requires a knowledge of node numbers and associated areas when the input is generated. The user would typically build a model without node-to-node connectors, make a preliminary execution of the code to obtain node numbers, and then set up the node-to-node connector input data.

A standard HEATING6 boundary condition is used to specify the heat transfer mechanism(s) that will be applied between nodes connected with node-to-node connectors. Similar to ordinary boundary conditions, they may be used to model radiation, convection, or natural convection and can be time and/or temperature dependent. However, they may not model a prescribed heat flux. The boundary condition is used to determine a conductance,  $h$ , between any two nodes, using the expression of Eq. (6.9). There is a constant multiplier applied to this conductance for each node-to-node connector. This multiplier, referred to as a connectivity, is entered in the input data deck. For a radiation problem this connectivity is the product of an exchange factor (simply the view factor for blackbody radiation) from node  $i$  to node  $j$  and the area associated with the base node,  $i$ .

To facilitate the utilization of HEATING6.1 node-to-node connectors in the HTAS1 control module, the OCULAR code has been developed as a module of SCALE. OCULAR is a radiation exchange factor computer code compatible with the axisymmetric r-z geometry of HEATING6.1. The code may be used to generate gray body exchange factors, as well as geometric configuration factors, which describe the radiative exchange in the cylindrical or annular enclosures that are characteristic of an axisymmetric geometry. OCULAR will be released as a functional module in the SCALE-4 package.

The addition of two- and three-dimensional spherical geometries gives HEATING6.1 a complete multidimensional modeling capability. However, with the mesh generation philosophy used in HEATING6, several situations arise in which there should be multiple nodes sharing the same physical location. HEATING6 currently handles this by either not allowing nodes at that location (e.g., at a radius of zero on a cylinder) or by not recognizing that the nodes are at the same location (e.g., for a 360° cylinder, nodes on the smaller and larger  $\theta$  edges of the model). With the inclusion of two- and three-dimensional spherical geometries, shared nodal locations are even more pervasive. For spherical cases, shared nodal locations occur at a radius of zero, at the union of a 360° sphere in  $\theta$  direction, and at nodes located along the line passing through the north and south poles of the sphere ( $\phi = \pm \pi/2$ .) In order to overcome these limitations and produce more realistic results, a shared nodal location philosophy has been introduced to the HEATING6.1 version of the code. All connections to any node at a shared nodal location are accumulated into the lowest node number at that location. No connections are made to the higher node numbers, and they essentially disappear from the solution. Information about heat generation rates and phase change for shared nodes is similarly treated as if it were associated with the lowest node number sharing the location. In the HEATING6.1 output, all nodes sharing the same location have the same temperature, and nodal temperatures can be obtained at the radial center of cylindrical and spherical problems.

#### 6.4 GRAPHICAL DISPLAY CAPABILITIES

Two codes, REGPLOT6 and HEATPLOT-S, are included in the SCALE system to provide a graphical display of HEATING6 geometry models and temperature profiles. Both plotting codes use the DISSPLA (Display Integrated Software System and Plotting Language)<sup>53</sup> graphics package and generate compressed plot data sets that can be stored on disk or routed to various plotting devices.

REGPLOT6 is a plotting program that enables the user to graphically verify the accuracy of his HEATING6 input model. REGPLOT6 plots the region boundaries of a one-, two-, or three-dimensional model. The region numbers, the material names, the heat generation function numbers, the initial temperature function numbers, and the boundary condition function numbers may be plotted for each region in any plane of the model. This version of REGPLOT6 may be used with HEATING6 input data sets that specify a maximum of 300 regions and 300 materials. REGPLOT6 input data are specified by adding another data block (beginning with keyword REGP) to a HEATING6 input deck.

HEATPLOT-S may be used with the HEATING5<sup>70</sup> or HEATING6 generalized heat conduction codes to generate plots of temperature distributions. HEATPLOT-S has the capability of generating temperature contours, temperature-time profiles, and temperature-distance profiles. The contours and temperature profiles may be generated from the current temperature distribution or from temperature changes relative to the initial temperature distribution. HEATPLOT-S requires as input the data set created by using the plotting option of HEATING5/HEATING6 and user-supplied card image input data. HEATPLOT-S determines from the card image input data the temperature, time, and distance units, the types of plots generated, how the plots are scaled, and the problem times for which the plots are generated. For temperature contour plots, HEATPLOT-S determines the number of contours to be plotted and the planes and regions for which contours are plotted. In addition, HEATPLOT-S determines whether or not the plot axes are reversed and/or switched. For temperature-time profile plots and temperature-distance profile plots, HEATPLOT-S determines the nodes or lines for which profiles are plotted and whether each profile appears on a separate plot or whether all profiles appear on one plot.

#### 6.5 CAPABILITIES OF THE HTAS1 CONTROL MODULE

As noted in an earlier section, HEATING6 is a complex code that often requires a large amount of input and careful consideration of the time and/or space mesh. Thus, the Heat Transfer Analysis Sequence No. 1 (HTAS1) was developed within SCALE to generate the necessary HEATING6 input

and automatically manipulate the module to perform a two-dimensional (R-Z) thermal analysis for a specific class of shipping containers during normal, fire, and post-fire conditions. Keywords, free format, and extensive use of default parameters and options simplifies the HTAS1 input to the point that a novice user can easily obtain a shipping cask thermal analysis. Each shipping cask component (e.g., inner shell, neutron shield, etc.) is identified by a keyword and appropriate axial and radial thicknesses. A standard material properties library in HTAS1 makes identification of thermal properties a simple matter of designating the correct identifier for each component material of the cask. Default materials are available for each shipping cask component. Boundary conditions are generated automatically for each surface.

The HTAS1 sequence begins by establishing the steady-state pre-fire conditions based on an input fuel heat generation, a default solar heat load, and default radiative and natural convective boundary conditions per requirements of the U.S. Code of Federal Regulations, Part 71 of Title 10 (see ref. 77). From the input heat generation (available from the thermal decay heat calculated by the SAS2/ORIGEN-S modules of SCALE), HTAS1 establishes the heat flux impinging on the axial and radial wall of the inner shell. Following the steady-state analysis, the sequence proceeds through a 30-minute fire and post-fire transient lasting three hours. The default fire conditions are established to meet the requirements of ref. 77. Following the transient analysis, a post-fire steady-state analysis is performed. The available analyses and their respective keywords are shown in Table 6.3. The entire analytical sequence, or an optional segment of the sequence, is run with a single HTAS1 calculation using repeated calls to HEATING6. Each of the analyses noted above is specified by a keyword. Following each keyword, the user may alter the default values for the ambient temperature and the coefficients and exponents used in the heat transfer correlation for natural convection from radial and axial surfaces. The direct solution method and Crank-Nicolson implicit techniques using specified parameters are the default numerical techniques for the steady-state and transient analysis, respectively. When phase change is allowed, HTAS1 will use Levy's modified explicit procedure for the transient analyses. The default numerical technique may also be overridden for each phase of the sequence.

Table 6.3. Analysis specification keywords for HTAS1 model

|          |  |
|----------|--|
| INITIAL  | - initial steady state                 |
| PREFIRE  | - steady state immediately before fire |
| FIRE     | - fire transient                       |
| POSTFIRE | - transient immediately following fire |
| FINAL    | - final steady state                   |

The specific class of shipping containers that can be analyzed using HTAS1 are shipping casks which can be modeled as concentric cylinders that may be axially asymmetric. Figure 6.9 shows the basic geometric model and the dimensions that must be input. The mesh is specified by specifying the number of mesh intervals within each input thickness (per Fig. 6.9). Typical components include an inner and outer shell, water jacket, neutron and gamma shields, and impact limiters. A cavity, inner shell, and outer shell are required. The neutron shield and water jacket must appear as a pair. Allowance is made for optional removal of the water jacket and impact limiters (one or both) and/or loss of the neutron shield after any of the analyses noted above. HTAS1 has been developed to allow the user to input fin data or override default emissivity and thermal property data. The seven zone keywords and their associated default material are shown in Table 6.4. For the water-filled neutron shield, HTAS1 will use material 17, denoted as H20CONV, from its material property library. The effective thermal conductivity of material 17 was designed to simulate the effects of the natural circulation in a 4.5-in.-wide annulus (ref. 78). This temperature-dependent effective thermal conductivity was derived using a correlation by Liu, Mueller, and Landis for approximating the thermal conductivity due to natural convection through a medium enclosed in an annular space between concentric cylinders (ref. 79).

DWG. NO. K/G-83-7  
(U)

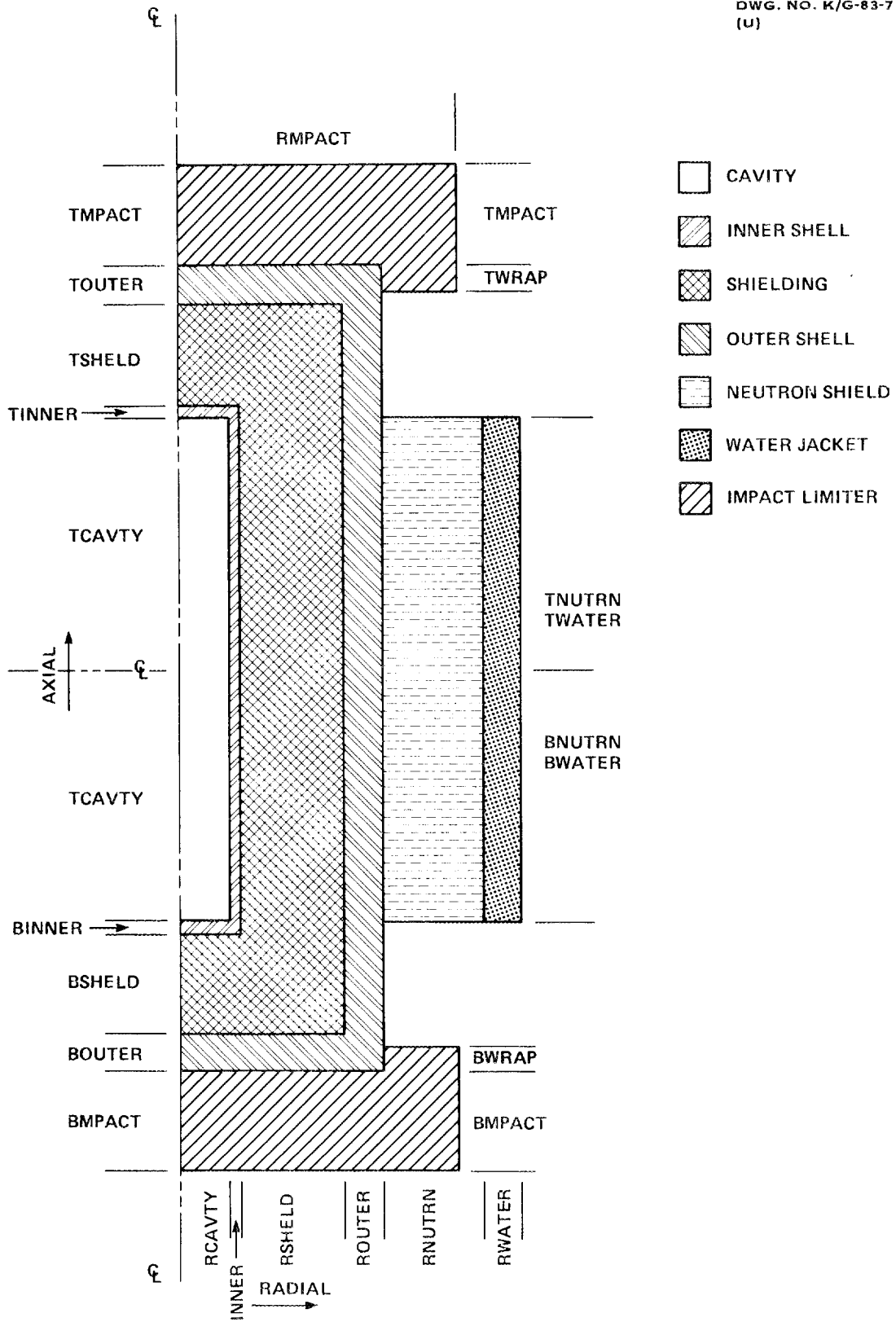


Fig. 6.9. Zone configuration in HTAS1 general model with physical dimension labels.

Table 6.4. Keywords for zones in HTAS1 model

| Zone keyword    | Default material index | Default material name | Default material description                                |
|-----------------|------------------------|-----------------------|---|
| CAVITY          |                        |                       | Void  |
| INNER SHELL     | 13                     | SST304                | Stainless Steel 304   |
| SHIELDING       | 11                     | LEAD                  | Lead  |
| OUTER SHELL     | 13                     | SST304                | Stainless Steel 304   |
| NEUTRON SHIELD  | 17                     | H20CON                | Water, effective conductivity simulating natural convection |
| WATER JACKET    | 13                     | SST304                | Stainless Steel 304   |
| IMPACT LIMITERS | 19                     | BALSA                 | Balsa wood, thermal conductivity across grain               |

HTAS1 automatically generates appropriate boundary conditions for the outer surfaces of the model based on the thermal analysis being performed, the boundary parameters associated with the thermal analysis, and the emissivities of the materials on the outer surfaces. Default emissivities per ref. 77 are provided. Allowed boundary conditions include natural convection to or from the surrounding medium, radiation to or from the surrounding medium, and a prescribed heat flux to simulate the solar heat load.

The film coefficient correlation to simulate the natural convective heat transfer effects across a surface has the form

$$h_c = h_n |T_s - T_a|^{h_c} \quad (6.13)$$

where

- $T_s$  = the surface temperature,
- $T_a$  = the ambient temperature for the thermal analysis involved,
- $h_n$  = the natural convective coefficient,
- $h_c$  = the natural convective exponent.

For a radial surface, the default values of  $h_n$  and  $h_c$  are 0.18 Btu/(hr-ft<sup>2</sup>-°F) and 1/3, respectively, to simulate the natural convective heat transfer due to the turbulent flow of air across the radial surface of a long, horizontal cylinder (ref. 80). For an axial surface, the default values of  $h_n$  and  $h_c$  are 0.19 Btu/(hr-ft<sup>2</sup>-°F) and 1/3, respectively, to simulate the natural convective heat transfer due to the turbulent flow of air across the end of a horizontal cylinder (ref. 80).

The effective heat transfer coefficient to simulate the radiative heat transfer at the surfaces of the model before and after the fire has the form (ref. 80)

$$h_r = \sigma \epsilon_s (T_s^2 + T_a^2)(T_s + T_a) , \quad (6.14)$$

where

$\sigma$  is the Stefan-Boltzmann constant or  $0.173 \times 10^{-8}$  Btu/(hr-ft<sup>2</sup>-°R<sup>4</sup>),  
 $\epsilon_s$  is the emissivity of the material on the surface of the model.

During the fire, the effective radiative heat transfer coefficient used by HTAS1 has the form (ref. 80)

$$h_r = \sigma \left( \frac{1}{\frac{1}{\epsilon_s} + \frac{1}{\epsilon_f} - 1} \right) (T_s^2 + T_f^2)(T_s + T_f), \quad (6.15)$$

where

$\epsilon_f$  is the emissivity of the fire,  
 $T_f$  is the temperature of the fire.

If loss of the neutron shield material is specified, HTAS1 generates a boundary condition to model one-dimensional radiative heat transfer between the opposing radial surfaces of the neutron shield. As default, the lost material is replaced by air which has an effective conductivity value of 0.1 Btu/hr-ft-°F to simulate natural convective effects that will occur in the resulting enclosure.

Subroutines from REGPLOT6 are included in HTAS1 so that the HEATING6 input generated by HTAS1 to describe the heat transfer model at each calculational phase can be graphically verified if the user selects the region plotting option. By default, plots of the regions, the materials, and the boundary condition function numbers are generated for each calculational phase. HEATING6 is not executed when region plots are generated. Therefore, a minimum of execution time can be used to verify that the input supplied to HTAS1 has produced the desired HEATING6 input. An example of a REGPLOT6 plot for the HTAS1 sample problem cask is shown in Fig. 6.10. Material \*3135 refers to the material with that identifying number from the HEATING6 thermal property library of ref. 11.

Temperature profile plots may also be generated by HTAS1 if the user desires. If the temperature profile plotting option is selected, one temperature distribution plot data set is written by HEATING6 during the fire transient calculations, and another temperature distribution plot data set is written by HEATING6 during the post-fire transient calculations. The user may save these plot data sets and later execute HEATPLOT-S to generate plots using these data sets as input.

Three default plots are generated by HTAS1 by simply including the keyword PLOT in the input. The first plot contains temperature vs time curves for the nodes in the center of the inner shell, the shielding, and the outer shell. If a node is not located in exactly the center of a particular zone, the node closest to the center of that zone is used. If the shielding is not modeled, the node that represents the inner shell is located on the radial fine grid line that is the border between the cavity and the inner shell, the node that represents the shielding is located on the radial fine grid line that is the border between the inner shell and the outer shell, and the node that represents the outer shell is located on the radial fine grid line that denotes the outer boundary of the outer shell. The second plot contains a curve that shows maximum temperature at any problem time vs the radial distance from the origin for all nodes on the axial centerline. The third plot contains a curve that shows the difference in volume-averaged temperatures between the inner shell and the outer shell as a function of time. These type plots were selected to aid in reviewing for possible melting and for evaluation of thermal stresses.

The shipping cask of Fig. 6.11 was analyzed using HTAS1 with slight changes in the model due to the HTAS1 requirement for having concentric cylinders (i.e., the axial and radial gamma shields were

Map of the Materials

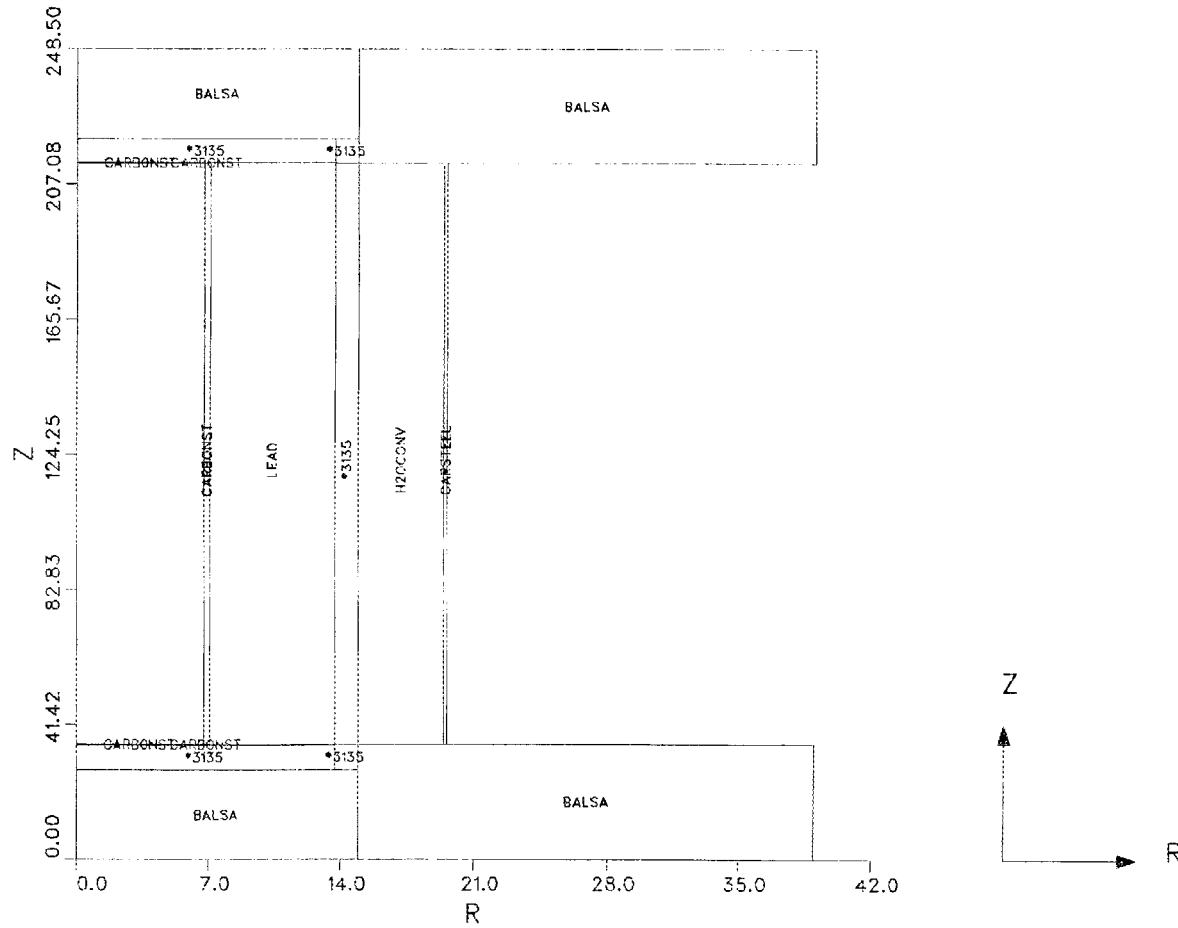


Fig. 6.10. Example of REGPLOT6 output for HTAS1 sample problem 2.

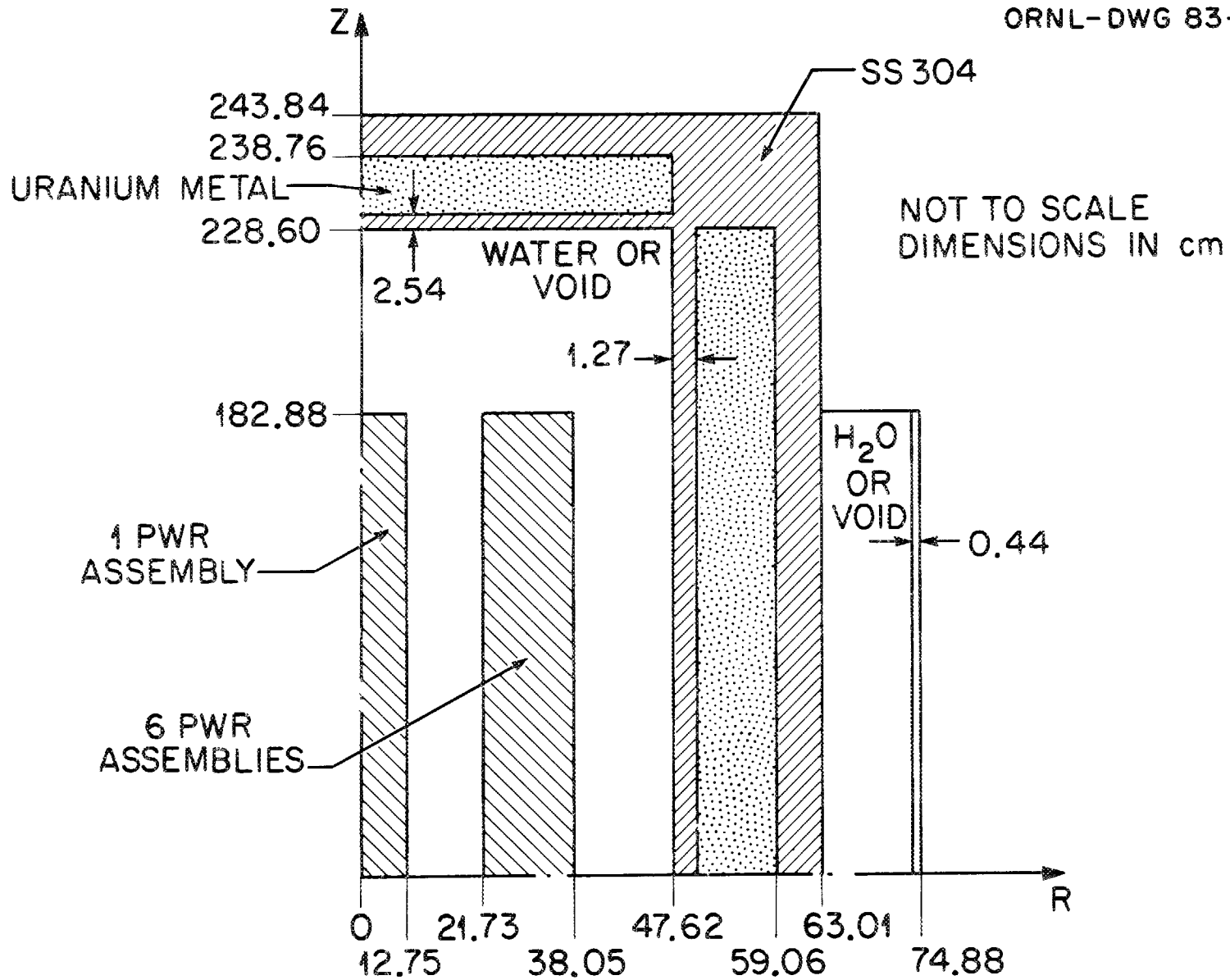


Fig. 6.11. Typical shipping cask calculational model.

connected). The simple input for this analysis is shown in Fig. 6.12. Note that the input is in mixed English units (inches, Btu/hr, minutes, and °F). The integer values following the axial and radial thicknesses of each cask component are the number of mesh intervals for that thickness. The first entry on the cavity (210000) card is the heat generation rate. Note that material 12 (uranium metal) was used for the gamma shield, thus overriding the default material (lead). Also, fins were added to the axial and radial outer shell surfaces, and the neutron shield was deleted (water removed, replaced with air, and surface emissivities set at 0.6) following the PREFIRE steady-state analysis. Parameters entered after the PREFIRE, POSTFIRE, and FINAL analysis denote changes to various default values. The analysis yielded a maximum shield temperature of 453°C and a maximum outer shell temperature of 562°C during the accident transient, well below the melting temperature of either cask material (uranium metal and SS304).

## 6.6 VERIFICATION EFFORTS

In the development of each new version of the HEATING series of codes, great care was taken to ensure that the code did produce accurate solutions to heat transfer problems. Similarly, extensive checking was performed on HEATING6 during its development and subsequent use. Unfortunately, for the most part, the checking that was done was not documented, nor was a formal verification study ever presented in a citable document. Recently, an effort was undertaken to produce a document that provides: (1) a rigorous verification of the analysis options available with HEATING6 against published analytical solutions, (2) a check of boundary conditions for which analytical solutions are not available, and (3) a set of reference cases to benchmark the code.<sup>81</sup>

Twenty-three cases with known analytic solutions were identified and are presented in ref. 81 to validate several of the analysis options available with HEATING6. Any differences between the two temperature solutions and sources of error are discussed where appropriate to illustrate the behavior of both the analytic and HEATING6 solutions. All of the differences between HEATING6 solutions and the analytical solutions are acceptably small for engineering applications. In fact, the agreement can generally be described as excellent. Detailed verification cases for radiation, natural convection, and surface-to-surface-type boundary conditions are not included due to a lack of analytical solutions. Only one of the eight finned-surface boundary conditions is included. Additionally, the one-dimensional cylindrical (z) geometry is not validated in this study.

There are several important analysis options in HEATING6 for which complete analytical solutions are neither available nor easily derivable. However, the absence of complete analytical solutions does not totally preclude some verification of these options. One approach is to develop a simple problem which includes the option of interest. By judicious design of the problem, it may be possible to extract information from the HEATING6 solution that can be compared directly to a simple calculation. This is not as rigorous a test as a detailed comparison to an analytical solution, but it can confirm that the behavior of the numerical solution is consistent with theory. The testing of boundary conditions is particularly amenable to this type of approach. If there is no heat generation within the model, then any changes in energy storage or temperature gradient are a direct result of heat transfer at the boundaries. This permits an easy check of the boundary condition. The verification cases of this type presented in ref. 81 demonstrate that HEATING6 produces results consistent with analytical values for all of the boundary conditions tested.

The HEATING code has evolved through many versions, and this evolution is continuing. It is imperative that modifications to the code do not adversely impact existing features. The verification cases noted above offer a means of checking for many such inadvertent changes to the code. However, these cases are not sufficient to adequately check all features of the code since they only exercise one option at a time. Any problems resulting as a consequence of the interaction of two or more features would not be discovered. Inadvertent changes can also be a problem when the code is implemented on a

ORNL DWG. 87-13392

```
=HTASI
TYPICAL PWR SHIPPING CASK

CAVITY 18.75 5 84.75 5 210000
INNER SHELL 0.5 1 1.0 1 1.25 1
SHIELDING 4.0 5 3.0 4 3.75 4
MATERIAL 12
OUTER SHELL 1.5 2 2.0 2 1.5 2
FINS 1 1
7.0 0.75 0.75 2.5 0.0 1.0
7.0 0.75 0.75 2.5 0.0 1.0
NEUTRON SHIELD 4.5 4 63.75 80.25
DELETE PREFIRE 0 0.6 0.6
WATER JACKET .125 1
PREFIRE 100 .3827
FIRE
POSTFIRE 1.80 100 .3827
FINAL 100 .3827
%
END
```

Fig. 6.12. Typical shipping cask input for HTASI.

different computer system than the one on which it was developed and verified. For these reasons, ref. 81 presents a selection of test cases that were chosen to benchmark the performance of the code. These complicated test cases exercise several analysis options simultaneously. They serve as a basis of comparison for any future modifications to the code or implementation of the code on other computer systems.

In addition to the above verification effort, the developers have been involved with recent comparative benchmark efforts undertaken in the U.S. by Sandia National Laboratories (SNL) and internationally by the Organization for Economic Cooperation and Development (OECD). The SNL effort involved four cask model test problems which were independently solved using many of the major publicly released thermal analysis codes in the U.S. The geometry for model problem 4 is shown in Fig. 6.13. Regions I, II, and IV of the model are solid materials, while Region III is a void. The problem involved a steady-state, 30-minute fire, and a post-fire transient that provided the first major test of the node-to-node connector option available in HEATING6.1. Comparison with other radiation-enhanced codes in the U.S. showed excellent agreement (within 2%) for all times and temperature locations.<sup>82</sup>

The international cask heat transfer problems developed under the auspices of the OECD have provided another good test of the new radiation capabilities in HEATING6.1. One problem involved an experiment with a simulated 16 x 16 PWR fuel assembly within an aluminum enclosure. The enclosure was filled with helium gas. Comparison of the HEATING6.1 results with the experimental results shown in Fig. 6.14 indicates good agreement and provides a thorough test of the node-to-node connector capability.<sup>83</sup>

## 6.7 SUMMARY

The HEATING6 functional module is an extremely versatile analytic tool that has been used worldwide by analysts for a multitude of applications besides transport/storage casks. The HTAS1 control module has a more limited spectrum of uses and users. Currently, the module is predominantly used by the U.S. Nuclear Regulatory Commission staff to aid in the review of transport cask licenses. The U.S. Department of Energy (DOE) also plans to use HTAS1 to some extent in reviewing casks designed or built for and/or used by the DOE.

This paper has provided a review of the thermal analysis capabilities available in the SCALE computational system. The major tool is the HEATING6 general heat conduction code. Features of the numerical model and the user interface were reviewed to illustrate both the flexibility available to the user as well as the caution that must be exercised to assure accurate results. The REGPLOT6 and HEATPLOT-S modules are used for graphical output of the HEATING6 geometric model and temperature maps. The HTAS1 control module was developed to remove much of the difficulties associated with using HEATING6 for cask analysis problems. It allows an unexperienced HEATING6 user to obtain an adequate thermal evaluation of a cask with a minimum of effort. However, simplicity of use should not necessarily remove the caution that the user must exercise, particularly in regard to the mesh spacing, to assure an accurate result. The verification efforts undertaken by the developers are an ongoing process. Problems that test and verify the analytic capabilities of the HEATING6 and HEATING6.1 module have been developed and catalogued for reference during future code development or maintenance.

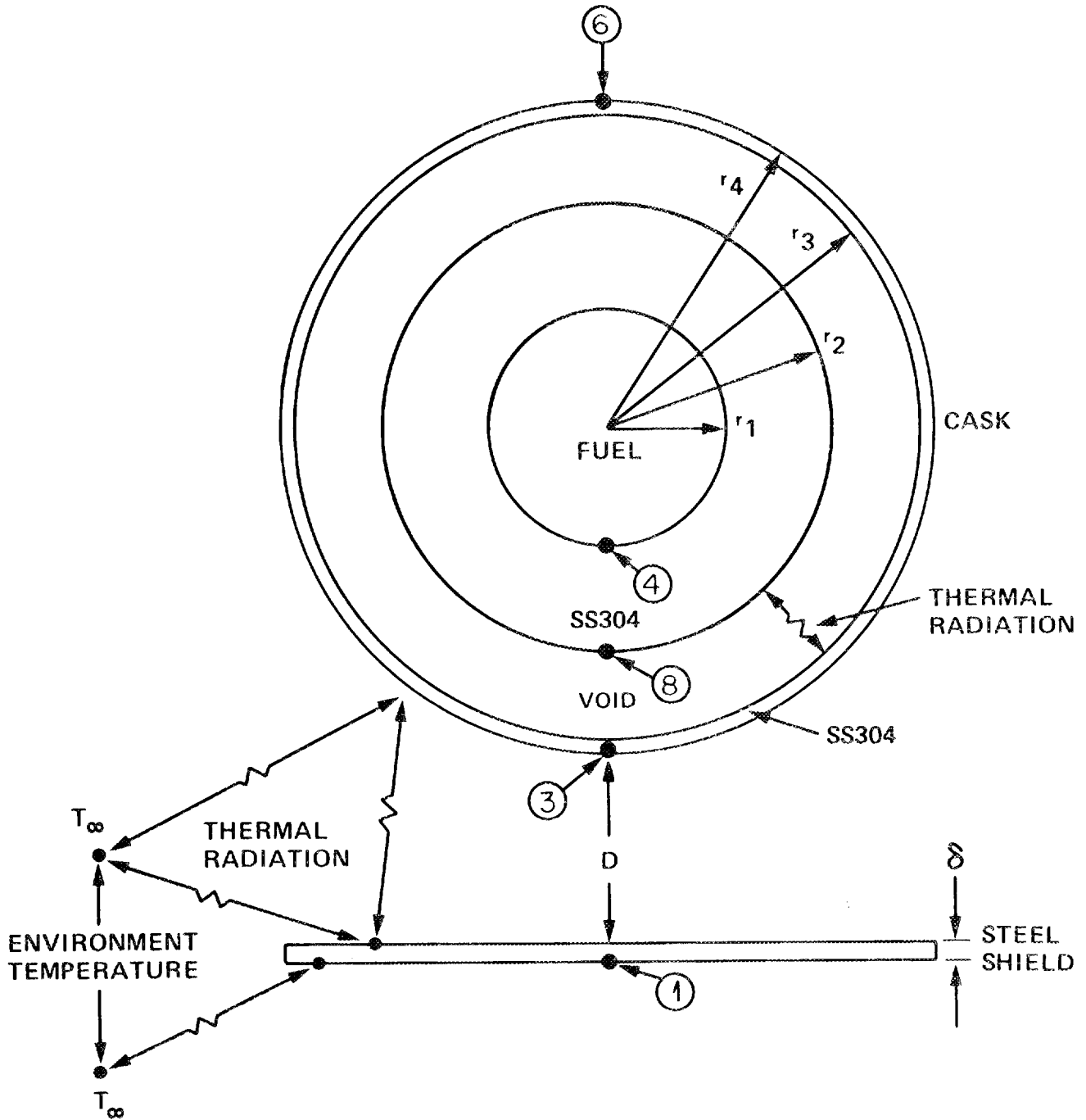


Fig. 6.13. Cask model problem with annular regions and radiation shield.

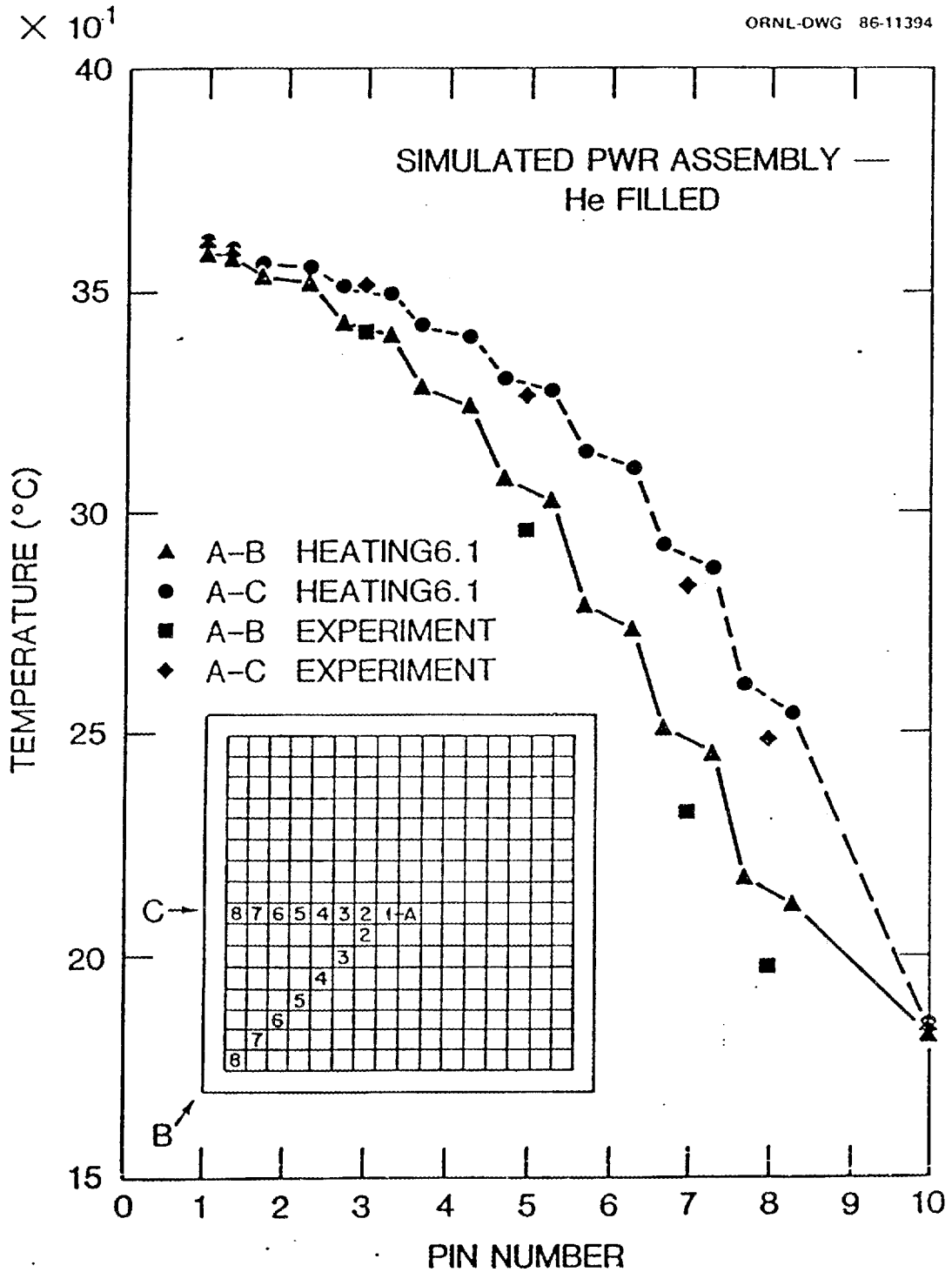


Fig. 6.14. HEATING6.1 and experimental results for helium-filled simulated PWR assembly in an enclosure.

## 7. REFERENCES

1. G. E. Whitesides and N. F. Cross, *KENO — A Multigroup Monte Carlo Criticality Program*, CTC-5, Union Carbide Corp., Nuclear Division (1969).
2. R. H. Odegaarden, "Application of SCALE System to Nuclear and Thermal Review of Radioactive Material Package Designs," *Proceedings of the Fifth International Symposium on Packaging and Transportation of Radioactive Materials*, Vol. II, p. 837, May 7-12, 1978.
3. R. M. Westfall and L. M. Petrie, "Standardized Safety Analysis of Nuclear Fuel Shipping Containers," *Proceedings of the Fifth International Symposium on Packaging and Transportation of Radioactive Materials*, Vol. II, p. 842, May 7-12, 1978.
4. *SCALE: A Modular Code System for Performing Standardized Computer Analyses for Licensing Evaluation*, Vols. 1-3, NUREG/CR-0200, U.S. Nuclear Regulatory Commission (originally issued July 1980, reissued January 1982, Revision 1 issued July 1982, Revision 2 issued June 1983, Revision 3 issued December 1984).
5. N. M. Greene et al., *AMPX: A Modular Code System for Generating Coupled Multigroup Neutron-Gamma Libraries from ENDF/B*, ORNL-TM-3706, Union Carbide Corp., Nuclear Division, Oak Ridge Nat. Lab., Oak Ridge, TN (March 1976).
6. E. A. Straker et al., *The MORSE Code — A Multigroup Neutron and Gamma-Ray Monte Carlo Transport Code*, ORNL-4585, Union Carbide Corp., Nuclear Division, Oak Ridge Nat. Lab., Oak Ridge, TN (1970).
7. M. J. Bell, *ORIGEN — The ORNL Isotope Generation and Depletion Code*, ORNL-4628, Union Carbide Corp., Nuclear Division, Oak Ridge Nat. Lab., Oak Ridge, TN (May 1973).
8. W. E. Ford et al., *A 218-Neutron-Group Master Cross Section Library for Criticality Safety Studies*, ORNL/CSD/TM-4, Union Carbide Corp., Nuclear Division, Oak Ridge Nat. Lab., Oak Ridge, TN (July 1976).
9. R. M. Westfall and J. R. Knight, "SCALE System Cross Section Validation with Shipping-Cask Critical Experiments," *Trans. Am. Nucl. Soc.* 33, 368 (November 1979).
10. Radiation Shielding Information Center (Oak Ridge National Laboratory) Data Package DLC-23/CASK, "40 Group Coupled Neutron and Gamma-Ray Cross-Section Data," contributed by Oak Ridge National Laboratory.
11. A. L. Edwards, *A Compilation of Thermal Property Data for Computer Heat-Conduction Calculations*, UCRL-50589, Lawrence Radiation Laboratory (1969).
12. G. E. Hansen and W. H. Roach, *Six and Sixteen Group Cross Sections for Fast and Intermediate Critical Assemblies*, LAMS-2543, Los Alamos Scientific Laboratory (November 1961).
13. V. I. Neeley and H. E. Handler, *Measurement of Multiplication Constant for Slightly Enriched Homogeneous UO<sub>3</sub>-Water Mixtures and Minimum Enrichment for Criticality*, HW-70310, Hanford Works (August 1961).
14. V. I. Neeley et al., *k<sub>∞</sub> of Three Weight Percent <sup>235</sup>U Enriched UO<sub>3</sub> and UO<sub>2</sub>(NO<sub>3</sub>) Hydrogenous Systems*, HW-66882, Hanford Works (September 1961).
15. W. E. Ford, III, et al., *A 218-Group Neutron Cross-Section Library in the AMPX Master Interface Format for Criticality Safety Studies*, ORNL/CSD/TM-4, Union Carbide Corp., Nuclear Division, Oak Ridge Nat. Lab. (July 1976).
16. R. M. Westfall et al., "Procedure for Determining Broad Energy Group Structure for Criticality Safety Calculations," *Trans. Am. Nucl. Soc.* 22, 291 (November 1975).

17. G. D. Joanou and J. S. Dudek, *GAM-II: A B<sub>3</sub> Code for the Calculation of Fast-Neutron Spectra and Multigroup Constants*, GA-4265, General Atomic (September 1963).
18. H. C. Honeck, *THERMOS: A Thermalization Transport Theory Code for Reactor Lattice Calculations*, BNL-5826, Brookhaven National Laboratory (September 1961).
19. M. E. Easter, *Validation of KENO V.a and Two Cross-Section Libraries for Criticality Calculations of Low-Enriched Uranium Systems*, ORNL/CSD/TM-223, Martin Marietta Energy Systems, Inc., Oak Ridge Nat. Lab. (1985).
20. J. R. Knight, *Validation of the Monte Carlo Criticality Program KENO V.a for Highly Enriched Uranium Systems*, ORNL/CSD/TM-221, Martin Marietta Energy Systems, Inc., Oak Ridge Nat. Lab. (1984).
21. G. W. Morrison et al., "A Coupled Neutron and Gamma Ray Multigroup Cross Section Library for Use in Shielding Calculations," *Trans. Am. Nucl. Soc.* 15, 535 (June 1972).
22. C. V. Parks et al., "Intercomparison of Cross-Section Libraries used for Spent Fuel Cask Shielding Analyses," **Proceedings of the Topical Conference on Theory and Practice in Radiation Protection and Shielding**, Vol. 2, p. 559, Knoxville, Tennessee, April 22-24, 1987
23. D. K. Trubey et al., *American National Standard Neutron and Gamma-Ray Flux-to-Dose Rate Factors*, ANSI/ANS-6.1.1-1977 (N666) American Nuclear Society (1977).
24. **Handbook of Chemistry and Physics**, Chemical Rubber Pub. Co., Cleveland, OH (1985).
25. **Chart of the Nuclides**, General Electric Co., San Jose, CA (1984).
26. W. A. Rhoades and R. L. Childs, *An Updated Version of the DOT IV One- and Two-Dimensional Neutron/Photon Transport Code*, ORNL-5851, Union Carbide Corp., Nuclear Division, Oak Ridge Nat. Lab. (July 1982).
27. J. R. Knight, *SUPERDAN: Computer Programs for Calculating the Dancoff Factor of Spheres, Cylinders, and Slabs*, ORNL/NUREG/CSD/TM-2, Union Carbide Corp., Nuclear Division, Oak Ridge Nat. Lab. (March 1978).
28. A. G. Croff, "ORIGEN2 - A Revised and Updated Version of the Oak Ridge Isotope Generation and Depletion Code," ORNL-5621, Union Carbide Corp., Nuclear Division, Oak Ridge Nat. Lab. (July 1980).
29. Allen G. Croff, "ORIGEN2: A Versatile Computer Code for Calculating the Nuclide Compositions and Characteristics of Nuclear Materials," *Nuclear Technology* 62, 335, 1983.
30. O. W. Hermann and R. M. Westfall, "ORIGEN-S: SCALE System Module to Calculate Fuel Depletion, Actinide Transmutation, Fission Product Buildup and Decay, and Associated Radiation Source Terms," as described in Sect. F7 of **SCALE: A Modular Code System for Performing Standardized Computer Analyses for Licensing Evaluation**, NUREG/CR-0200, Vol. 2 (January 1982, Revised June 1983 and December 1984).
31. D. R. Vondy, *Development of a General Method of Explicit Solution to the Nuclide Chain Equations for Digital Machine Calculations*, ORNL/TM-361, Union Carbide Corp., Nuclear Division, Oak Ridge Nat. Lab. (October 1962).
32. J. C. Ryman, *ORIGEN-S Data Libraries*, Sect. M6 of **SCALE: A Modular Code System for Performing Standardized Computer Analyses for Licensing Evaluation**, Vol. 3, NUREG/CR-0200, U.S. Nuclear Regulatory Commission (April 1983, Revised December 1984).
33. C. W. Kee, *A Revised Light Element Library for the ORIGEN Code*, ORNL/TM-4896, Union Carbide Corp., Nuclear Division, Oak Ridge Nat. Lab. (May 1975).

34. Radiation Shielding Information Center (Oak Ridge National Laboratory) Data Package DLC-38/ORYX-E, **ORIGEN Yields and Cross Sections - Nuclear Transmutation and Decay Data from ENDF/B**, contributed by Oak Ridge National Laboratory (September 1979).
35. ENDF/B-IV Fission Product Library Tapes 414-419, National Neutron Cross Section Center, Brookhaven National Laboratory (December 1974 and Rev. 1 December 1975).
36. Radiation Shielding Information Center (Oak Ridge National Laboratory) Code Package CCC-217/ORIGEN-79, "Isotope Generation and Depletion Code --- Matrix Exponential Method," contributed by Oak Ridge National Laboratory (September 1979).
37. A. G. Croff, R. L. Haese, and N. B. Gove, *Updated Decay and Photon Libraries for the ORIGEN Code*, ORNL/TM-6055, Union Carbide Corp., Nuclear Division, Oak Ridge Nat. Lab. (February 1979).
38. W. B. Ewbank et al., *Nuclear Structure Data File: A Manual for Preparation of Data Sheets*, ORNL-5054, Union Carbide Corp., Nuclear Division, Oak Ridge Nat. Lab. (June 1975).
39. W. B. Ewbank, "Evaluated Nuclear Structure Data File (ENSDF) for Basic and Applied Research," paper presented at the Fifth International CODATA Conference, Boulder, CO (June 1976).
40. D. C. Kocher, "Radioactive Decay Data Tables," Oak Ridge Nat. Lab., DOE/TIC-11026 (1981).
41. D. L. Johnson, *Evaluation of Neutron Yields from Spontaneous Fission of Transuranic Isotopes*, HEDL-SA-973, Hanford Engineering Development Laboratory (1975).
42. W. J. Swiatecki, "Systematics of Spontaneous Fission Half-Lives," *Phys. Rev.* **100**, 937, 1955.
43. J. K. Bair and J. Gomez del Campo, "Neutron Yields from Alpha-Particle Bombardment," *Nucl. Sci. Eng.* **71**, 18 (1979).
44. J. K. Bair and F. X. Haas, "Total Neutron Yields from the Reactions  $^{13}\text{C}(\alpha,n)^{16}\text{O}$  and  $^{17,18}\text{O}(\alpha,n)^{20,21}\text{Ne}$  (E)," *Phys. Rev. C* **7**, 1356, 1973.
45. J. K. Bair and H. B. Willard, "Level Structure in  $\text{Ne}^{22}$  and  $\text{Si}^{30}$  from the Reactions  $\text{O}^{18}(\alpha,n)\text{Ne}^{21}$  and  $\text{Mg}^{26}(\alpha,n)\text{Si}^{29}$ ," *Phys. Rev.* **128**, 299, 1962.
46. C. M. Lederer et al., *Table of Isotopes*, 6th ed., Wiley, New York (1967).
47. D. H. Stoddard, *Radiation Properties of  $^{244}\text{Cm}$  Produced for Isotopic Power Generators*, DP-939, Savannah River Laboratory (1964).
48. S. J. Rimshaw and E. E. Ketchen, "Curium Data Sheets," ORNL-4357, Union Carbide Corp., Nuclear Division, Oak Ridge Nat. Lab. (1969).
49. D. H. Stoddard and E. L. Albenesium, *Radiation Properties of  $^{238}\text{Pu}$  Produced for Isotopic Power Generators*, DP-984, Savannah River Laboratory (July 1965).
50. A. G. Khabakhpashev, "The Spectrum of Neutrons from a Po- $\alpha$ -O Source," *Atomnaya Energiya* **7**, 71 (1959).
51. O. W. Hermann, "COUPLE: SCALE System Module to Process Problem-Dependent Cross Sections and Neutron Spectral Data for ORIGEN-S Analyses," Sect. F6 of **SCALE: A Modular Code System for Performing Standardized Computer Analyses for Licensing Evaluation, Vol. 2**, NUREG/CR-0200, U.S. Nuclear Regulatory Commission (originally issued July 1980, reissued January 1982, Revision 1 issued July 1982, Revision 2 issued June 1983, Revision 3 issued December 1984).

52. J. C. Ryman et al., *Fuel Inventory and Afterheat Power Studies of Uranium-Fueled Pressurized Water Reactor Fuel Assemblies Using the SAS2 and ORIGEN-S Modules of SCALE with an ENDF/B-V-Updated Cross-Section Library*, NUREG/CR-2397 (ORNL/CSD-90), U.S. Nuclear Regulatory Commission (June 1982).
53. DISSPLA User's Manual, Integrated Software Systems Corporation, San Diego, CA (1981).
54. L. M. Petrie and N. F. Cross, *KENO IV — An Improved Monte Carlo Criticality Program*, ORNL-4938, Union Carbide Corp., Nuclear Division, Oak Ridge Nat. Lab. (1975). Also see Sect. F5 of the SCALE Manual, Ref. 4.
55. T. J. Hoffman, *The Optimization of Russian Roulette Parameters for KENO*, ORNL/TM-7539, Union Carbide Corp., Nuclear Division, Oak Ridge Nat. Lab. (1982).
56. M. J. Lorek, *Improved Criticality Search Techniques for Low- and High-Enriched Systems*, ORNL/NUREG/CSD/TM-13, NUREG/CR-2122, U.S. Nuclear Regulatory Commission (1981).
57. G. R. Handley et al., *Validation of the Monte Carlo Criticality Program KENO IV and the Hansen-Roach Sixteen-Energy-Group Cross Sections for High Assay Uranium Systems*, Y-2234, Union Carbide Corp., Nuclear Division, Oak Ridge Y-12 Plant (1981).
58. J. R. Knight, *Validation of the Monte Carlo Criticality Program KENO V.a for Highly Enriched Uranium Systems*, ORNL/CSD/TM-221, Martin Marietta Energy Systems, Inc., Oak Ridge Nat. Lab. (1984).
59. M. E. Easter, *Validation of KENO V.a and Two Cross-Section Libraries for Criticality Calculations of Low-Enriched Uranium Systems*, ORNL/CSD/T-223, K/HS-74, Martin Marietta Energy Systems, Inc., Oak Ridge Nat. Lab. (1985).
60. L. M. Petrie and J. T. Thomas, *Assessment of Computational Performance in Nuclear Criticality*, ORNL/CSD/TM-224, Martin Marietta Energy Systems, Inc., Oak Ridge Nat. Lab. (1985).
61. A. M. Hathout et al., *Validation of Three Cross-Section Libraries Used with the SCALE System for Criticality Safety Analysis*, NUREG/CR-1917, ORNL/NUREG/CSD/TM-19, U.S. Nuclear Regulatory Commission (June 1981).
62. M. E. Easter and R. T. Primm, III, *Validation of the SCALE Code System and Two Cross-Section Libraries for Plutonium Benchmark Experiments*, ORNL/TM-9402, Martin Marietta Energy Systems, Inc., Oak Ridge Nat. Lab. (January 1985).
63. W. C. Jordan, N. F. Landers, and L. M. Petrie, *Validation of KENO V.a Comparison with Critical Experiments*, ORNL/CSD/TM-238, Martin Marietta Energy Systems, Inc., Oak Ridge Nat. Lab. (1986).
64. "Standard Problem Exercise on Criticality Codes for Spent LWR Fuel Transport Containers," by a CSNI Group of Experts on Nuclear Criticality Safety Computations, CSNI Report No. 71, OECD, Paris, France (May 1982).
65. "Standard Problem Exercise on Criticality Codes for Large Arrays of Packages of Fissile Materials," by a CSNI Working Group, CSNI Report No. 78, OECD, Paris, France (August 1984).
66. M. B. Emmett, *The MORSE Monte Carlo Radiation Transport Code System*, ORNL-4972, Union Carbide Corp., Nuclear Division, Oak Ridge Nat. Lab. (February 1975).
67. J. A. Bucholz, "XSDOSE: A Module for Calculating Fluxes and Dose Rates at Points Outside a Shield," Sect. F4 of *SCALE: A Modular Code System for Performing Standardized Computer Analyses for Licensing Evaluation*, Vols. 1-3, NUREG/CR-0200, U.S. Nuclear Regulatory Commission (originally issued July 1980, reissued January 1982, Revision 1 issued July 1982, Revision 2 issued June 1983, Revision 3 issued December 1984).

68. E. A. Straker, P. N. Stevens, D. C. Irving, and V. R. Cain, *The MORSE Code — A Multigroup Neutron and Gamma-Ray Monte Carlo Transport Code*, ORNL-4585, Union Carbide Corp., Nuclear Division, Oak Ridge Nat. Lab.(1970).
69. T. J. Hoffman and J. S. Tang, *XSDRNPM-S Biasing of MORSE-SGC/S Shipping Cask Calculations*, NUREG/CR-2342, ORNL/CSD/TM-175, U.S. Nuclear Regulatory Commission (June 1982).
70. C. V. Parks et al., *Assessment of Shielding Analysis Methods, Codes, and Data for Spent Fuel Transport/Storage Applications*, ORNL/CSD/TM-246, Martin Marietta Energy Systems, Inc. (to be published at Oak Ridge National Laboratory).
71. W. D. Turner, D. C. Elrod, and I. I. Siman-Tov, *HEATING5 - An IBM 360 Heat Conduction Program*, ORNL/CSD/TM-15, Union Carbide Corp., Nuclear Division, Oak Ridge Nat. Lab. (March 1977).
72. R. S. Varga, *Matrix Iterative Analysis*, Prentice-Hall, Incorporated, Englewood Cliffs, New Jersey (1962).
73. J. J. Dorgarra, C. B. Moler, J. R. Bunch, and G. W. Stewart, "LINPACK User's Guide," *SIAM*, Philadelphia, Pennsylvania (1979).
74. W. M. Rohsenow and I. P. Hortnett, *Handbook of Heat Transfer*, McGraw-Hill, New York, pp. 3-115-3-119 (1973).
75. D. Q. Kern and A. D. Kraus, *Extended Surface Heat Transfer*, McGraw-Hill, New York (1972).
76. K. A. Gardner, "Efficiency of Extended Surface," *Transactions of the ASME*, pp. 621-631 (November 1945).
77. Part 71 of Title 10, Chapter 1, Code of Federal Regulations — Energy, Rules and Regulations, U.S. Nuclear Regulatory Commission (August 24, 1983).
78. *IF300 Shipping Cask, Consolidated Safety Analysis Report*, NEDO-10084-2, Nuclear Fuel and Services Division, General Electric, San Jose, CA (October 1979).
79. Chen-Ya Lin, W. K. Mueller, and F. Landis, "Natural Convection Heat Transfer in Long Horizontal Cylindrical Annuli," *Trans. Am. Soc. Mech. Engrs. V.*, 976 (1961).
80. W. H. McAdams, *Heat Transmission*, McGraw-Hill, New York (1954).
81. C. B. Bryan, K. W. Childs, G. E. Giles, *HEATING6 Verification*, K/CSD/TM-61, Martin Marietta Energy Systems, Inc., Oak Ridge Gaseous Diffusion Plant (December 1986).
82. C. B. Bryan and K. W. Childs, *Thermal Codes Benchmarking — HEATING6 Results*, K/CSD/TM-57, Martin Marietta Energy Systems, Inc., Oak Ridge Gaseous Diffusion Plant (August 1985).
83. K. W. Childs and C. B. Bryan, *HEATING6 Analysis of International Thermal Benchmark Problem Sets 1 and 2*, ORNL/CSD/TM-239, Martin Marietta Energy Systems, Inc., Oak Ridge Nat. Lab. (October 1986).

**Appendix A**

**CHANGES AND CORRECTIONS IN THE SCALE SYSTEM: 1980-1986**



## Appendix A

### CHANGES AND CORRECTIONS IN THE SCALE SYSTEM: 1980-1986

#### SCALE-0

SCALE-0 was released in 1980 and contained the control modules CSAS1 and CSAS2 for performing criticality analysis via XSDRNPM-S or KENO IV, respectively. Four criticality libraries were made available (16-group Knight-modified Hansen-Roach, 123-group GAM-THERMOS, 27-group ENDF/B-IV, and 218-group ENDF/B-IV), and resonance cross-section treatment was performed with NITAWL-S and BONAMI-S. A subroutine library and standard composition library were also provided.

#### SCALE-1

SCALE-1 was released in 1982. Besides the SCALE-0 programs and data libraries, SCALE-1 contained the following:

1. an enhanced criticality analysis control module called CSAS4 which used KENO V for performing the criticality analysis and provided an optimum pitch search option,
2. a shielding analysis control module called SAS3 which used the MARS system for geometry input and MORSE-SGC/S for the shielding analysis,
3. ORIGEN-S and corresponding data libraries for fuel depletion, spent fuel decay, and shielding source terms,
4. COUPLE for generating problem-dependent cross-section or neutron spectral data to ORIGEN-S,
5. ICE-S for mixing multigroup cross sections,
6. HEATING6 for heat transfer analyses,
7. JUNEBUG for geometry plotting of MARS and KENO IV geometries, and
8. XSDOSE for evaluating the dose and flux at a point outside a shield.

Three shielding libraries (coupled 22n-18 $\gamma$  group CASK library, 18-group gamma library, and a coupled 27n-18 $\gamma$  group library) were provided with this release. Some minor changes to the CSAS1 and CSAS2 control modules were also made in SCALE-1 to correct several minor errors or problems. A relatively major inconsistency in NITAWL-S was also fixed to eliminate negative groupwise constants when using zircalloy under certain specific conditions. Also, gadolinium (ID 64000) thermal-capture cross sections were updated to correct errors previously occurring in the resonance processing. Depending on the amount of gadolinium in the problem,  $k_{\text{eff}}$  values can change significantly (decrease) from that obtained with the data originally released with SCALE-0.

#### SCALE-2

In 1983, SCALE-2 was released. The programs and libraries of SCALE-1 were included as revised or corrected to enhance the system or fix known errors. Revisions and corrections include the following:

1. Substantial changes were made to the MARS geometry subroutine library to correct tracking errors that occurred in several MORSE-SGC/S problems and to restructure commons and data transfers for improved efficiency.

2. MORSE-SGC/S was corrected to prevent erroneous results from being obtained with several classes of problems: (a) those that have point detectors with the use of "OR's" in the geometry zone descriptions or that calculate an uncollided flux; (b) those that do an energy-dependent analysis, and (c) those that have arrays in the geometry where the length of the array data is an odd number.
3. JUNEBUG was updated to correct several known errors.
4. Internal commons and/or program interfaces were altered in SAS3, MORSE-SGC/S and JUNEBUG to match the updated MARS library.
5. BONAMI was updated to correct an error in the Dancoff expression for the input options ISSOPT=8 or ISSOPT=9.
6. All control modules except CSAS1 and CSAS2 were altered to check the validity of an input solution name. Previously, problems with invalid solution names ran using incorrect data for the solution.
7. KENO V was updated to eliminate the possibility of skipping a block on the direct access file (occurred when calculated data exactly filled a block) and to correct results for the average fission group and unit self-multiplication in problems with super grouping.
8. Numerous minor modifications were made to HEATING6 to correct errors and add features required by the new control module HTAS1. Changes included (a) an option to eliminate the nodal melting ratio map for transient calculations, (b) improvements to fix minor storage problems, (c) a correction to eliminate abnormal terminations when the initial time step size of zero was used, and (d) corrections to eliminate an error when using the fin effectiveness technique to model natural convection over a finned surface.
9. The resonance range for several nuclides was changed in the 27-group neutron cross-section data to be consistent with the NITAWL treatment. Tests performed with the new data indicate no significant effect on previous results.
10. Decay data for several nuclides in the light element and actinide libraries were updated.

New programs added to SCALE with SCALE-2 were (1) the heat transfer analysis control module HTAS1 which uses HEATING6 to analyze the prefire, fire, and post-fire conditions of a transport cask accident scenario, and (2) the shielding analysis control module SAS2 which performs burnup analysis via ORIGEN-S and a subsequent radial shielding calculation via XSDRNPM-S. An expanded 27-group library was also provided with SCALE-2 to provide data for a number of fission product nuclides useful in depletion calculations.

### SCALE-3

SCALE-3 offers some significant changes over the SCALE-2 release. New programs (and/or data) and revisions are as follows:

1. The Materials Information Processor used by CSAS4, SAS2, and SAS3 has been updated to correct some minor errors and to allow more (optional) resonance data to be input.
2. MARS and MORSE-SGC/S were updated to correct several minor errors and to add warning and error messages (MARS) useful in detecting input or tracking problems.
3. KENO V was replaced with KENO V.a which has enhanced geometry features and optional printer plots of the geometry. KENO V input will also work with KENO V.a.

4. CSAS4 was updated to allow interfacing with KENO V.a, provide two new analytical sequences, and provide improved search options. An error in CSAS4 has been corrected. The error caused the second buckling DZ to be set to the first buckling DY for multiregion problems containing a void and utilizing a buckled cylinder or slab.
5. SAS2 was improved by enhancing the restart feature to allow a different number of fuel zones to be used for the shielding portion of the analysis than that originally specified in the initial case.
6. HTAS1 has been enhanced to allow geometry and output plots.
7. XSDRNPM-S has been updated to (a) improve the calculation of reaction rates, (b) put the calculation of the quadrature set in double precision, and (c) allow mixed reaction rates to be specified with the same MT identifiers used for microscopic reaction rates.
8. ORIGEN-S has been modified to (a) calculate an improved neutron source strength, (b) add computation of a neutron source spectra, and (c) save data in a form useful for plotting.
9. ICE-S was modified to normalize the flux used in evaluation of the mixing factor for generating the fission spectrum.
10. BONAMI-S and the 16-group Hansen-Roach data were modified to correct an inconsistency in the evaluation of  $\sigma_p$  used to interpolate Bondarenko factors from the data tables. The inconsistency has little or no effect on  $k_{\text{eff}}$  results for highly enriched metal systems. The inconsistency becomes more important for moderated systems and becomes very significant for slightly moderated, low-enriched systems (where  $\sigma_p$  ranges between 30 and 150). Table A.1 provides  $k_{\text{eff}}$  analytic results for some low-enriched experiments using the old and new Bondarenko treatment.
11. JUNEBUG has been replaced with JUNEBUG-II. The new version is considerably more efficient in terms of run time and data storage and has been modified to remove errors detected by users.
12. Data for several new materials were added to the Standard Composition Library and several elements were added to the isotope distribution table.
13. For some nuclides in the 123-group GAM-THERMOS library, the higher-order  $P_n$  coefficients have been changed to make them legitimate expansions.
14. HEATING6 has been updated to correct some errors detected in the expressions for the fin effectiveness and eliminate an error with one option employed in calculating the fin effectiveness.
15. The subroutine library has been revised to (a) correct some errors detected in the free-form reading routine for arrays, YREAD, and (b) modify applicable routines to (hopefully) allow use of 3380 diskpaks.
16. KENO IV has been updated to correct an error in the scattering direction of a split particle. Previous versions of KENO IV neglected to store the initial direction of the particle if a splitting occurred before the particle scattered.
17. PICTURE, CESAR, HEATPLOT, and REGPLOT6 are new programs being added to the SCALE system. PICTURE produces printer plots of MARS geometries; HEATPLOT and REGPLOT6 produce compressed plot files of HEATING6 output and geometry models, respectively; and CESAR is a module which searches a data base to obtain SCALE input data for analyzing a particular criticality experiment or set of experiments.

Table A.1. 16-group results for critical experiments of low-enriched slightly moderated uranium systems\*

| Problem | Enr.<br>wt% | H:U-238 | H:U-235 | New Bondarenko<br>treatment<br>16 Group Xsects |           | Old Bondarenko<br>treatment<br>16 Group Xsects |           |
|---------|-------------|---------|---------|--|-----------|--|-----------|
|         |             |         |         | K(eff)   | Deviation | K(eff)   | Deviation |
| 11      | 2.0         | 4.0     | 195.2   | 0.99587  | .00365    | 1.02801  | .00399    |
| 12      | 2.0         | 4.0     | 195.2   | 0.99744  | .00327    | 1.02386  | .00371    |
| 21      | 3.0         | 4.2     | 133.4   | 1.01363  | .00401    | 1.04861  | .00437    |
| 22      | 3.0         | 4.2     | 133.4   | 1.01660  | .00445    | 1.04053  | .00459    |
| 23      | 3.0         | 4.2     | 133.4   | 1.00874  | .00485    | 1.03795  | .00380    |
| 24      | 3.0         | 4.2     | 133.4   | 1.01190  | .00479    | 1.03600  | .00478    |
| 25      | 3.0         | 4.2     | 133.4   | 1.00980  | .00498    | 1.03692  | .00465    |
| 26      | 3.0         | 4.2     | 133.4   | 1.00565  | .00397    | 1.03993  | .00492    |
| 27      | 3.0         | 4.2     | 133.4   | 1.00860  | .00411    | 1.04139  | .00448    |
| 28      | 3.0         | 4.2     | 133.4   | 1.01929  | .00407    | 1.02522  | .00447    |
| 13      | 2.0         | 6.1     | 293.9   | 1.00337  | .00389    | 1.03082  | .00446    |
| 14      | 2.0         | 6.1     | 293.9   | 0.99609  | .00395    | 1.02370  | .00368    |
| 4       | 1.4         | 6.1     | 421.8   | 0.99647  | .00337    | 1.02051  | .00318    |
| 5       | 1.4         | 6.1     | 421.8   | 0.99776  | .00326    | 1.03049  | .00318    |
| 6       | 1.4         | 6.1     | 421.8   | 1.00764  | .00311    | 1.02484  | .00323    |
| 15      | 2.0         | 8.4     | 406.3   | 1.00108  | .00378    | 1.01288  | .00363    |
| 29      | 3.0         | 8.7     | 276.9   | 0.99487  | .00462    | 1.02674  | .00513    |
| 30      | 3.0         | 8.7     | 276.9   | 0.99257  | .00382    | 1.01798  | .00528    |
| 31      | 3.0         | 8.7     | 276.9   | 1.00132  | .00450    | 1.02314  | .00407    |
| 32      | 3.0         | 8.7     | 276.9   | 0.99154  | .00420    | 1.01886  | .00447    |
| 16      | 2.0         | 10.3    | 495.9   | 0.99737  | .00325    | 1.01583  | .00341    |
| 17      | 2.0         | 12.7    | 613.6   | 0.98408  | .00342    | 1.01767  | .00369    |
| 18      | 2.0         | 12.7    | 613.6   | 0.98871  | .00316    | 1.00822  | .00309    |
| 19      | 2.0         | 20.1    | 971.7   | 0.99527  | .00292    | 1.00263  | .00276    |
| 20      | 2.0         | 20.1    | 971.7   | 0.98804  | .00273    | 1.00172  | .00239    |
| 33      | 4.98        | 25.9    | 488.0   | 1.00028  | .00374    | 0.99709  | .00404    |
| 34      | 4.98        | 25.9    | 488.0   | 0.99565  | .00413    | 1.00070  | .00402    |
| 35      | 4.98        | 26.0    | 490.0   | 0.98574  | .00415    | 0.99341  | .00457    |
| 36      | 4.98        | 26.3    | 496.0   | 0.98733  | .00416    | 0.99651  | .00478    |

\*Mike Easter, *Validation of KENO V.a and Two Cross-Section Libraries for Criticality Calculations of Low Enriched Uranium Systems*, ORNL/CSD/TM-223, Martin Marietta Energy Systems, Inc., Oak Ridge Nat. Lab. (July 1985).

### SCALE 3.1

In May 1986, RSIC was alerted of several errors and/or inconsistencies that existed in the initial SCALE-3 tape release. The changes are provided below.

1. CSAS4 and KENO V.a were updated to correct several errors that could yield incorrect answers
  - a. specification of PAX=YES on the KENO V.a parameter card caused a printer to be incorrectly set that altered the random number sequence;
  - b. for large systems with shared boundaries, it was possible for the wrong material to be used in one of the regions;
  - c. for a KENO V.a restart case that wrote another restart file on a different unit, the boundary conditions were incorrectly specified in a subsequent case if the restart file was used;
  - d. when a box type was specified and a unit number skipped, the unit orientation data was not entered and some information in the neutron bank was lost; and
  - e. a loop occurred when a particle exited a hemicylindrical region and entered a region containing holes, and the particle did not move in the direction of the cut face due to the direction cosine component in that direction being zero or very very small.
2. SAS2 was modified to correct an error in the  $^{238}\text{U}$  resonance calculation for the fuel region. The error caused  $^{238}\text{U}$  to be used as one of the moderators in the NITAWL calculation.
3. MORSE-SGC/S was updated to correct errors that caused the code not to run for certain input situations.
4. SAS3 was changed to allow selection of all gamma response functions and correct an error in the number of Legendre coefficients specified for MORSE-SGC/S.
5. Two subroutines (ACTIE and OAKTRE) from the MARS Library were altered to eliminate the possibility of an infinite loop when data was input incorrectly and to correct a wrong index in the concentric sphere option.
6. Until now, subroutine RESDA in the Material Information Processor has found two nuclides in a mixture with the largest slowing down power and passed these to NITAWL to use as the first and second moderators in the resonance calculation. For most cases that have been treated, this works well, but cases exist where a third moderator has very nearly the same slowing down power as the selected second moderator. Therefore, RESDA has been changed to pass an "average" moderator to NITAWL as the second moderator which preserves the total slowing down power of all nuclides except the resonance nuclide and the first moderator. This change will make minor differences in all calculations where a mixture with a resonance nuclide has more than three nuclides. For cases where this is important, it can make as much as 1.5-2.0% difference in  $k_{\text{eff}}$ .
7. Standard Composition Library Data for the total cross section of nickel in Inconel has been corrected. Use of a non-physical value ( $\sigma_T < \sigma_S$ ) caused the automatic mesh generator not to function where this nuclide was used.
8. Due to bad magic words in the binary library from which it was created, the following arrays were omitted from the card image file for the 27-group neutron library:

|       |          |    |        |        |    |
|-------|----------|----|--------|--------|----|
| Be-9  | MT=1007, | P3 | Re-185 | MT=52, | P3 |
| O-16  | MT=1007, | P3 | Pu-241 | MT=56, | P3 |
| Br-79 | MT=61,   | P3 | Cm-244 | MT=60, | P3 |
| Zr    | MT=52,   | P3 |        |        |    |

It is not anticipated that any of these changes would provide any significant effect on previously calculated results.

Only an IBM version of the entire SCALE package is available. However, the codes and data in SCALE-0 are available in a CDC version that has been updated to be current with the SCALE-3 release. A FORTRAN-77 version of many SCALE models and assembler routines is also available from RSIC as code package CCC-475. With the SCALE-4 release, both IBM and CRAY FORTRAN-77 versions of the package will be available.

**Appendix B**

**FEATURES OF THE ORIGEN-S PROGRAM**



## Appendix B

### FEATURES OF THE ORIGEN-S PROGRAM

The code solves problems having the following characteristics or features:

1. An "irradiation" problem is solved using a set of initial nuclide or element concentrations and the "nuclear data library" for a given reactor flux.
2. A "post-irradiation" problem which may be part of irradiation subcase or a new subcase.
3. A "decay-only" problem involving no irradiation.
4. A problem is solved using a "continuous feed" feature, where the concentrations are enhanced with a continuous rate of feed for given isotopes. This applies to fluid fuel reactors.
5. A problem is solved using a "continuous chemical processing" feature, where the concentrations of given elements are depleted by a continuous removal rate through chemical processing.
6. A "continuation" problem may be requested, where an irradiation or decay subcase begins with the concentrations prevailing at any time specified during the last subcase.
7. Either the same or a different "nuclear data library" may be requested in a continuation subcase. This allows for different flux spectra to be applied, in order to account for the time dependence of flux within a reactor.
8. A continuation problem is solved using a "batch removal" feature, where given fractions of specified elements are removed through chemical batch processing before calculation continues.
9. A "blending case" is executed, which always will contain several subcases. Different concentrations are used in two or more of the subcases. A given fraction of the material from each of the streams, or subcases, at specified times are added together to form the initial concentrations for subsequent "blended stream" subcases. While different libraries are permitted, there should not be any variation in the lists of nuclides from library to library. Any number of problems not related to the blending option may be solved within the case.
10. The "nuclear data library" input to the code may be in either the "binary" or "card image" mode. Only the "card image" library can be edited. The binary library saves about half the computer time of a ten-time-step problem, can be automatically updated using COUPLE, and automatically provides the library sizes which must be user-specified for the "card image" library.
11. There is a division of the isotopes and isomers into three separate groups. The problem computation may be restricted to any combination of the three groups, eliminating needless time or printing in processing an unwanted group. The nuclides of each group (or library) are:
  - a. fuel nuclides and their heavy metal reaction and decay products plus  $^4\text{He}$ ,
  - b. fission products,
  - c. light elements common in power reactor coolants, clad, and structural material or in research reactor experimental cells.
12. The problem input may be punched in the free-field style, with the numerous conveniences of the FIDO Input System (see Sect. M10 of ref. 4).

13. A variety of units is allowed in the input of some of the problem parameters:
- starting nuclide concentrations may be in grams, gram-atoms, weight ppm or atom ppm,
  - reactor irradiation may be in terms of thermal flux or power,
  - time in six different units.
14. The nuclide concentration and associated answers may be converted to a large variety of units for listing. The units available during irradiation depend upon the input units. Possible output units are:
- gram-atoms,
  - weight ppm,
  - atom ppm,
  - atoms/(barn-cm),
  - total delayed gamma source spectra in photons/sec, MeV/sec, or MeV/w-s of burnup,
  - fraction of total neutron absorption rates,
  - total neutron production,
  - total neutron absorption,
  - infinite medium neutron multiplication constant,  $k_{\infty}$ .

Output units available during the decay period are:

- gram-atoms,
  - grams,
  - curies,
  - thermal power afterheat in watts,
  - gamma power afterheat in watts,
  - cubic meters of air containing nuclide quantity to produce density equal to Radiation Concentration Guide (RCG) limit for air,
  - cubic meters of water to equal RCG for water,
  - neutron sources from  $\alpha,n$  reaction,
  - neutron sources from spontaneous fission,
  - total gamma source spectra in photons sec, MeV sec, or MeV w-s of burnup,
  - neutron source spectra from  $\alpha,n$  plus spontaneous fission in neutrons/sec.
15. In general, only tables in the units specified are listed and these are divided into only those groups (see 11) selected. These may be listed by either nuclide or element. Quantities below the cut-off for the unit may be deleted.
16. The gamma photon release rate spectra may be computed using three different photon constant data bases. The most recent data base<sup>37</sup> has improved quality and can be periodically updated.

17. An energy group structure may be input for producing gamma source spectra. The sources may be punched or saved as an output file. The sources from the three libraries or groups (see 11) may be combined.
18. The photon data base in the "nuclear data library" may be updated from improved constants in the other data bases.
19. Principal photon sources, by nuclide, may be listed by energy group from the fission products. The percent of source used to select nuclides may be controlled by input.
20. A computation model has been applied to the fission products which produces both time-dependent decay concentrations and their time integral over the time step.
21. Starting concentrations may be punched. Also the totals of many of the tables listed may be punched.
22. All concentrations (g-atoms) at any or all time steps may be saved on a binary tape. A restart feature allows a case to start with any of the saved values.
23. The core storage required for executing the program automatically expands and contracts to fit the problem.
24. All input data, normally punched on cards, may be input from a binary written interface — allowing easy recycle into and out of the program.
25. The removable thermal energy per fission, which is dependent on time and concentration, is computed for each time step by default. Also, an input option allows users to select 200 MeV fission.
26. There is a table of contents of page numbers starting each subcase.
27. Substantially improved data have been applied in calculating neutron sources, along with new models for  $\alpha, n$  reactions and the energy-dependent neutron spectra.



## INTERNAL DISTRIBUTION

- |        |                   |        |  |
|--------|-------------------|--------|--|
| 1.     | C. W. Alexander   | 49.    | R. T. Primm  |
| 2-6.   | C. B. Anthony     | 50.    | R. R. Rawl   |
| 7-11.  | J. L. Bartley     | 51.    | J. P. Renier   |
| 12.    | L. D. Bates       | 52.    | J. W. Roddy  |
| 13.    | B. L. Broadhead   | 53-57. | R. W. Roussin  |
| 14.    | C. B. Bryan       | 58.    | J. C. Ryman  |
| 15.    | J. A. Bucholz     | 59.    | J. Saling  |
| 16.    | S. P. Cerne       | 60-62. | C. H. Shappert   |
| 17.    | K. W. Childs      | 63.    | L. B. Shappert   |
| 18.    | S. N. Cramer      | 64.    | C. O. Slater   |
| 19.    | H. L. Dodds       | 65.    | G. R. Smolen   |
| 20.    | H. R. Dyer        | 66.    | R. M. Stinnett   |
| 21.    | M. B. Emmett      | 67.    | J. S. Tang   |
| 22.    | D. E. Fields      | 68.    | J. T. Thomas   |
| 23.    | W. E. Ford        | 69.    | J. N. Tunstall   |
| 24.    | P. B. Fox         | 70.    | J. C. Turner   |
| 25.    | G. E. Giles       | 71.    | M. W. Waddell  |
| 26.    | N. M. Greene      | 72-76. | R. M. Westfall   |
| 27-31. | N. Hatmaker       | 77.    | G. E. Whitesides/R. P. Leinius                             |
| 32.    | O. W. Hermann     | 78.    | P. T. Williams   |
| 33.    | C. M. Hopper      | 79.    | R. Q. Wright   |
| 34.    | W. C. Jordan      | 80.    | Central Research Library                                   |
| 35.    | N. F. Landers     | 81.    | ORNL Y-12 Technical Library,<br>Document Reference Section |
| 36.    | A. P. Malinauskas | 82.    | Laboratory Records Department                              |
| 37-41. | B. F. Maskewitz   | 83.    | Laboratory Records, ORNL (RC)                              |
| 42.    | J. V. Pace        | 84.    | ORNL Patent Office   |
| 43-47. | C. V. Parks       |        |  |
| 48.    | L. M. Petric      |        |  |

## EXTERNAL DISTRIBUTION

85. S. Ailes, Battelle Project Management Division, 505 King Avenue, Columbus, OH 43201
86. G. Allen, Sandia National Laboratories, P. O. Box 5800, Albuquerque, NM 87185
87. H. I. Avci, Battelle Pacific Northwest Laboratory, Office of Waste Technology Development, 7000 S. Adams Street, Willowbrook, IL 60521
88. A. F. Avery, AEE Winfrith, Reactor Physics Division, Bldg. B.21, Dorchester, GB-Dorset DT2 8DH, United Kingdom
89. L. Barrett, U.S. Department of Energy, Office of Civilian Radioactive Waste Management, RW-232, Washington, DC 20545
90. C. Boggs-Mayes, U.S. Department of Energy, Chicago Operations Office, 9800 S. Cass Avenue, Argonne, IL 60439
91. T. Bump, Argonne National Laboratory, 9700 S. Cass Ave., Argonne, IL 60439
92. M. Cosack, Physikalisch Technische Bundesanstalt, Bundesallee 100, 3300 Braunschweig, Federal Republic of Germany

93. J. M. Creer, Battelle Pacific Northwest Laboratory, P.O. Box 999, Richland, WA 99352
94. M. Diop, CEN Saclay, DRE/SERMA/LEP, F-91191 GIF/YVETTE CEDEX, France
95. Division of Engineering, Mathematics and Geosciences, U.S. Department of Energy, Washington, DC 20545
96. M. Dohnal, Chem. Eng. Dept., Tech. Univ. Brno, Kravi hora 2, 611 00 Brno, Czechoslovakia
97. C. C. Dwight, U.S. Department of Energy, Idaho Operations Office, Idaho Falls, ID 83402
98. E. Easton, Transportation Branch, Office of Nuclear Material Safety & Safeguards, U.S. Nuclear Regulatory Commission, MS 396-SS, Washington, DC 20555
99. T. Eng, U.S. Department of Energy, Office of Civilian Radioactive Waste Management, RW-232, Washington, DC 20545
100. F. P. Falci, Manager, Nuclear Materials Transportation R&D, U.S. Department of Energy, DP-121, Washington, DC 20545
101. L. Fisher, Lawrence Livermore National Laboratory, P.O. Box 808, Livermore, CA 94550
102. H. Geiser, Wissenschaftlich-Technische Ingenieurberatung GMBH, Mozartstrasse 13, 5177 Titz-Rodingen, Federal Republic of Germany
103. R. E. Glass, Sandia National Laboratories, Division 6322, P.O. Box 5800, Albuquerque, NM 87185
104. G. Gualdrini, ENEA-TIB/FICS, C.R.E. "E. Clementel", Via Mazzini, 2, I-40139 Bologna, Italy
105. J. Hale, U.S. Department of Energy, Office of Civilian Radioactive Waste Management, RW-233, Washington, DC 20545
106. C. Heeb, Battelle Pacific Northwest Laboratory, P. O. Box 999, Richland, WA 99352
107. M. M. Heiskell, U.S. Department of Energy, Oak Ridge Operations, P.O. Box E, Oak Ridge, TN 37830
108. J. R. Hilley, U.S. Department of Energy, Office of Civilian Radioactive Waste Management, Washington, DC 20545
109. J. F. Jaeger, Eidgenoessisches Institut fuer Reaktorforschung, CH-5303 Wuerenlingen, Switzerland
110. U. Jenquin, Battelle Pacific Northwest Laboratory, P.O. Box 999, Richland, WA 99352
111. K. Klein, Office of Civilian Radioactive Waste Management, U.S. Department of Energy, Washington, DC 20545
112. C. Kouts, Office of Civilian Radioactive Waste Management, U.S. Department of Energy, Washington, DC 20545
113. W. Lake, Transportation & Certification Branch, Office of Nuclear Material Safety & Safeguards, U.S. Nuclear Regulatory Commission, MS 396-SS, Washington, DC 20555
114. R. Lambert, EPRI, P. O. Box 10412, Palo Alto, CA 94303
115. D. Langstaff, U.S. Department of Energy, Richland Operations Office, P. O. Box 550, Richland, WA 99352
116. J. Leatham, U.S. Department of Energy, EG&G Idaho, P. O. Box 1625, Idaho Falls, ID 83415
117. R. A. Libby, Battelle Pacific Northwest Laboratory, 2030 M St. NW, Washington, DC 20026
118. E. Livesey, Manager, Process Technology Group, Process and Technical Services, Rutherford House, British Nuclear Fuels, Risley Warrington Cheshire WA36AS, United Kingdom
119. A. Luksic, Battelle Pacific Northwest Laboratory, P. O. Box 999, Richland, WA 99352
120. S. Mancioffi, ENEA/DISP-ARA-RAM, Via Vitaliano Brancati 48, I-00144 Rome, Italy
121. C. Marotta, Transportation Branch, Office of Nuclear Material Safety & Safeguards, U.S. Nuclear Regulatory Commission, MS 396-SS, Washington, DC 20555
122. M. Mason, Transnuclear, 1 North Broadway, White Plains, NY 10601

123. C. J. Mauck, U.S. Department of Energy, MS DP-4-1, Washington, DC 20545
124. R. S. McKee, Battelle Pacific Northwest Laboratory, P.O. Box 999, Richland, WA 99352
125. D. Mennerdahl, E. Mennerdahl Systems, Pl 457, S-186 00 Vallengarna, Sweden
126. R. L. Murray, P. O. Box 5596, Raleigh, NC 27650
127. R. H. Odegaard, Transportation Branch, Office of Nuclear Material Safety & Safeguards, U.S. Nuclear Regulatory Commission, MS 396-SS, Washington, DC 20555
128. Office of Assistant Manager, Energy Research and Development, Department of Energy, Oak Ridge Operations, P.O. Box E, Oak Ridge, TN 37831
129. O. Ozer, EPRI, P. O. Box 10412, Palo Alto, CA 94303
130. R. W. Peterson, Battelle Columbus Laboratories, 505 King Avenue, Columbus, OH 43201
131. F. Prohammer, Argonne National Laboratory, 9700 S. Cass Ave., Argonne, IL 60439
132. W. A. Pryor, U.S. Department of Energy, P. O. Box E, Oak Ridge, TN 37831
133. A. Renard, Belgonucleaire, 25, rue du Champ de Mars, Bruxelles, Belgium
134. J. P. Roberts, Office of Nuclear Material Safety & Safeguards, U.S. Nuclear Regulatory Commission, MS 396-SS, Washington, DC 20555
135. J. N. Rogers, Div. 8324, Sandia Laboratories, Livermore, CA 94550
136. T. W. Rowland, U.S. Department of Energy, Idaho Operations Office, Idaho Falls, ID 83402
137. T. L. Sanders, Sandia National Laboratories, Division 6323, P. O. Box 5800, Albuquerque, NM 87185
138. M. Shay, Battelle Pacific Northwest Laboratory, P. O. Box 999, Richland, WA 99352
139. D. E. Shelor, Office of Civilian Radioactive Waste Management, U.S. Department of Energy, Washington, DC 20545
140. D. Smith, Branch Manager, QA, Science Applications International Corporation, Nevada Nuclear Waste Storage Investigations, Valley Bank Center, Suite 458, 101 Convention Center Drive, Las Vegas, NV 89109
141. H. L. Steinberg, U.S. Department of Energy, Office of Civilian Radioactive Waste Management, RW-233, Washington, DC 20545
142. C. J. Temus, Nuclear Packaging, Inc., 1010 South 336th Street, Federal Way, WA 98003
143. J. Thornton, Duke Power Co., P. O. Box 33189, Charlotte, NC 28242
144. J. L. Torres, U.S. Department of Energy, DP-4, Washington, DC 20545
145. J. Voglewede, U.S. Nuclear Regulatory Commission, MS 623-SS, Washington, DC 20555
146. F. Wasastjerna, Nuclear Engineering Lab., Technical Research Centre of Finland, P.O.B. 169, SF-00181 Helsinki 18, Finland
147. A. H. Wells, Nuclear Assurance Corporation, 5720 Peachtree Parkway, Norcross, GA 30092
148. J. T. West, Los Alamos National Laboratory, P. O. Box 1663, Los Alamos, NM 87545
149. W. Weyer, Wissenschaftlich-Technische Ingenieurberatung GMBH, Mozartstrasse 13, 5177 Titz-Rodingen, Federal Republic of Germany
150. D. S. Williams, Bechtel North American Power Corporation, 15740 Shady Grove Road, Gaithersburg, MD 20877-1454
151. M. L. Williams, LSU Nuclear Science Center, Baton Rouge, LA 70803
152. R. F. Williams, EPRI, P. O. Box 10412, Palo Alto, CA 94303
153. E. Wilmot, U.S. Department of Energy, Office of Civilian Radioactive Waste Management, RW-233, Washington, DC 20545
- 154-155. Office of Scientific and Technical Information, U.S. Department of Energy, Oak Ridge, TN 37831
- 156-305. Given distribution under category GM.